Universität Konstanz

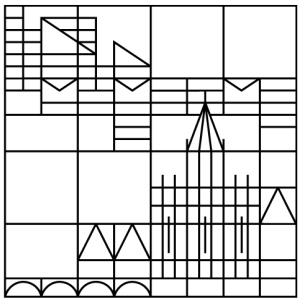

Master Thesis

Quantum Transport Group

Prof. Dr. Wolfgang Belzig

Decoherence dynamics of topological spin chains

Hannes Weisbrich

Supervisor
Dr. Gianluca Rastelli
and Prof. Dr. Wolfgang Belzig
Konstanz, May 22, 2018

Acknowledgments

I want to thank all people who supported me during my studies and this work.

Special thanks to my supervisors Dr. Gianluca Rastelli and Prof. Dr. Wolfgang Belzig for their time they invested in the discussions and the weekly meetings with me. I really enjoyed these discussions and they always helped me to expand my knowledge in physics.

I also want to thank the whole research group for the nice atmosphere during the last year.

Furthermore, I want to express my special gratitude to my family for the support during my studies which gave me the opportunity to study physics.

Hannes Weisbrich
Konstanz, 2018

Abstract

This thesis examines the transverse Ising chain under the influence of the environment represented by a bosonic bath. In the transverse Ising chain the spins are coupled to their nearest neighbor perpendicular to a transverse field, a model representing a chain of qubits with nearest neighbor interaction. This model features a quantum phase transition from the trivial phase to the topological phase ([1], [2]), and can be mapped onto the fermionic Kitaev chain via the Jordan-Wigner transformation ([3]) with the characteristic majorana zero mode (or unpaired majorana fermions) in the topological phase ([4]), localized at the ends of the chain. Hence there are two degenerate ground states in the topological regime, which are separated by an energy gap to excitations, whereas the trivial regime has only one ground state. How these characteristics influence the decoherence dynamics of the ground state and the zero energy mode (in the topological regime) is investigated within this thesis. Qubits are affected by dephasing and energy relaxation, as they are not perfectly isolated to the environment, hence a realistic model of a chain of qubits is also affected by this kind of dissipation. We focus on the pure dephasing regime where the qubits are only affected by dephasing, which we can assume for qubits with energy relaxation time much larger than the decoherence time $T_1 >> T_2$ (e.g. Fluxonium qubits with $T_1 \approx 1000\mu s$ and $T_2 \approx 10\mu s$ [5]). We show how the dynamics are influenced by the correlation of the dissipation, for global correlated dissipation via the total spin of the chain and for locally correlated dissipation through each spin of the chain. Moreover, the influence of the chain length on the dynamics is compared for the closed and open chain. At low temperature the spin chain shows protection against decoherence for the two ground states due to its topological properties.
The first chapter of this thesis gives a short overview over the most important concepts and definitions within this thesis, namely the Lindblad equation, topology and dissipation in single and separated qubits. The second chapter is about the properties of isolated spin chains. The third chapter examines the closed spin chain with dissipation, whereas the last chapter is about the open spin chain with dissipation.

German Summary

Diese Arbeit untersucht Quanten-Spin-Ketten unter dem Einfluss der Umgebung. Im Modell der Quanten-Spin-Kette sind die Spins mit ihrem nächsten Nachbarn senkrecht zu einem transversalen Feld gekoppelt, welches beispielsweise eine Kette von Qubits mit Wechselwirkung zum nächsten Nachbarn darstellt. Das Modell beinhaltet einen Quantenphasenübergang von der trivialen Phase in die topologische Phase ([1], [2]) und kann über die Jordan-Wigner-Transformation auf die fermionische Kitaev-Kette abgebildet werden ([3]), mit den charakteristischen Majorana Moden (oder ungepaarten Majorana Fermionen) in der topologischen Phase ([4]), welche an den Enden der Kette lokalisiert sind. Dabei gibt es in der topologischen Phase zwei entartete Grundzustände, die durch eine Energielücke zu Anregungen getrennt sind, während die triviale Phase nur einen Grundzustand hat. Wie diese Eigenschaften die Dekohärenz des Grundzustandes und der niedrigsten Anregung beeinflussen, wird in dieser Arbeit untersucht.
Im Allgemeinen sind Qubits von Dekohärenz und Energieverlust betroffen, da sie nicht perfekt gegen die Umgebung isoliert sind. Diese Art der Dissipation muss man auch für eine realistisches Modell der Quanten-Spin-Kette annehmen. Wir werden das Regime, bei der die Qubits nur von Dekohärenz betroffen sind, genauer betrachten. Dies ist realistisch für Qubits, deren Energierelaxationszeit T_1 viel größer ist als die Dekohärenzzeit T_2 (z.B. Fluxonium Qubits mit $T_1 \approx 1000\mu s$ und $T_2 \approx 10\mu s$ [5]). Dabei zeigen wir, wie die Korrelation der Dekohärenz/Fluktuationen zwischen den einzelnen Spins die Dynamik der Kette beeinflusst. Zudem wird der Einfluss der Kettenlänge auf die Dynamik der Quanten-Spin-Kette untersucht. Bei niedrigen Temperaturen zeigt die Spin-Kette aufgrund ihrer topologischen Eigenschaften einen Schutz gegen Dekohärenz für die beiden entarteten Grundzustände.
Das erste Kapitel dieser Arbeit gibt einen kurzen Überblick über die wichtigsten Konzepte und Definitionen dieser Arbeit, die Lindblad-Gleichung, Topologie und Dissipation in einzelnen und getrennten Qubits. Das zweite Kapitel befasst sich mit den Eigenschaften isolierter Spin-Ketten. Im dritten Kapitel geht es um den Spin-Ring mit Dissipation und das letzte Kapitel befasst sich mit der offenen Spin-Kette mit Dissipation.

Contents

Chapter 1

Introduction

One of the most outstanding challenges in quantum physics is the understanding of interacting quantum many body systems for implementing the properties of such systems in quantum information and quantum transport. As such quantum systems generally cannot be described by statistical observables, computational approaches for these systems are hard to apply for classical computers. Another approach is using controllable quantum systems to simulate these interacting quantum many body systems ([6]). From the theoretical point of view general models as the quantum XY model or the quantum Ising model were studied as a bench test to unveil the characteristics of quantum many body systems.
The Quantum Ising model with its different variations was already studied 50 years ago (see [7][8][9][10]) as a universal model for many-body systems and quantum magnetism. The model encompasses a quantum phase transition ([1][11]) featuring quantum correlation and entanglement ([12][13]). The model was intensively studied due to its rich physical properties in the vicinity of the quantum criticality, as quenching in a driven chain ([14][15][16]) and the Kibble-Zurek mechanism ([2][17]) showing non-equilibrium dynamics during a sudden change of the Hamiltonians parameters, as well as the Loschmidt echo of a two level system coupled to the Ising chain ([18]) quantifying the sensitivity of quantum evolution to the criticality.
The Ising model can be also characterized by topology, in which different classes of Hamiltonians are characterized by a topological quantum number, revealing the relation between topological properties and a quantum phase transition ([19][20]). By a mapping onto fermionic chains with the Jordan-Wigner transformation ([21]), one can connect the topology with localized end states corresponding to majorana bound modes ([4]) in fermionic chains, which obey non-abelian statistics and thus could be used for fault-tolerant quantum computation ([22]).
Recent progress allows to create artificial quantum chains experimentally, as done with Rydberg atoms ([23]), trapped ions ([24][25]), optical lattices ([26]) and superconducting qubits ([27][28][29]). For such artificial chains it is important to understand the dissipation mechanisms, as these chains cannot be considered as isolated systems. Hence a dissipative model is required to describe these dissipative spin chains.
Numerical methods determined the criticality and phase diagrams of spin chains influenced by single site dissipation along the spin-spin interaction ([30][31][32]), but the dynamics of the ground state influenced by single site dissipation has yet to be unveiled. Since topological states promise robustness against certain classes of dissipation ([33]), there is a relation between topology and dissipative dynamics.

1.1 Lindblad equation

Consider a general system H_s, which is weakly coupled to the environment H_B by H_I, such that the total Hamiltonian can be expressed as

$$H = H_s + H_I + H_B \,. \tag{1.1.1}$$

In the interaction picture the time evolution of the density matrix is described by the von Neumann equation ([34]):

$$\frac{d\rho}{dt} = -i\,[H_I(t), \rho(t)] \;, \tag{1.1.2}$$

which can be represented in the integral form as

$$\rho(t) = \rho(0) - i\int_0^t dt'\,[H_I(t'), \rho(t')] \;. \tag{1.1.3}$$

Inserting eq.1.1.3 into eq.1.1.2 and taking the trace over the bath, as we are only interested in the dynamics of the system and not the bath, leads to

$$\frac{d\rho_s(t)}{dt} = -\int_0^t dt'\,tr_B\,[H_I(t), [H_I(t'), \rho(t')]] \;, \tag{1.1.4}$$

with $\rho_s = tr_B(\rho)$ the density matrix of the system. For simplicity we assumed that $tr_B[H_I(t), \rho(0)] = 0$.
This equation is not closed as the systems density matrix ρ_s still does depend on the density matrix of the whole system ρ. To get a closed equation for ρ_s one can assume weak coupling between the bath and the system. Hence the bath is only negligibly affected by the system, such that $\rho(t) \approx \rho_s(t) \otimes \rho_B$, which is called Born approximation

$$\frac{d\rho_s(t)}{dt} = -\int_0^t dt'\,tr_B\,[H_I(t), [H_I(t'), \rho_s(t') \otimes \rho_B]] \;. \tag{1.1.5}$$

This equation is not local in time, as the result of $\rho_s(t)$ depends on all past times $\rho_s(t')$. We can do two further approximation if the typical time scale of the system τ_s is much larger than the typical time of the bath τ_B (rapidly decaying bath correlation). The first one is that we assume that $\rho_s(t') = \rho_s(t)$, such that the result does only depend on the present state (no memory effects) to get the time local Redfield equation

$$\frac{d\rho_s(t)}{dt} = -\int_0^t dt'\,tr_B\,[H_I(t), [H_I(t'), \rho_s(t) \otimes \rho_B]] \;. \tag{1.1.6}$$

For the second approximation one has to substitute t' with $t - t'$ and change the upper limit of the integral to ∞ to finally arrive at the Markovian quantum master equation

$$\frac{d\rho_s(t)}{dt} = -\int_0^t dt'\,tr_B\,[H_I(t), [H_I(t'), \rho_s(t) \otimes \rho_B]] \;. \tag{1.1.7}$$

Thus the Markovian master equation can only resolve the dynamics of the system larger as the typical time scale of the bath τ_B.
The interaction Hamiltonian between the bath and the system H_I can be expressed as

$$H_I = \sum_\alpha A_\alpha \otimes B_\alpha \,, \tag{1.1.8}$$

where A_α are the operators from the system coupled to the operators $\hat{B}_\alpha$ from the bath. One can express these operators in the spectral decomposition

$$A_\alpha(\omega) = \sum_{\epsilon' - \epsilon = \omega} \Pi(\epsilon) A_\alpha \Pi(\epsilon') \,, \tag{1.1.9}$$

where $\Pi(\epsilon)$ is the projector onto the subspace with energy ϵ.
Hence the time evolution of an operator $A_\alpha(\omega)$ is well defined by

$$A_\alpha(\omega)(t) = e^{-i\omega t} A_\alpha(\omega) \,. \tag{1.1.10}$$

Using the spectral decomposition of the interaction Hamiltonian in the Markovian quantum master equation leads to

$$\frac{d\rho_s(t)}{dt} = \sum_{\omega,\omega'} \sum_{\alpha,\beta} e^{i(\omega'-\omega)t} \Gamma_{\alpha\beta}(\omega) \left(A_\beta(\omega)\rho_s(t) A_\alpha^\dagger(\omega') - A_\alpha^\dagger(\omega') A_\beta(\omega) \rho_s(t) \right) + h.c. \,, \tag{1.1.11}$$

with $A_\alpha(\omega)^\dagger = A_\alpha(-\omega)$ and the half Fourier transform of the bath correlator

$$\Gamma_{\alpha\beta}(\omega) = \int_0^\infty dt' e^{i\omega t'} tr_B \left(B_\alpha^\dagger(t) B_\beta(t-t') \rho_B \right) \,. \tag{1.1.12}$$

The fast oscillating terms in eq.1.1.11, for which $\omega \neq \omega'$, can be neglected in the Rotating Wave Approximation (RWA) as they average out on larger time scale

$$\frac{d\rho_s(t)}{dt} = \sum_{\omega} \sum_{\alpha,\beta} \Gamma_{\alpha\beta}(\omega) \left(A_\beta(\omega)\rho_s(t) A_\alpha^\dagger(\omega') - A_\alpha^\dagger(\omega') A_\beta(\omega) \rho_s(t) \right) + h.c. \,. \tag{1.1.13}$$

By defining the real and imaginary part of Γ

$$\kappa_{\alpha\beta}(\omega) = \Gamma_{\alpha\beta}(\omega) + \Gamma_{\alpha\beta}^*(\omega) = \int_{-\infty}^\infty dt' e^{i\omega t'} tr_B \left(B_\alpha^\dagger(t') B_\beta(0) \rho_B \right) \tag{1.1.14}$$

$$S_{\alpha\beta}(\omega) = \frac{1}{2i} \left(\Gamma_{\alpha\beta}(\omega) - \Gamma_{\alpha\beta}^*(\omega) \right) \,, \tag{1.1.15}$$

one arrives finally at the Lindblad equation

$$\begin{aligned} \frac{d\rho_s(t)}{dt} = \sum_{\omega} \sum_{\alpha,\beta} \Bigg(& - i S_{\alpha\beta}(\omega) \left[A_\alpha^\dagger(\omega) A_\beta(\omega), \rho_s(t) \right] \\ & + \kappa_{\alpha\beta}(\omega) \left(A_\beta(\omega) \rho_s(t) A_\alpha^\dagger(\omega) - \frac{1}{2} \left\{ A_\alpha^\dagger(\omega) A_\beta(\omega), \rho_s(t) \right\} \right) \Bigg) \,, \end{aligned} \tag{1.1.16}$$

whereas the first (imaginary) part is the Lamb shift, which only yields a renormalization of the energy levels of the system due to the interaction with the bath. The second part describes the dissipative dynamics of the system.

1.2 Dissipation in a single spin

Consider a single qubit with frequency ω_q, the Hamiltonian can be expressed with the Pauli matrix σ_z

$$H_q = \frac{\omega_q}{2}\sigma_z \,. \tag{1.2.1}$$

The qubit has the two eigenstates $|e\rangle$ and $|g\rangle$, the excited state and the ground state respectively. Such that σ_z is

$$\sigma_z = |e\rangle\langle e| - |g\rangle\langle g| \,. \tag{1.2.2}$$

Any arbitrary state or every change of the qubit can be expressed with a linear combination of the Pauli matrices $\sigma_x = |e\rangle\langle g| + |g\rangle\langle e|$, $\sigma_y = -i\,|e\rangle\langle g| + i\,|g\rangle\langle e|$ and σ_z with the relation

$$\sigma_i\sigma_j = \delta_{ij}\mathbb{1} - i\sum_{k=1}^{3}\epsilon_{ijk}\sigma_k \,, \tag{1.2.3}$$

where ϵ_{ijk} is the Levi-Civita symbol and $\sigma_1 = \sigma_x$, $\sigma_2 = \sigma_y$ and $\sigma_3 = \sigma_z$.
Thus it is sufficient to use a linear combination of Pauli matrices to describe every possible coupling of a qubit with the environment. The coupling Hamiltonian reads as

$$H_I = \sum_i \sigma_i \hat{B}_i \,, \tag{1.2.4}$$

with the time evolution in the interaction picture

$$H_I(t) = \sigma_z\hat{B}_z(t) + \frac{1}{2}\left(\sigma_+ e^{i\omega_q t} + \sigma_- e^{-i\omega_q t}\right)\hat{B}_x(t) + \frac{i}{2}\left(\sigma_+ e^{i\omega_q t} - \sigma_- e^{-i\omega_q t}\right)\hat{B}_y(t) \,. \tag{1.2.5}$$

Using the Rotating Wave Approximation yields the Lindblad equation

$$\begin{aligned}\frac{d\rho_s(t)}{dt} = {}& \kappa_0\left(\sigma_z\rho_s\sigma_z - \rho_s\right) + \frac{1}{2}\kappa_{xy}(\omega_q)\left(\sigma_+\rho_s\sigma_- - \frac{1}{2}\left\{\sigma_-\sigma_+, \rho_s\right\}\right) \\ & + \frac{1}{2}\kappa_{xy}(-\omega_q)\left(\sigma_-\rho_s\sigma_+ - \frac{1}{2}\left\{\sigma_+\sigma_-, \rho_s\right\}\right) \,,\end{aligned} \tag{1.2.6}$$

with $\kappa_\alpha(\omega) = \int_{-\infty}^{\infty} dt' e^{i\omega t'} tr_B\left(B_\alpha^\dagger(t')B_\alpha(0)\rho_B\right)$, $2\kappa_{xy}(\omega) = \kappa_x(\omega) + \kappa_y(\omega)$ and $\kappa_0 = \lim_{\omega\to 0}\kappa_z(\omega)$.
Thus the energy relaxation $\langle\sigma_z\rangle(t)$ is described by

$$\frac{d\langle\sigma_z\rangle}{dt} = \left(\kappa_{xy}(\omega_q) + \kappa_{xy}(-\omega_q)\right)\left(\langle\sigma_z\rangle(t) - \langle\sigma_z\rangle_{eq}\right) \,, \tag{1.2.7}$$

with $\langle\sigma_z\rangle_{eq} = \frac{\kappa_{xy}(-\omega_q)-\kappa_{xy}(\omega_q)}{\kappa_{xy}(\omega_q)+\kappa_{xy}(-\omega_q)}$, such that the energy relaxation rate T_1 is

$$T_1 = \frac{1}{\kappa_{xy}(\omega_q) + \kappa_{xy}(-\omega_q)} \,. \tag{1.2.8}$$

The dephasing dynamics can be described by $\langle\sigma_x\rangle(t)$

$$\frac{\langle\sigma_x\rangle(t)}{dt} = -\left(\frac{1}{2T_1} + 2\kappa_0\right)\langle\sigma_x\rangle(t)\,. \tag{1.2.9}$$

Hence the decoherence time T_2 is defined as

$$\frac{1}{T_2} = \frac{1}{2T_1} + 2\kappa_0 = \frac{1}{2T_1} + \frac{1}{T_\phi}\,, \tag{1.2.10}$$

with $T_\phi = \frac{1}{2\kappa_0}$ the pure dephasing time.
Hence in the limit of $T_2 << T_1$ the σ_z-coupling to the bath is the dominant coupling to the environment. In experiments the energy relaxation time of qubits is in most cases larger as the dephasing time $T_1 > T_2$ (e.g. [5] and [35]), such that the pure dephasing (due to σ_z coupling) of the qubit always plays an important role. In certain qubit architectures there is even the case that $T_2 << T_1$, e.g. for flux and fluxonium qubits (see [5] and [36]), such that in the pure dephasing regime (in the regime of $t \sim T_2$) the $\sigma_{x,y}$-coupling to the bath can be neglected, as the energy relaxation gets only important for times, which are magnitudes larger as the dephasing time.

1.3 Pure dephasing rate

The case of a qubit affected by pure dephasing can be determined exactly ([34])

$$H = \frac{\omega_q}{2}\sigma_z + \sigma_z \sum_k g_k\left(\hat{b}_k + \hat{b}_k^\dagger\right) + \sum_k \omega_k \hat{b}_k^\dagger \hat{b}_k \tag{1.3.1}$$

where we assumed a bosonic bath as environment.
Hence the time ordered evolution operator in the interaction picture is

$$U(t) = \mathcal{T}\exp\left(-i\int_0^t dt' \sum_k g_k\left(\hat{b}_k e^{-i\omega_k t'} + \hat{b}_k^\dagger e^{i\omega_k t'}\right)\right)\,. \tag{1.3.2}$$

As the commutator of the interaction term is

$$[H_I(t), H_I(t')] = -2i\sum_k g_k^2 \sin\left(\omega_k(t-t')\right)\,, \tag{1.3.3}$$

the time ordered expression simplifies to

$$\begin{aligned} U(t) &= \exp\left(-\frac{1}{2}\int_0^t dt' \int_0^t dt''[H_I(t'), H_I(t'')]\theta(t'-t'')\right)\exp\left(-i\int_0^t dt' H_I(t')\right) \\ &= \exp\left(i\int_0^t dt' \int_0^t dt'' \sum_k g_k^2 \sin\left(\omega_k(t'-t'')\right)\theta(t'-t'')\right)\hat{V}(t)\,, \end{aligned} \tag{1.3.4}$$

where the first term leads to a time dependent phase factor in the time evolution (no operators appear here), and the operator $\hat{V}(t)$ which determines the evolution of our system

$$\hat{V}(t) = \exp\left(\frac{\sigma_z}{2}\sum_k\left(\alpha_k(t)\hat{b}_k^\dagger - \alpha_k^*(t)\hat{b}_k\right)\right)\,, \tag{1.3.5}$$

with

$$\alpha_k = 2g_k \frac{1 - e^{i\omega_k t}}{\omega_k} \,. \tag{1.3.6}$$

Thus the density matrix elements of the system can be determined by

$$\langle m| \rho_s(t) |\tilde{m}\rangle = \langle m| tr_B \left(\hat{V}(t) \rho_s(0) \hat{V}^{-1}(t) \right) |\tilde{m}\rangle \tag{1.3.7}$$

with $m, \tilde{m} = 0, 1$ for the two possible states in the qubit.
Inserting eq.1.3.5 into eq.1.3.7 we have

$$\begin{aligned} \langle 0| \rho_s(t) |0\rangle &= \langle 0| \rho_s(0) |0\rangle \\ \langle 1| \rho_s(t) |1\rangle &= \langle 1| \rho_s(0) |1\rangle \\ \langle 1| \rho_s(t) |0\rangle &= \langle 0| \rho_s(t) |1\rangle^* = e^{-\Gamma_0(t)} \langle 1| \rho_s(0) |0\rangle \,, \end{aligned} \tag{1.3.8}$$

with the dephasing rate $\Gamma_0(t)$

$$\begin{aligned} \Gamma_0(t) &= \sum_k \ln tr_B \left(\exp \left[\alpha_k(t) \hat{b}_k^\dagger - \alpha_k^*(t) \hat{b}_k \right] \right) = -\frac{1}{2} \sum_k |\alpha_k|^2 \left\langle \left\{ \hat{b}_k, \hat{b}_k^\dagger \right\} \right\rangle_B \\ &= -\sum_k \frac{4g_k^2}{\omega_k^2} \coth \left(\frac{\omega_k}{2k_B T} \right) (1 - \cos(\omega_k t)) \,. \end{aligned} \tag{1.3.9}$$

In the continuum limit of our bath modes we have

$$\Gamma_0(t) = \int_0^\infty d\omega K(\omega) \coth \left(\frac{\omega}{2k_B T} \right) \frac{1 - \cos(\omega t)}{\omega^2} \tag{1.3.10}$$

with $K(\omega)$ the spectral density, which we assume to be ohmic with a cutoff frequency Ω

$$K(\omega) = \eta \omega e^{-\omega/\Omega} \,, \tag{1.3.11}$$

where η determines the coupling strength to the environment.
Hence the dephasing rate can be determined to (see appendix A)

$$\Gamma_0(t) = \frac{\eta}{2} \ln(1 + \Omega^2 t^2) + \eta \ln \left(\frac{\sinh(\pi k_B T t)}{\pi k_B T t} \right) \,. \tag{1.3.12}$$

For short times the decoherence function $\Gamma_0(t)$ does depend on the cutoff frequency Ω, whereas in the Markovian regime with $\pi k_B T t >> 1$ we have

$$\Gamma_0(t) \approx \eta \pi k_B T t = \frac{t}{T_\phi} \tag{1.3.13}$$

leading to an exponential decay of the coherence with the rate $\frac{1}{T_\phi} = \eta \pi k_B T$.

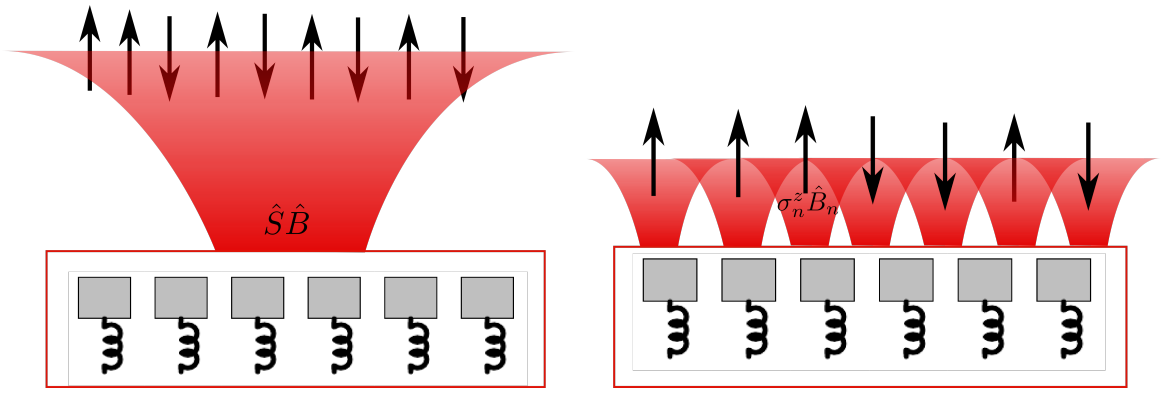

(a) global correlated bath (b) local correlated bath

Figure 1.1: Schematic picture of the two different correlations of the bath (represented by the oscillators). In a global correlated bath the interaction to the environment is via the total spin $\hat{S} = \sum_n \sigma_n^z$ and for local correlated bath via the single spin independently.

1.4 Dissipation in a set of N non-interacting spins

The case of non-interacting qubits affected by pure dephasing gives already insight how dissipation scales with the size of the system. Consider N qubits affected by pure dephasing

$$H = \frac{\omega_q}{2} \sum_{n=1}^{N} \sigma_n^z + \sum_{n=1}^{N} \sum_k \sigma_n^z \hat{B}_n \,. \tag{1.4.1}$$

The Lindblad takes the form

$$\frac{d\rho_s}{dt} = \sum_{n_1,n_2} \kappa_{n_1,n_2} \left(\sigma_{n_2}^z \rho_s \sigma_{n_1}^z - \frac{1}{2} \{ \sigma_{n_1}^z \sigma_{n_2}^z, \rho_s \} \right) , \tag{1.4.2}$$

with $\kappa_{n_1,n_2} = \lim_{\omega \to 0} \int_{-\infty}^{\infty} dt' e^{i\omega t'} tr_B \left(B_{n_1}^\dagger(t') B_{n_2}(0) \rho_B \right)$.
In general κ_{n_1,n_2} can be an arbitrary function of the correlation length (distance of n_1 to n_2). Assuming a global correlation, such that $\kappa_{n_1,n_2} = \kappa = 1/(2T_\phi)$ (with T_ϕ the dephasing rate of a single qubit) is independent on the spin sites (correlation length of the bath is much larger as the length of the chain) leads to

$$\frac{d\rho_s}{dt} = \frac{1}{2T_\phi} \sum_{n_1,n_2} \left(\sigma_{n_2}^z \rho_s \sigma_{n_1}^z - \frac{1}{2} \{ \sigma_{n_1}^z \sigma_{n_2}^z, \rho_s \} \right) . \tag{1.4.3}$$

For an arbitrary state $|\{m_j\}\rangle = \prod_j |m\rangle_j$, where $|m\rangle_j$ describes the state of the j-th qubit we have

$$\frac{d \langle \{m_j\} | \rho_s | \{\tilde{m}_j\} \rangle}{dt} = -\frac{1}{T_\phi} \left(\sum_j m_j - \sum_j \tilde{m}_j \right)^2 \langle \{m_j\} | \rho_s | \{\tilde{m}_j\} \rangle \,. \tag{1.4.4}$$

The dephasing rate scales quadratically with the differences of excited qubits of the two arbitrary states, such that there is a decoherence free subspace for states with the same number of excited qubits. The maximum dephasing rate is N^2 times the rate of the single qubit.

For local correlation of the dissipation we have $\kappa_{n_1,n_2} = \kappa\delta_{n_1,n_2}$. In this case the Lindblad reads as

$$\frac{d\rho_s}{dt} = \frac{1}{2T_\phi}\sum_n \left(\sigma_n^z \rho_s \sigma_n^z - \rho_s\right) , \tag{1.4.5}$$

hence for states $|\{m_j\}\rangle$, where m_j describes the state of the jth qubit, we have

$$\frac{d\left\langle\{m_j\}\right| \rho_s \left|\{\tilde{m}_j\}\right\rangle}{dt} = -\frac{1}{T_\phi}\sum_j |m_j - \tilde{m}_j| \left\langle\{m_j\}\right| \rho_s \left|\{\tilde{m}_j\}\right\rangle . \tag{1.4.6}$$

In this locally correlated bath the dephasing time scales linearly with the difference of each qubit of the two states, such that the decoherence free subspace does not appear anymore in this case and the maximal dephasing rate is N times the rate of the single qubit.
As we can see the correlation of the fluctuations in an ensemble of spins can play a major role in the dissipative dynamics of the whole system.

1.5 Topology

Topology is the study of mathematical objects, which can be classified into different topological classes. Consider for example a sphere, it can be continuously deformed into other objects e.g. a disk, such that these objects belong to the same topological class. As it is not possible to deform a sphere continuously into an object with a hole, they belong to different topologically classes, which is determined by the number of holes in this case. Generally such objects and their respective topological classification by an integer number can be expressed by an integral of local quantities. The Gauss-Bonnet theorem states that the Gaussian curvature K over a surface S defines an integer topological invariant, the Euler characteristic ([37])

$$\xi = \frac{1}{2\pi}\int_S K dS . \tag{1.5.1}$$

Topological invariants can be also used to classify Hamiltonians, which may be e.g.

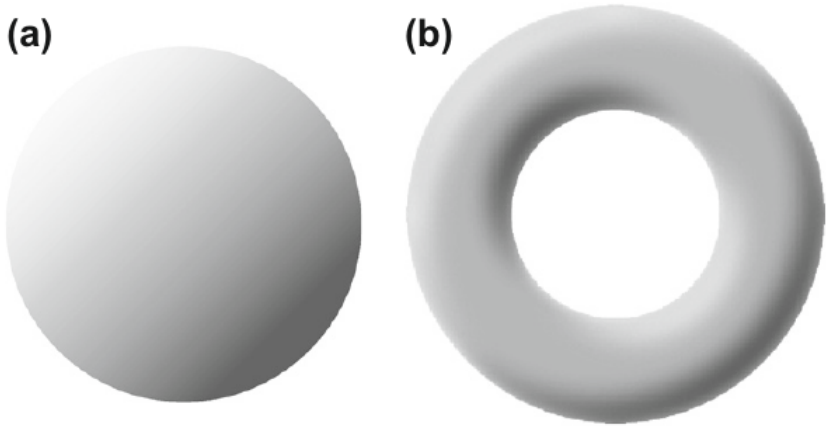

Figure 1.2: (a) Sphere with zero holes and (b) doughnut with one hole, representing two different topological classes from [37].

the ground state degeneracy (dimension) of an Hamiltonian.
Continuous transformation of a quantum system can be interpreted as an adiabatic evolution of an Hamiltonian $H(\vec{R})$ in the parameter space $\vec{R}$. For such adiabatic slow evolutions (in comparison to the energy gaps of the system), the system stays in the slowly changed eigenstate, as the slow evolution does not allow a transition to other eigenstates of the Hamiltonian. However a phase is accumulated during the adiabatic evolution of the state $|\psi_n(t)\rangle$

$$|\psi_n(t)\rangle) = e^{i\theta_n(t)} e^{i\gamma_n(t)} |n(\vec{R(t)})\rangle \ , \tag{1.5.2}$$

with $|n(\vec{R}(t))\rangle$ the eigenstate of the Hamiltonian, the dynamical phase θ_n and the geometrical phase γ_n

$$\theta_n(t) = -\int_0^t E_n(\vec{R}(t'))dt' \tag{1.5.3}$$

$$\gamma_n(t) = i\int_0^t \langle n(\vec{R}(t'))| \frac{d}{dt'} |n(\vec{R}(t'))\rangle \, dt' \, . \tag{1.5.4}$$

For a cyclic evolution, the geometric phase becomes the (gauge-invariant) Berry phase and can be expressed in terms of the cyclic adiabatic evolution $\vec{R}$ (see [38] and [39])

$$\gamma_n(C) = \oint_C A_n(\vec{R})d\vec{R} = \int_S d\vec{S}\vec{F}_n, \, , \tag{1.5.5}$$

whereas A_n is the Berry connection

$$A_n(\vec{R}) = i \langle n(\vec{R}| \frac{d}{d\vec{R}} |n(\vec{R})\rangle \ , \tag{1.5.6}$$

and $\vec{F}_n = \vec{\nabla}_{\vec{R}} \times A_n(\vec{R})$ the Berry curvature. The Berry phase can only take multiple values of 2π and thus it is reasonable to define a topological invariant number, the Chern number C_n, which can take only integer values

$$C_n = \frac{1}{2\pi}\int_S \vec{F}_n d\vec{S} \, , \tag{1.5.7}$$

and can be used to define different topological classes of Hamiltonians. E.g. for the Ising models the Chern number can be used to describe the amount of zero modes ([20]), and thus can be also used to identify the quantum phase transition ([19]), which occurs when the Chern number changes its number.

Chapter 2

Ising chain

The transverse Ising model is a chain of N spins with nearest neighbor interaction with coupling strength J and a transverse field t to each spin in the chain

$$H = -t\sum_{i}^{N}\sigma_i^z - J\sum_{i}^{N-1}\sigma_i^x\sigma_{i+1}^x - J_{N,1}\sigma_N^x\sigma_1^x\,, \tag{2.0.1}$$

One can distinguish two different chains, the closed chain with closed boundary condition ($J_{N,1} = J$), which refer to a ring with N spins and the second case with open boundary conditions ($J_{N,1} = 0$), which refers to a spin chain with two open ends.
This model of the Ising chain can be used for example to describe a chain of N qubits with nearest neighbor interaction. The chain features a quantum phase transition from the topological phase $t < J$ (with two degenerate ground states) to the trivial phase $t > J$. To unveil the transition and the eigenstates of the spin chain, one can transform the spin operators to fermionic operators with the Jordan-Wigner transformation (see [7]).

2.1 Closed Boundary Condition

First consider the spin ring with $J_{N,1} = J$. With the spin-flip operator

$$\sigma_i^{\pm} = \frac{1}{2}\left(\sigma_i^x \pm i\sigma_i^y\right) \tag{2.1.1}$$

the Hamiltonian reads

$$H = -t\sum_{i}^{N}\sigma_i^z - J\sum_{i}^{N-1}\left(\sigma_i^+ + \sigma_i^-\right)\left(\sigma_{i+1}^+ + \sigma_{i+1}^-\right) - J\left(\sigma_N^+ + \sigma_N^-\right)\left(\sigma_1^+ + \sigma_1^-\right). \tag{2.1.2}$$

2.1.1 Jordan-Wigner transformation

One can introduce fermionic operators with the Jordan-Wigner transformation (see [7] or [10])

$$\hat{c}_n^\dagger = \prod_{m=1}^{n-1}\left(e^{i\frac{\pi}{2}(1-\sigma_m^z)}\right)\sigma_n^- = \hat{\nu}_n\sigma_n^- \tag{2.1.3}$$

$$\hat{c}_n = \sigma_n^+\prod_{m=1}^{n-1}\left(e^{-i\frac{\pi}{2}(1-\sigma_m^z)}\right) = \sigma_n^+\hat{\nu}_n^\dagger\,. \tag{2.1.4}$$

These satisfy the fermionic anti commutation relations $\{\hat{c}_m,\hat{c}_n^\dagger\}=\delta_{mn}$, $\{\hat{c}_m,\hat{c}_n\}=0$ and $\{\hat{c}_m^\dagger,\hat{c}_n^\dagger\}=0$.
Since $[\sigma_n^z, \sigma_m^\pm] = 0$ (for $m \neq n$) it follows that

$$\hat{c}_n^\dagger = \prod_{m=1}^{n-1} \left(e^{i\frac{\pi}{2}(1-\sigma_m^z)}\right) \sigma_n^- = \sigma_n^- \prod_{m=1}^{n-1} \left(e^{i\frac{\pi}{2}(1-\sigma_m^z)}\right) = \sigma_n^- \hat{\nu}_n \tag{2.1.5}$$

$$\hat{c}_n = \sigma_n^+ \prod_{m=1}^{n-1} \left(e^{-i\frac{\pi}{2}(1-\sigma_m^z)}\right) = \prod_{m=1}^{n-1} \left(e^{-i\frac{\pi}{2}(1-\sigma_m^z)}\right) \sigma_n^+ = \hat{\nu}_n^\dagger \sigma_n^+. \tag{2.1.6}$$

With $\hat{\nu}_n = \hat{\nu}_n^\dagger$ (see appendix B.1).
The total Hamiltonian in the fermionic picture reads as (full derivation can be seen in the appendix B.2)

$$H = -t \sum_{n=1}^{N} (1 - 2\hat{n}_n) - J \sum_{n=1}^{N-1} \left(\hat{c}_n^\dagger \hat{c}_{n+1} + \hat{c}_{n+1}\hat{c}_n + h.c.\right) - \hat{P}\left(\hat{c}_N^\dagger \hat{c}_1^\dagger + \hat{c}_1 \hat{c}_N + \hat{c}_N^\dagger \hat{c}_1 + \hat{c}_1^\dagger \hat{c}_N\right). \tag{2.1.7}$$

With the parity operator

$$\hat{P} = \prod_{m=1}^{N} (1 - 2\hat{n}_m), \tag{2.1.8}$$

which takes the value $+1$ for an even number of fermionic quasiparticles and -1 for an odd number of fermionic quasiparticles.
The Hamiltonian has nearly the form of a quadratic fermionic Hamiltonian, only the parity operator is not quadratic in the fermionic operators. To get rid of the parity operator one can project the Hamiltonian onto the subspaces of even and odd parity. To do so one can introduce the projector of the parity operator

$$\hat{P}^\pm = \frac{1}{2}\left(\mathbb{1} \pm \prod_{m=1}^{N} e^{i\pi\hat{n}_m}\right) = \frac{1}{2}\left(\mathbb{1} \pm \prod_{m=1}^{N} \sigma_m^z\right) = \frac{1}{2}\left(\mathbb{1} \pm \prod_{m=1}^{N} (1 - 2\hat{n}_m)\right), \tag{2.1.9}$$

such that the Hamiltonian can be expressed as

$$H = \left(\hat{P}^+ + \hat{P}^-\right) H \left(\hat{P}^+ + \hat{P}^-\right) = \hat{P}^+ H \hat{P}^+ + \hat{P}^- H \hat{P}^- = H^+ + H^- \tag{2.1.10}$$

$$H^\pm = H_k^\pm + H_x^\pm. \tag{2.1.11}$$

The term of the transverse field $H_k^\pm$ reads

$$H_k^\pm = \hat{P}^\pm (-t) \sum_{n=1}^{N} (1 - 2\hat{n}_n)\, \hat{P}^\pm, \tag{2.1.12}$$

and the interaction term H_x is transformed to

$$H_x^\pm = \hat{P}^\pm (-J) \left(\sum_{n=1}^{N-1} \left(\left(\hat{c}_n^\dagger \hat{c}_{n+1} + \hat{c}_{n+1}\hat{c}_n + h.c.\right) \mp \left(\hat{c}_N^\dagger \hat{c}_1 + \hat{c}_1 \hat{c}_N + h.c.\right)\right)\right) \hat{P}^\pm. \tag{2.1.13}$$

With the convention that the subspace of even parity H_x^+ must obey the condition $\hat{c}_{N+1} = -\hat{c}_1$ and the subspace of odd parity H_x^- fulfills the condition $\hat{c}_{N+1} = \hat{c}_1$ the full Hamiltonian can be simplified to

$$H^{\pm} = \hat{P}^{\pm}(-J)\sum_{n=1}^{N}\left(\hat{c}_n^{\dagger}\hat{c}_{n+1} + \hat{c}_{n+1}\hat{c}_n + h.c.\right) - t\left(\sum_{n=1}^{N} 1 - 2\hat{n}_n\right)\hat{P}^{\pm}. \tag{2.1.14}$$

2.1.2 Fourier transformation of the even parity subspace

For the even parity subspace (with even number of fermionic quasiparticles) the condition $\hat{c}_{N+1} = -\hat{c}_1$ has to be fulfilled. This condition only allows odd values of k in the Fourier transformation

$$\hat{c}_n = \frac{e^{-i\frac{\pi}{4}}}{\sqrt{N}}\sum_{k^+}\left(e^{i\frac{\pi n k^+}{N}}\hat{c}_{k^+}\right), \tag{2.1.15}$$

where the sum goes over all odd values $k^+ = \pm 1, \pm 3, ..., \pm(N-3), \pm(N-1)$ (N was set to an even number for simplification) to fulfill the condition $\hat{c}_{N+1} = -\hat{c}_1$.
Therefore the first part of the interaction term can be transformed to

$$\sum_{n=1}^{N}\left(\hat{c}_n^{\dagger}\hat{c}_{n+1} + h.c.\right) = \sum_{k^+}\hat{c}_{k^+}^{\dagger}\hat{c}_{k^+} 2\cos\left(\frac{\pi}{N}k^+\right). \tag{2.1.16}$$

And the second term of the interaction reads

$$\sum_{n=1}^{N}\hat{c}_n\hat{c}_{n+1} + h.c. = \sum_{k^+}\sin\left(\frac{\pi}{N}k^+\right)\left(\hat{c}_{k^+}\hat{c}_{-k^+} + \hat{c}_{-k^+}^{\dagger}\hat{c}_{k^+}^{\dagger}\right). \tag{2.1.17}$$

The full derivation can be seen in the appendix B.3.
The term of the transverse field transforms to

$$\sum_{n=1}^{N}\hat{c}_n^{\dagger}\hat{c}_n = \sum_{k^+}\hat{c}_{k^+}^{\dagger}\hat{c}_{k^+}. \tag{2.1.18}$$

Hence the even parity subspace Hamiltonian is

$$H^+ = -tN + \sum_{k^+}\left[\left(2t - 2J\cos\left(\frac{\pi}{N}k^+\right)\right)\hat{c}_{k^+}^{\dagger}\hat{c}_{k^+} - J\sin\left(\frac{\pi}{N}k^+\right)\left(\hat{c}_{k^+}\hat{c}_{-k^+} + \hat{c}_{-k^+}^{\dagger}\hat{c}_{k^+}^{\dagger}\right)\right]. \tag{2.1.19}$$

2.1.3 Fourier transformation of the odd parity subspace

For the odd parity subspace (odd number of quasiparticles) the condition $\hat{c}_N = \hat{c}_1$ has to be fulfilled, thus only even values of k appear in the Fourier transformation

$$\hat{c}_n = \frac{e^{i\frac{\pi}{4}}}{\sqrt{N}}\sum_{k^-}\left(e^{i\frac{\pi n k^-}{N}}\hat{c}_{k^-}\right), \tag{2.1.20}$$

with the even values $k^- = 0, \pm 2, ..., \pm(N-2), \pm N$.
Therefore the terms can be transformed in the same way as for the even subspace

$$\sum_{n=1}^{N} \left(\hat{c}_n^\dagger \hat{c}_{n+1} + h.c.\right) = \sum_{k^-} \hat{c}_{k^-}^\dagger \hat{c}_{k^-} 2\cos\left(\frac{\pi}{N}k^-\right) \tag{2.1.21}$$

$$\sum_{n=1}^{N} \left(\hat{c}_n \hat{c}_{n+1} + h.c.\right) = \sum_{k^-} \sin\left(\frac{\pi}{N}k^-\right)\left(\hat{c}_{k^-}\hat{c}_{-k^-} + \hat{c}_{-k^-}^\dagger \hat{c}_{k^-}^\dagger\right) \tag{2.1.22}$$

$$\sum_{n=1}^{N} \hat{c}_n^\dagger \hat{c}_n = \sum_{k^-} \hat{c}_{k^-}^\dagger \hat{c}_{k^-} \,. \tag{2.1.23}$$

And the odd parity subspace Hamiltonian can be expressed as

$$H^- = -tN + \sum_{k_e} \left[\left(2t - 2J\cos\left(\frac{\pi}{N}k^-\right)\right)\hat{c}_{k^-}^\dagger \hat{c}_{k^-} - J\sin\left(\frac{\pi}{N}k^-\right)\left(\hat{c}_{k^-}\hat{c}_{-k^-} + \hat{c}_{-k^-}^\dagger \hat{c}_{k^-}^\dagger\right)\right]. \tag{2.1.24}$$

Note that the difference between the odd parity Hamiltonian H^- and the even parity Hamiltonian H^+ are only the different k values.

2.1.4 Bogoliubov transformation

In the following the Hamiltonian H is considered for both subspaces, since the Bogoliubov transformation works for both subspaces the same way. For even k the Hamiltonian refers to the odd subspace and for odd k the Hamiltonian refers to the even subspace.
The two subspace Hamiltonians can be simplified with the following expressions:

$$\xi_k = 2\left[t - J\cos\left(\frac{\pi}{N}k\right)\right] \tag{2.1.25}$$

$$\Delta_k = 2J\sin\left(\frac{\pi}{N}k\right) \tag{2.1.26}$$

$$\begin{aligned} H &= -Nt + \sum_k \left(\xi_k \hat{c}_k^\dagger \hat{c}_k + \frac{1}{2}\Delta_k\left(\hat{c}_k \hat{c}_{-k} + \hat{c}_{-k}^\dagger \hat{c}_k^\dagger\right)\right) \\ &= -Nt + \frac{1}{2}\sum_k \xi_k + \frac{1}{2}\sum_k \begin{pmatrix}\hat{c}_k^\dagger & \hat{c}_{-k}\end{pmatrix}\begin{pmatrix}\xi_k & \Delta_k \\ \Delta_k & -\xi_k\end{pmatrix}\begin{pmatrix}\hat{c}_k \\ \hat{c}_{-k}^\dagger\end{pmatrix} \end{aligned} \tag{2.1.27}$$

To diagonalize this Hamiltonian a Bogoliubov transformation, as done in the appendix B.4, is applied with

$$\hat{c}_k = u_k \hat{\gamma}_k + v_k \hat{\gamma}_{-k}^\dagger \tag{2.1.28}$$

$$\hat{c}_{-k}^\dagger = -v_k \hat{\gamma}_k + u_k \hat{\gamma}_{-k}^\dagger \,, \tag{2.1.29}$$

whereas $u_k^2 + v_k^2 = 1$, $u_k^2 = 1/2(1 + \xi_k/E_k)$ and $v_k^2 = 1/2(1 - \xi_k/E_k)$. The diagonalized Hamiltonian with the new quasiparticle operators $\hat{\gamma}_k$ reads

$$H = -Nt + \frac{1}{2}\sum_k (\xi_k - E_k) + \sum_k E_k(\hat{\gamma}_k^\dagger \hat{\gamma}_k) \,, \tag{2.1.30}$$

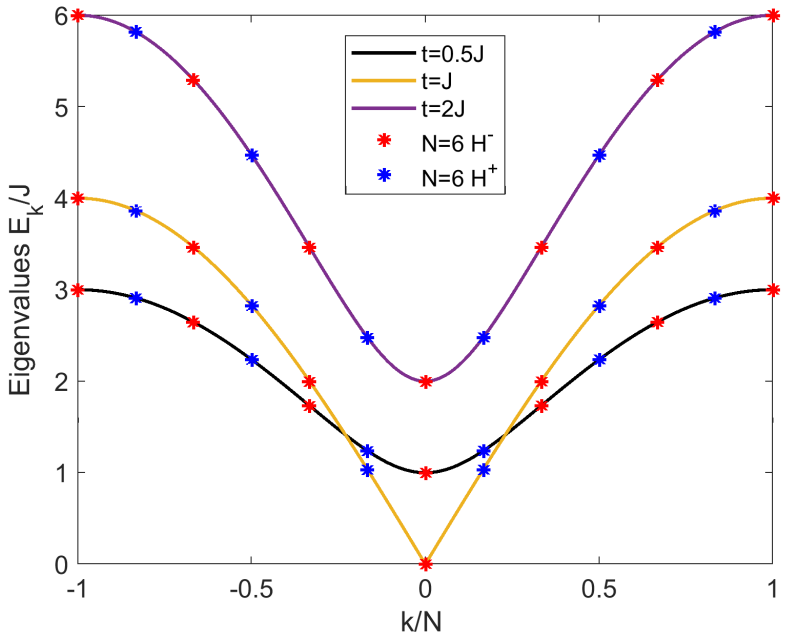

Figure 2.1: Single particle spectrum E_k for different values of t/J with the marked positions for a spin chain of $N = 6$ spins referring to the different parity subspaces. The eigenvalues are degenerate for all states but $k = 0$ and $k = N$.

with the excitation energy of the new quasiparticles $E_k = \sqrt{\xi_k^2 + \Delta_k^2}$.
This result can be used for the odd and even parity subspace Hamiltonians, only that for

$$H^- : k = k^- = 0, \pm 2, ..., \pm(N-2), \pm N \tag{2.1.31}$$
$$H^+ : k = k^+ = \pm 1, \pm 3, ..., \pm(N-1). \tag{2.1.32}$$

Thus the full Hamiltonian of the transverse Ising ring reads as

$$H = \sum_{\sigma=\pm} \left[\hat{P}^\sigma \left(E_0^\sigma + \sum_{k^\sigma} E_k (\hat{\gamma}_k^\dagger \hat{\gamma}_k) \right) \hat{P}^\sigma \right] \tag{2.1.33}$$
$$E_0^\pm = -Nt + \frac{1}{2} \sum_{k^\pm} (\xi_k - E_k) \ . \tag{2.1.34}$$

Therefore the single particle spectrum of even parity (H^+) is different to the spectrum of odd parity (H^-), which is shown in Fig.2.1 and Fig.2.2.

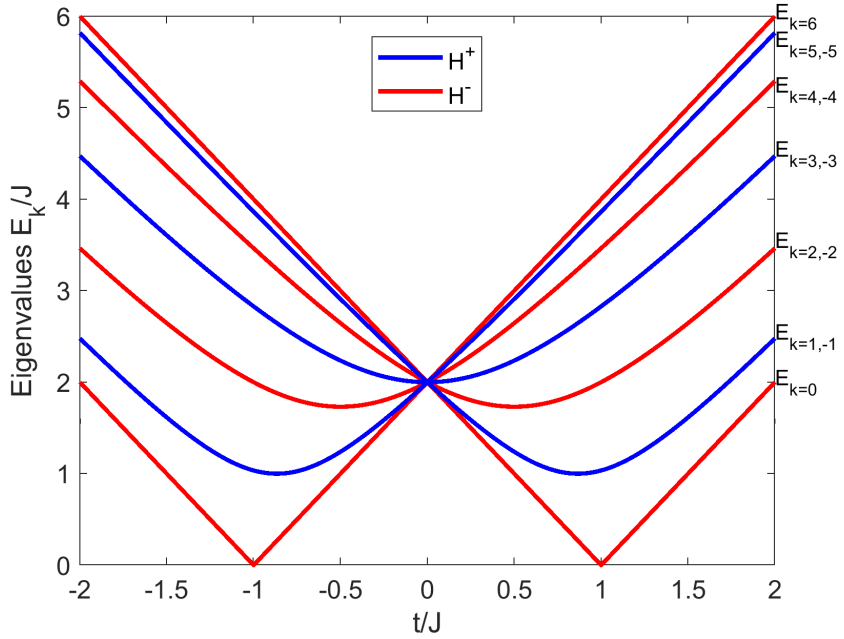

Figure 2.2: Single particle spectrum of the spin chain with closed boundary condition with $N = 6$ spins. These energy levels refers either to the odd or even parity subspace of the System. Note that the energy levels are degenerate as discussed in Fig.2.1. One can see that for an even number of spins the eigenvalues are zero at the critical points $t = J$ and $t = -J$.

2.1.5 Ground state

The ground state is the even parity ground state (for $J > 0$ and $t > 0$) with

$$|GS^+\rangle = \prod_{k^+} \left(u_k + v_k c_k^\dagger c_{-k}^\dagger\right) |\emptyset\rangle \ , \tag{2.1.35}$$

where $|\emptyset\rangle$ is the fermionic vacuum.
Thus only even number of excitations are allowed in the even parity subspace, e.g.

$$\hat{P}^+ \gamma_{k1^+}^\dagger \gamma_{k2^+}^\dagger \hat{P}^+ |GS^+\rangle = |k_1^+, k_2^+\rangle \tag{2.1.36}$$

For the odd parity subspace its more complex, for a clear picture we extract the fermionic state $k = 0$ (which energy can get negative) from the Hamiltonian

$$H^- = -2t + 2(t - J)\hat{c}_0^\dagger \hat{c}_0 - \frac{1}{2}\sum_{k^- \neq 0} E_k + \sum_{k^- \neq 0} E_k \gamma_k^\dagger \gamma_k \, . \tag{2.1.37}$$

One can see that the occupation of the fermionic state $\hat{c}_0^\dagger \hat{c}_0$ has positive energy for $t > J$ and negative energy for $t < J$, but as it has always the lowest energy in comparison to other states, it has to be occupied in the lowest state of the odd parity subspace. Hence the lowest possible state for this subspace can be defined as

$$|GS^-\rangle = \prod_{k^- \neq 0} \left(u_k + v_k c_k^\dagger c_{-k}^\dagger\right) |\emptyset\rangle \otimes \hat{c}_0^\dagger |\emptyset\rangle \tag{2.1.38}$$

$$= |vac_f\rangle \otimes \hat{c}_0^\dagger |\emptyset\rangle \tag{2.1.39}$$

Here we also have the double Bogoliubov excitation

$$\hat{P}^{-}\gamma^{\dagger}_{k1^{-}}\gamma^{\dagger}_{k2^{-}}\hat{P}^{-}\left|GS^{-}\right\rangle \tag{2.1.40}$$

with odd parity. Furthermore, we can also create excitation without $\hat{c}^{\dagger}_{0}\hat{c}_{0}$ occupied e.g.

$$\hat{P}^{-}\gamma^{\dagger}_{k1^{-}}\hat{c}_{k=0}\hat{P}^{-}\left|GS^{-}\right\rangle = \gamma^{\dagger}_{k1^{-}}\Pi_{k^{-}\neq 0}\left(u_k + v_k c^{\dagger}_{k}c^{\dagger}_{-k}\right)\left|\emptyset\right\rangle = \gamma^{\dagger}_{k1^{-}}\left|vac_f\right\rangle \tag{2.1.41}$$

We can see that the false bogoliubov vacuum $\left|vac_f\right\rangle$ of the odd parity subspace does not exist alone but is useful to define in terms of excitations. The energy difference between the lowest state $\left|GS^{-}\right\rangle$ with odd parity and other excitation, where the occupation at $k = 0$ is exchanged, is shown in Fig.2.3.
One can see that in the regime $t < J$ (where the fermionic state $k = 0$ has negative energy), we need extra energy to not occupy the fermionic state $\hat{c}^{\dagger}_{0}\hat{c}_{0}$, hence one can define the Bogoliubov operator as $\gamma^{\dagger}_{0} = \hat{c}_{0}$ (c_0 is a hole excitation). Thus the lowest state $\left|GS^{-}\right\rangle$ has the property

$$\gamma^{\dagger}_{0}\gamma_{0}\left|GS^{-}\right\rangle = \hat{c}_{0}\hat{c}^{\dagger}_{0}\left|GS^{-}\right\rangle = 0 \tag{2.1.42}$$

$$\gamma^{\dagger}_{k_1}\gamma^{\dagger}_{0}\left|GS^{-}\right\rangle = \left|k_1, 0\right\rangle \tag{2.1.43}$$

Thus the state $k = 0$ is not occupied in the Bogoliubov picture.
This is different in the regime $t > J$, here we gain energy by not occuping the fermionic state $\hat{c}^{\dagger}_{0}\hat{c}_{0}$ (and loose by occupying another state as $E_k > E_{k=0}$), hence one can define the Bogoliubov operator as $\gamma_0 = \hat{c}_0$ ($c^{\dagger}_{0}$ is a particle excitation) Thus the lowest state $\left|GS^{-}\right\rangle$ has the property

$$\gamma^{\dagger}_{0}\gamma_{0}\left|GS^{-}\right\rangle = \hat{c}^{\dagger}_{0}\hat{c}_{0}\left|GS^{-}\right\rangle = \left|GS^{-}\right\rangle \tag{2.1.44}$$

$$\gamma^{\dagger}_{k}\gamma^{\dagger}_{0}\left|GS^{-}\right\rangle = 0 \tag{2.1.45}$$

Hence the state $k = 0$ is occupied in the Bogoliubov picture, and we will use the notation of $\left|GS^{-}_{(k=0)}\right\rangle$ for $t > J$ to make clear that $k = 0$ is occupied.

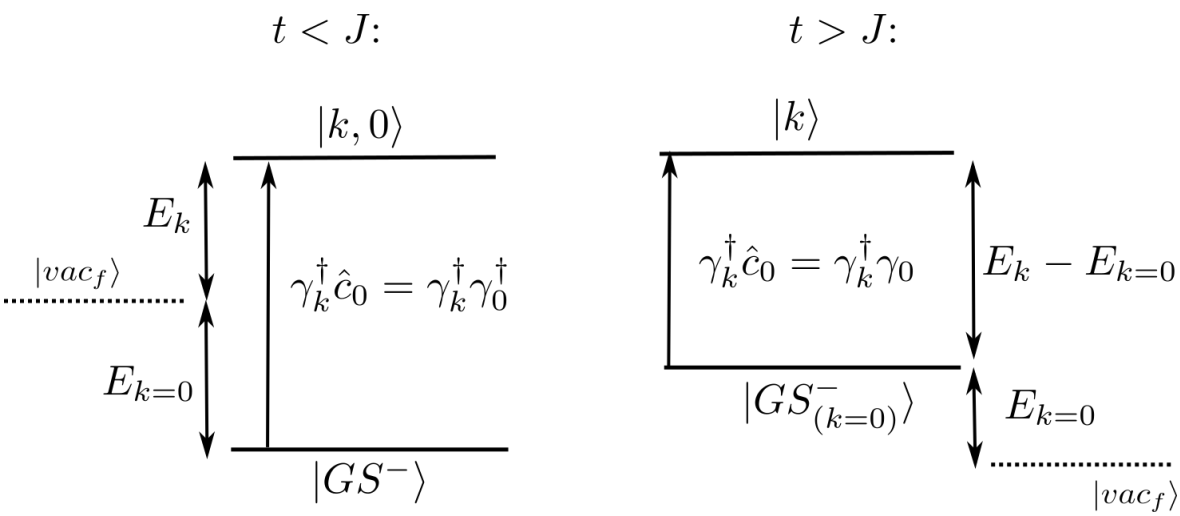

Figure 2.3: The lowest energy state $|GS^-\rangle$ of the odd parity subspace in which we define the false vacuum $|vac_f\rangle$ (no physical state).
In the regime $t < J$ the state $k = 0$ has negative energy thus replacing the occupation at $k = 0$ with another state needs the energy $E_{k=0} + E_k$. In the regime $t > J$ the state $k = 0$ has positive energy thus replacing the occupation at $k = 0$ with another state needs the energy $E_k - E_{k=0}$.

2.1.6 Ground state energy

The ground state energy with even parity can be determined directly from eq.2.1.34

$$E_{GS^+} = -Nt + \frac{1}{2}\sum_{k^+}(\xi_k - E_k) = -\frac{1}{2}\sum_{k^+} E_k \,. \tag{2.1.46}$$

For the odd parity subspace we have

$$\begin{aligned} H^- &= -Nt + \xi_0 \hat{n}_0 + \frac{1}{2}\sum_{k^-\neq 0} \xi_k - E_k + \sum_{k^-\neq 0} E_k \gamma_k^\dagger \gamma_k \\ &= -t + 2(t-J)\hat{n}_0 - \frac{1}{2}\sum_{k^-\neq 0} E_k + \sum_{k^-\neq 0} E_k \gamma_k^\dagger \gamma_k \,. \end{aligned} \tag{2.1.47}$$

Here was used that:

$$\frac{1}{2}\sum_{k^-\neq 0} \xi_k = \sum_{k^-\neq 0} \left(t - J\cos\left(\frac{\pi}{N}k\right)\right) = (N-1)t \,. \tag{2.1.48}$$

The odd parity subspace always needs at least one particle excitation to fulfill the odd parity condition. For $t, J > 0$ the state with the smallest energy is $k = 0$, with negative energy for $t < J$ and positive energy for $t > J$ (with the gap closing at $t = J$).
The state $\hat{n}_0$ occupied corresponds to the lowest odd parity state, hence the energy of the lowest possible state of the two subspaces can be expressed as

$$E_{GS^+} = -\frac{1}{2}\sum_{k^+} E_k \tag{2.1.49}$$

$$E_{GS^-} = t - J - \frac{1}{2}\sum_{k^-\neq 0} E_k \,. \tag{2.1.50}$$

The lowest energy states of even and odd parity and their energy difference are plotted in Fig.2.4 and Fig.2.5, whereas the lowest excitations are plotted in Fig.2.6.

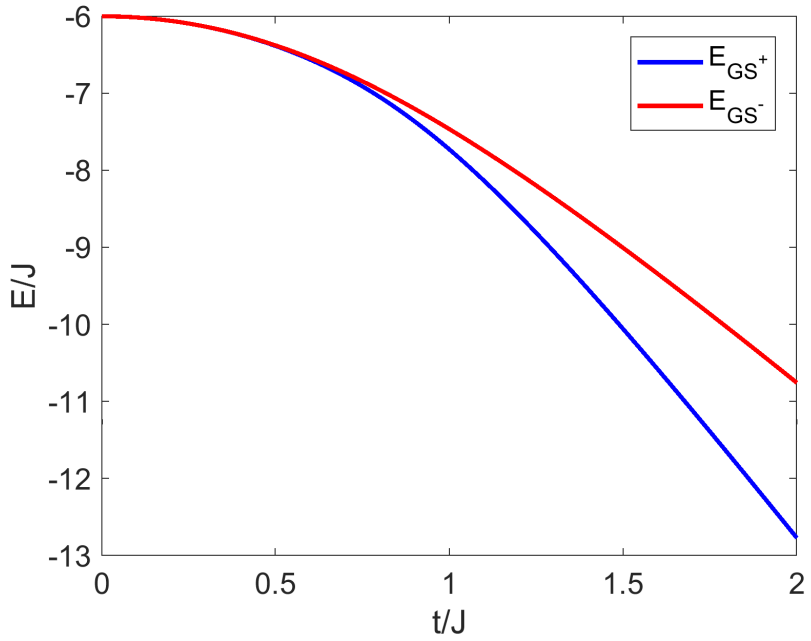

Figure 2.4: Energies of the two lowest states of the two subspaces for $N = 6$. One can see that there is a transition from a single ground state for $t > J$ (with even parity) to two degenerate groundstate for $t < J$ (with different parities).

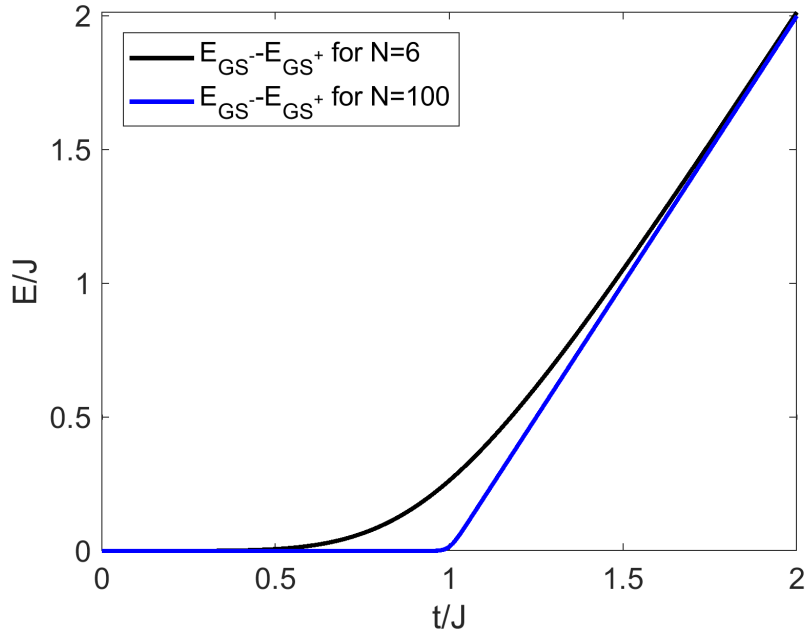

Figure 2.5: Energy difference $E^- - E^+$ of the two lowest states for $N = 6$ and $N = 100$ spins. It can be seen that in the thermodynamic limit $N \to \infty$ there is an direct transition (non analytic point) from a single ground state to two degenerate ground states at the critical point $t = J$.

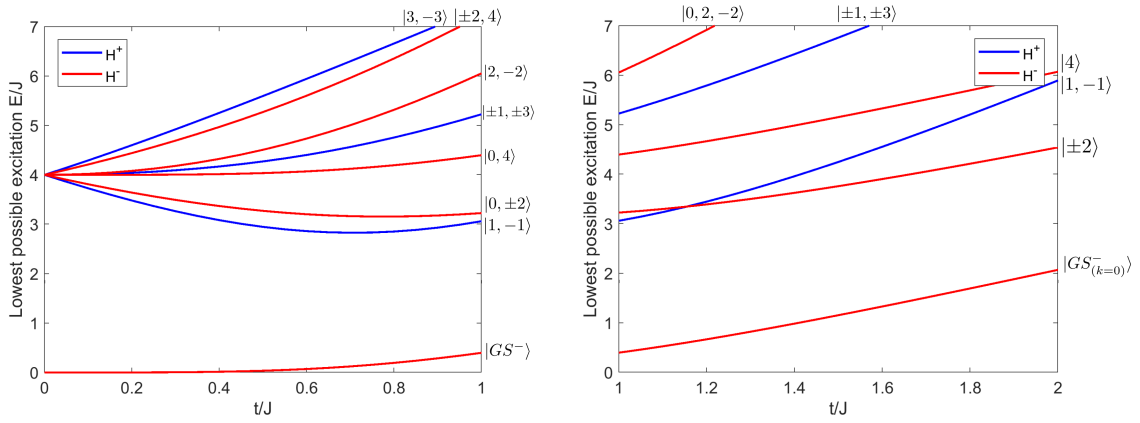

(a) $t < J$ (b) $t > J$

Figure 2.6: Energy of lowest possible excitations in respect to the ground state energy of the even parity subspace for $N = 4$ spins. Note that the excitations plotted here always have well defined parity. Besides the next lowest excitation (starting for $t = 0$ at $8J$) are not plotted here. The states with odd parity change their occupation of $k = 0$ at the critical point (in the Bogoliubov picture), as the hole excitation changes to a particle excitation at this point (see Fig.2.3).

2.1.7 Topology in the closed chain

To unveil the topological properties one can rewrite the Hamiltonian in the pseudo-spin form (see [19])

$$H^+ = 4 \sum_{k>0} \vec{r}(k) \vec{s}_k \tag{2.1.51}$$

$$\vec{r}(k) = (0, J \sin(k\pi/N), J \cos(k\pi/N) - t)\,, \tag{2.1.52}$$

which represents pseudo spins $\{s_k\}$ in a magnetic field $\vec{r}$ with

$$s_k^- = (s_k^+)^\dagger = \hat{c}_k \hat{c}_{-k} \tag{2.1.53}$$

$$s_k^z = \frac{1}{2}\left(\hat{c}_k^\dagger \hat{c}_k + \hat{c}_{-k}^\dagger \hat{c}_{-k} + 1\right)\,. \tag{2.1.54}$$

They satisfy Pauli's algebra with $[s_k^z, s_{k'}^\pm] = \pm\delta_{kk'} s_{k'}^\pm$ and $[s_k^+, s_{k'}^-] = 2\delta_{kk'} s_{k'}^z$.
In the thermodynamic limit the energy density of the ground state reads

$$\epsilon_g = \lim_{N\to\infty} E_g/N = -\frac{1}{2\pi}\int_{-\pi}^{\pi} |\vec{r}(k)| dk\,. \tag{2.1.55}$$

The right hand-side looks already like a topological number, as it traces a loop in the k space (see Fig.2.7), with

$$x(k) = J \sin(k\pi/N)\,, \tag{2.1.56}$$

$$y(k) = J \cos(k\pi/N) - t\,. \tag{2.1.57}$$

One can see that the loop for the transverse Ising model is a circle with radius J and the center shifted by t.
A quantum phase transition now occurs when $\partial\epsilon_g/\partial\lambda$ has a non-analytic point (with

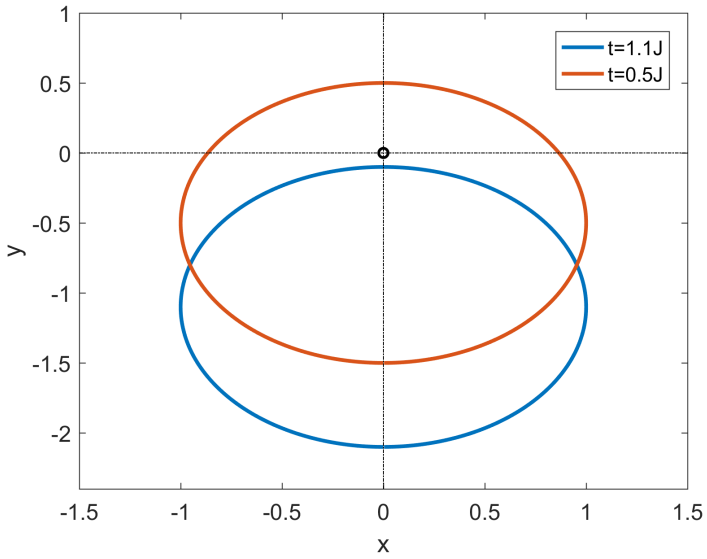

Figure 2.7: The loop described by eq.2.1.56 and eq.2.1.57 represented in the xy-space. The winding number takes the value $g = 1$ if the origin is inside the circle ($t < J$) and the value $g = 0$ if it is outside of the circle ($t > J$), showing that the topology changes at the critical point $t = J$.

$\lambda = J/t$), e.g. the second derivative diverges at this point.
This point can be also determined geometrically by the winding number g in the xy-space (see [19]) by

$$g = \frac{1}{2\pi} \oint_C \frac{1}{r^2}(ydx - xdy)\,, \tag{2.1.58}$$

which determines the number of clockwise rotations around the origin in our loop defined in eq.2.1.55. In our simple model we have a circle with radius J and the center shifted by t. Hence for $t > J$ the circle is shifted from the origin, such that the origin is outside of the circle leading to $g = 0$, thus this regime is referred as the trivial regime. For $J > t$ the origin is within the circle leading to $g = 1$, thus we are in the topological regime (see Fig.2.7).

2.2 Open Boundary condition

For open boundary condition, the chain has two open ends with $J_{N,1} = 0$. The Jordan-Wigner transformation can be used in the same way as for the case of the chain ring. In this case, the term with the parity operator drops out.

2.2.1 Diagonalization

The Ising chain with open boundary condition after the Jordan Wigner transformation takes the following form

$$\begin{aligned} H &= (-J)\sum_{n=1}^{N-1}\left(\hat{c}_n^\dagger \hat{c}_{n+1} + \hat{c}_{n+1}\hat{c}_n + h.c.\right) - t\left(\sum_{n=1}^{N} 1 - 2\hat{n}_n\right) \\ &= \left(\sum_{i,j}\left[t_{ij}\hat{c}_i^\dagger \hat{c}_j + \frac{1}{2}\Delta_{ij}\hat{c}_i^\dagger \hat{c}_j^\dagger + \frac{1}{2}\Delta_{ij}\hat{c}_j\hat{c}_i\right] - Nt\right) . \end{aligned} \tag{2.2.1}$$

With the matrices

$$t_{ij} = \begin{cases} -J & i = j \pm 1 \\ 2t & i = j \\ 0 & \text{else} \end{cases} \tag{2.2.2}$$

$$\Delta_{ij} = \begin{cases} -J & i = j - 1 \\ J & i = j + 1 \\ 0 & \text{else} \end{cases} . \tag{2.2.3}$$

Inserting these matrices into the general equation for the diagonalization of quadratic fermionic Hamiltonians (see appendix B.5) it follows

$$E_k\vec{\psi}_k = 2\underbrace{\begin{pmatrix} t & 0 & 0 & ... & & \\ -J & t & 0 & 0 & ... & \\ 0 & -J & t & 0 & 0 & ... \\ \vdots & \ddots & \ddots & \ddots & \ddots & \ddots \end{pmatrix}}_{A}\vec{\phi}_k \tag{2.2.4}$$

$$E_k\vec{\phi}_k = 2\underbrace{\begin{pmatrix} t & -J & 0 & ... & & \\ 0 & t & -J & 0 & ... & \\ 0 & 0 & t & -J & 0 & ... \\ \vdots & \ddots & \ddots & \ddots & \ddots & \ddots \end{pmatrix}}_{B}\vec{\psi}_k \tag{2.2.5}$$

$$\rightarrow \frac{E_k}{2t}\psi_{n,k} = \phi_{n,k} - \lambda\phi_{n-1,k} \tag{2.2.6}$$

$$\rightarrow \frac{E_k}{2t}\phi_{n,k} = \psi_{n,k} - \lambda\psi_{n+1,k}\,, \tag{2.2.7}$$

as a condition for the transformation for diagonalizing the Hamiltonian with $\phi_{0,k} = 0$ and $\psi_{N+1,k} = 0$.
The diagonal Hamiltonian after the transformation reads

$$H = \sum_k E_k \gamma_k^\dagger \gamma_k + E_{GS}\,, \tag{2.2.8}$$

whereas

$$\gamma_k = \sum_n \left(u_{n,k} \hat{a}_n + v_{n,k} \hat{a}_n^\dagger \right) \tag{2.2.9}$$

$$\phi_{n,k} = u_{n,k} - v_{n,k} \tag{2.2.10}$$

$$\psi_{n,k} = u_{n,k} + v_{n,k}\,. \tag{2.2.11}$$

Since eq.2.2.6 and eq.2.2.7 are symmetric in respect to $n \leftrightarrow N + 1 - n$ one can do the following Ansatz

$$\psi_n \propto \sin(k(N + 1 - n)) \tag{2.2.12}$$

$$\phi_n \propto s_k \sin(kn)\,, \tag{2.2.13}$$

with $s_k = \text{sign}((\sin(k)/\sin(kN))$.
From inserting the Ansatz into eq.2.2.6 and eq.2.2.7 one can derive two conditions for the transformation as done in the appendix B.8

$$\left(\frac{E}{2t}\right)^2 = 1 + \lambda^2 - 2\lambda\cos(k) \tag{2.2.14}$$

$$\frac{\lambda \sin(k)}{1 - \lambda\cos(k)} = -\tan(k(N + 1))\,. \tag{2.2.15}$$

The first equation shows the energy depending on k (same as for the ring chain), and the second equation describes the condition for the possible k values (different in the ring chain). Additionally this equation has also an imaginary solution for specific parameter regime of $\lambda = J/t$ (< 1), which leads to a localized solution of ψ_n and ϕ_n at the ends of the chain.

2.2.2 Localized states

The energy/eigenvalue of the imaginary solution of ϕ_n and ψ_n is

$$E = 2\sqrt{t^2 + J^2 + 2tJ\cos(iq)} = 2\sqrt{t^2 + J^2 + 2tJ\cosh(q)}\,, \tag{2.2.16}$$

and has to fulfill the condition 2.2.15

$$-\tanh((N + 1)q) = \frac{\lambda \sinh(q)}{1 - \lambda\cosh(q)} \tag{2.2.17}$$

$$\lambda e^{-q} = 1 + \lambda \left(e^q - e^{-q}\right) e^{-2q(N+1)} \left(\frac{1}{1 - e^{-2q(N+1)}}\right)\,. \tag{2.2.18}$$

This can be further simplified by an expansion in the limit of $Nq >> 1$. To the lowest order this yields

$$\lambda e^{-q} = 1 \tag{2.2.19}$$
$$q = \ln(\lambda)\,. \tag{2.2.20}$$

Thus the energy in lowest order is

$$E = 2t^2\sqrt{1+\lambda^2-\lambda\left(e^q+e^{-q}\right)} \tag{2.2.21}$$
$$= 2t^2\sqrt{1+\lambda^2-\lambda\left(\lambda+\frac{1}{\lambda}\right)} \tag{2.2.22}$$
$$= 0\,. \tag{2.2.23}$$

Hence the state is degenerate with the ground state within the limit of $Nq >> 1$, which is valid for $t/J << 1$ (when we are not close to the critical point $t = J$).
The first order correction ϵ of e^{-q}

$$e^{-q} = \frac{1}{\lambda} + \epsilon \tag{2.2.24}$$
$$\tag{2.2.25}$$

can be approximated by

$$\epsilon \approx \frac{\lambda^2-1}{\lambda}\left(\frac{1}{\lambda}\right)^{2(N+1)} \tag{2.2.26}$$
$$\rightarrow \left(\frac{E}{2t}\right)^2 \approx \epsilon\lambda(\lambda^2-1) \tag{2.2.27}$$

as derived in the appendix B.9. One can see that the energy correction for the localized state strongly depends on the number of spins N and λ. For an infinite chain length the correction drops out, as the ground state is doubly degenerate with the symmetric and anti-symmetric combination of ψ_n and ϕ_n, see Fig.2.8. If the chain length is finite, the symmetric and anti-symmetric combinations hybridize into the ground state $|GS\rangle$ and the nearly degenerate excitation $|0\rangle = \gamma^\dagger_{k_0}|GS\rangle$, as ϕ_n and ψ_n have a finite overlap. The imaginary solution ϕ_n and ψ_n have the (approximated) form (see appendix B.10) of

$$\psi_n = 2\frac{\sqrt{\lambda^2-1}}{\lambda^{N+1}}\sinh(q(N+1-n)) \approx \sqrt{\lambda^2-1}e^{-qn} \tag{2.2.28}$$
$$\phi_n = 2\frac{\sqrt{\lambda^2-1}}{\lambda^{N+1}}\sinh(qn) \approx \sqrt{\lambda^2-1}e^{-q(N+1-n)}\,, \tag{2.2.29}$$

and are plotted for different t/J and N in Fig.2.8, where you can see the overlap scaling with the number of spins N and the ratio t/J.

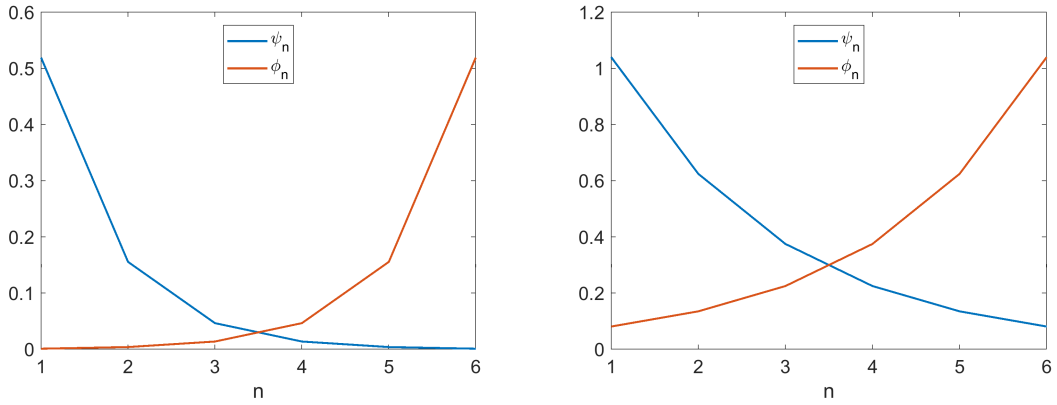

(a) $N = 6$ $t = 0.3J$

(b) $N = 6$ $t = 0.6J$

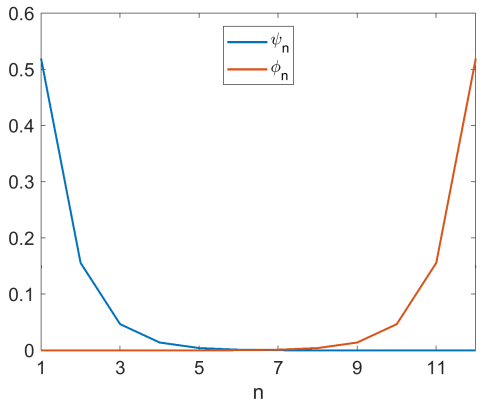

(c) $N = 12$ $t = 0.3J$

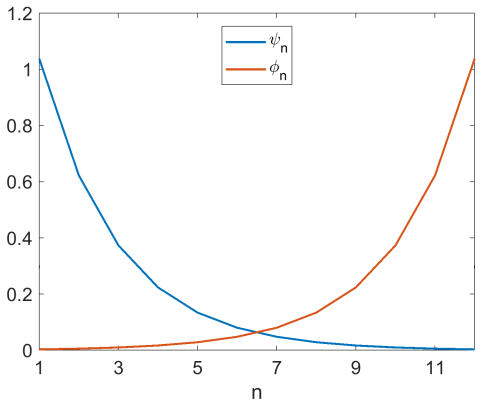

(d) $N = 12$ $t = 0.6J$

Figure 2.8: ϕ_n and ψ_n of the imaginary solution for different number of spins N and different ratio of t/J. As it can be seen the localization depends on the number of spins N and on the ratio t/J. The overlap of ψ_n with ϕ_n is proportional to the energy splitting between the ground state $|GS\rangle$ and the lowest excitation $|0\rangle$.

2.2.3 Ground state energy

The ground state energy E_{GS} in the diagonal Hamiltonian

$$H = \sum_k E_k \gamma_k^\dagger \gamma_k + E_{GS} \tag{2.2.30}$$

can be determined by inserting the transformation

$$\gamma_k = \sum_i \left(u_{ki} \hat{a}_i + v_{ki} \hat{a}_i^\dagger \right) \tag{2.2.31}$$

$$\gamma_k^\dagger = \sum_i \left(u_{ki}^* \hat{a}_i^\dagger + v_{ki}^* \hat{a}_i \right) \tag{2.2.32}$$

into the Hamiltonian

$$\begin{aligned} H &= \sum_k E_k \sum_{i,j} \left(u_{ki}^* \hat{c}_i^\dagger + v_{ki}^* \hat{c}_i \right) \left(u_{kj} \hat{c}_j + v_{kj} \hat{c}_j^\dagger \right) + E_0 \\ &= \sum_k E_k \sum_{i,j} \left(u_{ki}^* u_{kj} \hat{c}_i^\dagger \hat{c}_j + v_{ki}^* v_{kj} \hat{c}_i \hat{c}_j^\dagger + u_{ki}^* v_{kj} \hat{c}_i^\dagger \hat{c}_j^\dagger + v_{ki}^* u_{kj} \hat{c}_i \hat{c}_j \right) + E_0 \\ &= \left(u_{ki}^* u_{kj} \hat{c}_i^\dagger \hat{c}_j + v_{ki}^* v_{kj} (\delta_{ij} - \hat{c}_j^\dagger \hat{c}_i) + u_{ki}^* v_{kj} \hat{c}_i^\dagger \hat{c}_j^\dagger + v_{ki}^* u_{kj} \hat{c}_i \hat{c}_j \right) + E_0 \\ &= \left(u_{ki}^* u_{kj} \hat{c}_i^\dagger \hat{c}_j - v_{ki}^* v_{kj} \hat{c}_j^\dagger \hat{c}_i + u_{ki}^* v_{kj} \hat{c}_i^\dagger \hat{c}_j^\dagger + v_{ki}^* u_{kj} \hat{c}_i \hat{c}_j + v_{ki}^* v_{ki} \right) + E_0 \\ &= \left(\sum_{i,j} \left[t_{ij} \hat{c}_i^\dagger \hat{c}_j + \frac{1}{2} \Delta_{ij} \hat{c}_i^\dagger \hat{c}_j^\dagger + \frac{1}{2} \Delta_{ij} \hat{c}_j \hat{c}_i \right] - Nt \right) . \end{aligned} \tag{2.2.33}$$

By comparing the terms without the fermionic ladder operators the ground state energy can be determined

$$\begin{aligned} -Nt &= E_{GS} + \sum_k \sum_i E_k |v_{ki}|^2 \\ \rightarrow E_{GS} &= -Nt - \sum_k \sum_i E_k |v_{ki}|^2 . \end{aligned} \tag{2.2.34}$$

The ground state energy and the lowest excitation is plotted in Fig.2.9. The whole single particle spectrum in respect to this ground state energy is plotted in Fig.2.10 and Fig.2.11. Note that for the case of the open chain the single particle spectrum directly refers to the lowest excitation (since there are no condition for the parity, as for the closed chain).
As plotted in Fig.2.10 and Fig.2.11 the ground state is (approximately) degenerate to the lowest excitation for $t < J$ (depending on the chain length N and λ), hence it is often referred as the topological regime with two degenerate ground states ([20]) separated by an energy gap to excitations.
In the trivial regime $t > J$ has a single ground state separated by an energy gap to excitations. Thus a quantum phase transition occurs at the critical point $t = J$ (for $N \rightarrow \infty$), where the Chern number changes its value and the zero mode localized at the end of the chain appears ($t < J$).
In the following we use the notation of $\gamma_{k_0}^\dagger |GS\rangle = |0\rangle$ with energy $E_{k_0} = E_0$ the lowest excitation (which becomes degenerate with the ground state in the topological regime) and all higher excitation $\gamma_{k_i}^\dagger |GS\rangle = \gamma_i^\dagger |GS\rangle = |i\rangle$ with energy $E_{k_i} = E_i$ (whereas $i = 1...N-1$ with increasing energy as depicted in Fig.2.10 and Fig.2.11, e.g. the state $|N-1\rangle$ has always the largest energy E_{N-1}).

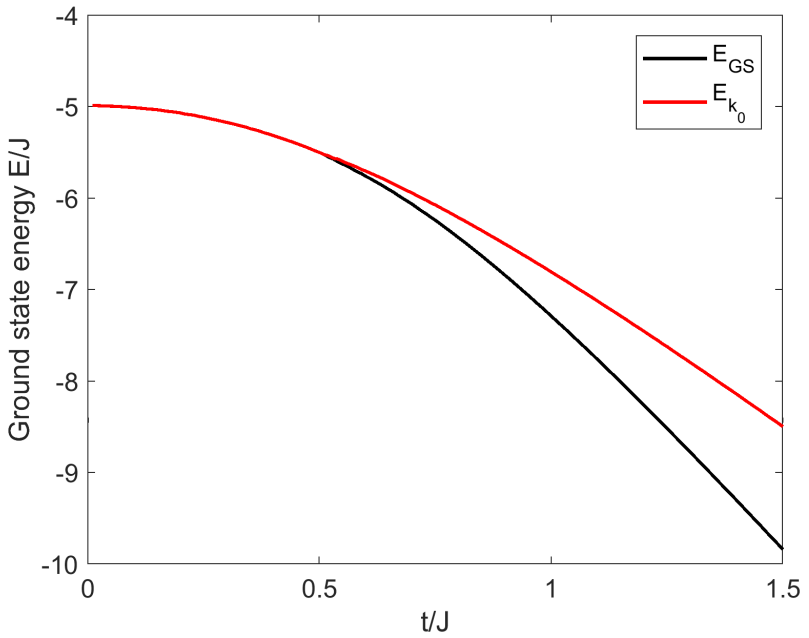

Figure 2.9: Ground state energy of the open Ising chain for $N = 6$ spins. For $t = 0$ the ground state energy starts at $-(N-1)J$, since there are N spins with in total $N-1$ nearest neighbors (due to the loose ends). For $J \ll t$ the ground state energy starts to decrease linearly with t, as the ground state in this regime refers to the case, where all spins are aligned in z-direction.

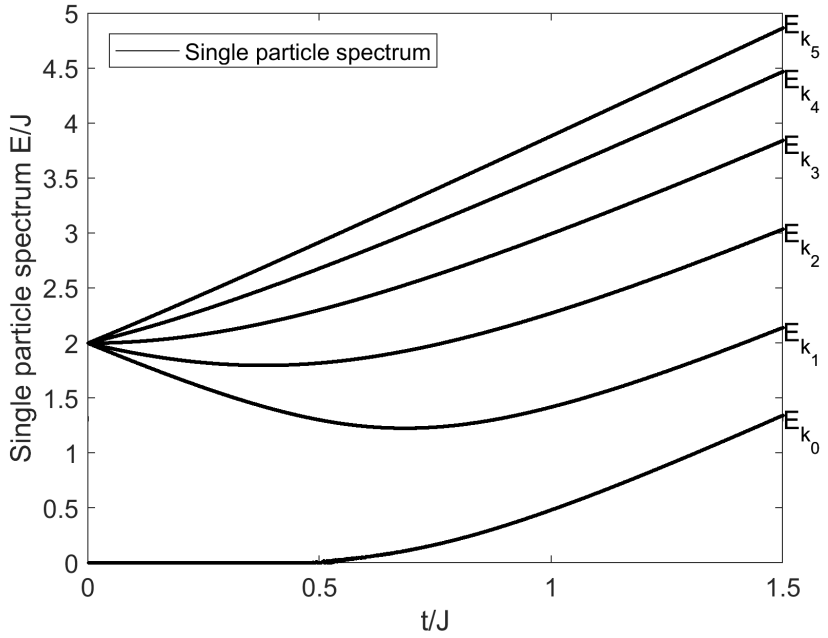

Figure 2.10: Single particle energy spectrum for the open chain with $N = 6$ spins. In a short chain the overlap of the localized modes leads to a larger energy splitting between the ground state $|GS\rangle$ and the lowest excitation $|0\rangle$ in the topological regime (t<J).

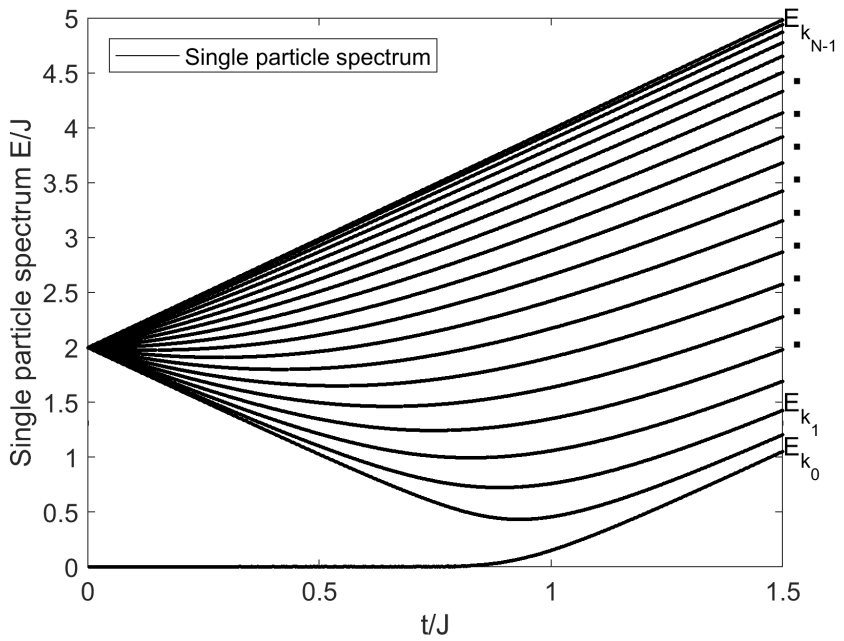

Figure 2.11: Single particle energy spectrum for the open chain with $N = 20$ spins. In a longer chain ground state $|GS\rangle$ and the lowest exciation $|0\rangle$ are (approximately) degenerate in the topological regime, due to the negligible overlap of the localized modes.

Chapter 3

Dissipation in the closed Ising chain

The interaction between the environment H_B and the spins is via the σ_z-direction and relates to the pure dephasing of the single spins, see 1.2. Assuming the dephasing time of the single spin $T_2 \ll T_1$ is much larger than the energy relaxation time (e.g. for flux/fluxonium qubits with $T_1 \approx 1000\mu s$ and $T_2 \approx 10\mu s$ [5] and [36]), the pure σ_z coupling is justified for $t \ll T_1$.

$$H = H_s + H_B + H_{int} \tag{3.0.1}$$

$$H_s = -t\sum_i^N \sigma_i^z - J\sum_i^{N-1} \sigma_i^x\sigma_{i+1}^x - J\sigma_N^x\sigma_1^x \tag{3.0.2}$$

$$H_{int} = \sum_{i=1}^N \sigma_i^z \hat{B}_i \tag{3.0.3}$$

$$\hat{B}_i = \text{operator of the bath} \tag{3.0.4}$$

3.1 Transformation of the interaction for the closed chain

The coupling of the bath to the spin chain has to be transformed into the eigenoperators of the Hamiltonian, hence with the Jordan Wigner transformation we have

$$\sigma_i^z = 1 - 2\hat{n}_i\,. \tag{3.1.1}$$

Thus the total interaction term of the chain to the bath reads

$$H_{int} = \left(P^+ + P^-\right)\sum_{i=1}^N (1-2\hat{n}_i)\,\hat{B}_i\left(P^+ + P^-\right)\,. \tag{3.1.2}$$

As one can see the σ_z coupling to the bath has to preserve the parity in our system. Therefore no transitions from the even to the odd parity subspace are induced by the bath. Hence the interaction Hamiltonian can be transformed for each subspace separately to

$$\hat{n}_n = \begin{cases} \frac{1}{N}\sum\limits_{k_1,k_2=odd} e^{-i\frac{\pi}{N}(k_1-k_2)n}\hat{c}_{k1}^\dagger\hat{c}_{k2} & \text{in } H^+ \\ \frac{1}{N}\sum\limits_{k_1,k_2=even} e^{-i\frac{\pi}{N}(k_1-k_2)n}\hat{c}_{k1}^\dagger\hat{c}_{k2} & \text{in } H^- \end{cases}\,. \tag{3.1.3}$$

With the eigenoperators the coupling term reads as

$$\begin{aligned} H_{int}^{\pm} &= \sum_{n=1}^{N} \frac{1}{N} \left(N - 2 \sum_{k_1,k_2} e^{-i\frac{\pi}{N}(k_1-k_2)n} \left(u_{k1}\gamma_{k1}^{\dagger} + v_{k1}\gamma_{-k1} \right) \left(u_{k2}\gamma_{k2} + v_{k2}\gamma_{-k2}^{\dagger} \right) \right) \hat{B}_n \\ &= \sum_{n=1}^{N} \hat{B}_n - 2 \sum_{n=1}^{N} \frac{1}{N} \sum_{k_1,k_2} e^{-i\frac{\pi}{N}(k_1-k_2)n} \left(u_{k1}u_{k2} - v_{k1}v_{k2} \right) \gamma_{k1}^{\dagger}\gamma_{k2}\hat{B}_n \\ &+ 2 \sum_{n=1}^{N} \frac{1}{N} \sum_{k_1,k_2} u_{k1}v_{k2} \left(e^{-i\frac{\pi}{N}(k_1+k_2)n} \gamma_{k1}^{\dagger}\gamma_{k2}^{\dagger} + h.c. \right) \hat{B}_n \,, \end{aligned} \tag{3.1.4}$$

where k is summed over all odd integer in the even subspace and over all even integer in the odd subspace. In the interaction picture in respect to H_{int} we can write

$$\frac{dA}{dt} = -i[A, H_s] \tag{3.1.5}$$

$$[\gamma_k, H_s] = E_k\gamma_k \tag{3.1.6}$$

$$[\gamma_k^{\dagger}, H_s] = -E_k\gamma_k^{\dagger} \,. \tag{3.1.7}$$

Thus the time dependent interaction reads in total as

$$\begin{aligned} H_{int}^{\pm}(t) &= \sum_{n=1}^{N} \hat{B}_n(t) - \frac{2}{N} \sum_{n=1}^{N} \sum_{k_1,k_2} e^{-i\frac{\pi}{N}(k_1-k_2)n} e^{i(E_{k1}-E_{k2})t} \left(u_{k1}u_{k2} - v_{k1}v_{k2} \right) \gamma_{k1}^{\dagger}\gamma_{k2}\hat{B}_n(t) \\ &+ \frac{2}{N} \sum_{n=1}^{N} \sum_{k_1,k_2} u_{k1}v_{k2} \left(e^{-i\frac{\pi}{N}(k_1+k_2)n} e^{i(E_{k1}+E_{k2})t} \gamma_{k1}^{\dagger}\gamma_{k2}^{\dagger} + h.c. \right) \hat{B}_n(t) \,, \end{aligned} \tag{3.1.8}$$

with odd or even k_1, k_2 in H^+ and H^- respectively. Hereafter we omit the first term of eq.3.1.8 as it simply corresponds to a renormalization of the bath's state.

3.2 Master equation

Starting from the Redfield equation we have

$$\frac{d\rho_s}{dt} = -\int_{t_0}^{t} dt' tr_B[H_{int,I}(t), [H_{int,I}(t'), \rho_s(t) \otimes \rho_B]] \tag{3.2.1}$$

with the bath correlator

$$F_{n_1,n_2}(t - t') = tr_B[B_{n_1}(t)B_{n_2}(t')\rho_B] \,. \tag{3.2.2}$$

Thus the Redfield can be expressed with the projection on the two subspaces

$$\begin{aligned}\frac{d\rho_s}{dt} = &-\int_{t_0}^{t} dt' \sum_{n_1,n_2} \Bigg\{ F_{n_1,n_2}(t-t') \Bigg(\left[\hat{P}^+\sigma^z_{n_1}(t)\hat{P}^+, \hat{P}^+\sigma^z_{n_2}(t')\hat{P}^+\rho_s(t)\right] \\ &+ \left[\hat{P}^-\sigma^z_{n_1}(t)\hat{P}^-, \hat{P}^-\sigma^z_{n_2}(t')\hat{P}^-\rho_s(t)\right] - \hat{P}^+\sigma^z_{n_2}(t')\hat{P}^+\rho_s(t)\hat{P}^-\sigma^z_{n_1}(t)\hat{P}^- \\ &- \hat{P}^-\sigma^z_{n_2}(t')\hat{P}^-\rho_s(t)\hat{P}^+\sigma^z_{n_1}(t)\hat{P}^+ \Bigg) \\ &+ F_{n_2,n_1}(t'-t) \Bigg(\left[\rho_s(t)\hat{P}^+\sigma^z_{n_2}(t')\hat{P}^+, \hat{P}^+\sigma^z_{n_1}(t)\hat{P}^+\right] + \left[\rho_s(t)\hat{P}^-\sigma^z_{n_2}(t')\hat{P}^-, \hat{P}^-\sigma^z_{n_1}(t)\hat{P}^-\right] \\ &- \hat{P}^+\sigma^z_{n_1}(t)\hat{P}^+\rho_s(t)\hat{P}^-\sigma^z_{n_2}(t')\hat{P}^- - \hat{P}^-\sigma^z_{n_1}(t)\hat{P}^-\rho_s(t)\hat{P}^+\sigma^z_{n_2}(t')\hat{P}^+ \Bigg) \Bigg\}, \end{aligned} \tag{3.2.3}$$

such that the Redfield can be splitted up into three parts, the first one which operates only in the even subspace (terms with only $\hat{P}^+$), the second part only in the odd subspace (terms with only $\hat{P}^-$) and the last terms which have projectors of both subspaces. The derivation for the Lindblad superoperator for the first two terms is the same, only the sum over k-values are different.

3.3 Global bath coupling

For a global coupling the interaction is independent of the spin site, as the bath interacts with the total spin of the chain.

$$H_{int} = \left(\sum_i \sigma^z_i\right)\hat{B} = \hat{S}\hat{B} \tag{3.3.1}$$

Thus the bath correlator can be simplified to

$$F_{n_1,n_2}(t-t') = F(t-t') = tr_B[\hat{B}(t)\hat{B}(t')\rho_B]\,. \tag{3.3.2}$$

In the master equation the terms can be simplified (here one part as an example) to

$$\sum_{n_1,n_2} F_{n_1,n_2}(t-t')\sigma^z_{n_1}(t)\sigma^z_{n_2}(t')\rho_s(t) = F(t-t')\left(\sum_{n_1}\sigma^z_{n_1}(t)\right)\left(\sum_{n_2}\sigma^z_{n_2}(t')\right)\rho_s(t)\,. \tag{3.3.3}$$

Thus the equation simplifies as the spin site dependence can be summed out to

$$\begin{aligned}\sum_n \sigma_n^z(t) &= \sum_n \Bigg(1 - \frac{2}{N}\sum_{k_1,k_2} e^{-i\frac{\pi}{N}(k_1-k_2)n} e^{i(E_{k1}-E_{k2})t}\left(u_{k1}u_{k2} - v_{k1}v_{k2}\right)\gamma_{k1}^\dagger\gamma_{k2} \\ &\quad + \frac{2}{N}\sum_{k_1,k_2} u_{k1}v_{k2}\left(e^{-i\frac{\pi}{N}(k_1+k_2)n} e^{i(E_{k1}+E_{k2})t}\gamma_{k1}^\dagger\gamma_{k2}^\dagger + h.c.\right)\Bigg) \\ &= N - 2\sum_{k_1,k_2}\delta_{k_1,k_2} e^{i(E_{k1}-E_{k2})t}\left(u_{k1}u_{k2} - v_{k1}v_{k2}\right)\gamma_{k1}^\dagger\gamma_{k2} \\ &\quad + 2\sum_{k_1,k_2}\delta_{k_1,-k_2} u_{k1}v_{k2}\left(e^{i(E_{k1}+E_{k2})t}\gamma_{k1}^\dagger\gamma_{k2}^\dagger + h.c.\right) \\ &= N - 2\sum_{k_1}\left(u_{k1}^2 - v_{k1}^2\right)\gamma_{k1}^\dagger\gamma_{k1} \\ &\quad + 2\sum_{k_1} u_{k1}v_{-k_1}\left(e^{i2E_{k1}t}\gamma_{k1}^\dagger\gamma_{-k1}^\dagger + h.c.\right). \end{aligned} \tag{3.3.4}$$

Here was used that $1/N\sum_{k1,k2} e^{i\pi/N(k_1-k_2)} = \delta_{k1,k2}$, since k_1 and k_2 are either both even or both odd, such that the difference is always even (see appendix C.1).
Inserting this into the master equation and using the Rotating Wave Approximation (where only slow rotating terms are kept, see 1.1) leads to the following Lindblad super operators (neglecting the Lamb-shift):

$$\begin{aligned}\hat{L}^\pm(\rho_s) &= 4\kappa_0\sum_{k1,k2}\frac{\xi_{k1}\xi_{k2}}{E_{k1}E_{k2}}\left(\hat{P}^\pm\gamma_{k1}^\dagger\gamma_{k1}\hat{P}^\pm\rho_s\hat{P}^\pm\gamma_{k2}^\dagger\gamma_{k2}\hat{P}^\pm - \frac{1}{2}\left\{\hat{P}^\pm\gamma_{k1}^\dagger\gamma_{k1}\gamma_{k2}^\dagger\gamma_{k2}\hat{P}^\pm, \rho_s\right\}\right) \\ &+ \sum_{k1,k2}\delta_{E_{k1},E_{k2}}\kappa(2E_{k1})\frac{\Delta_{k1}\Delta_{k2}}{E_{k1}E_{k2}}\left(\hat{P}^\pm\gamma_{-k1}\gamma_{k1}\hat{P}^\pm\rho_s\hat{P}^\pm\gamma_{k2}^\dagger\gamma_{-k2}^\dagger\hat{P}^\pm - \frac{1}{2}\left\{\hat{P}^\pm\gamma_{k2}^\dagger\gamma_{k2}^\dagger\gamma_{-k1}\gamma_{k1}\hat{P}^\pm, \rho_s\right\}\right) \\ &+ \sum_{k1,k2}\delta_{E_{k1},E_{k2}}\kappa(-2E_{k1})\frac{\Delta_{k1}\Delta_{k2}}{E_{k1}E_{k2}}\left(\hat{P}^\pm\gamma_{k1}^\dagger\gamma_{-k1}\hat{P}^\pm\rho_s\hat{P}^\pm\gamma_{-k2}\gamma_{k2}\hat{P}^\pm - \frac{1}{2}\left\{\hat{P}^\pm\gamma_{-k2}\gamma_{k2}\gamma_{k1}^\dagger\gamma_{-k1}^\dagger\hat{P}^\pm, \rho_s\right\}\right)\end{aligned} \tag{3.3.5}$$

$$\hat{L}^0(\rho_s) = \kappa_0\sum_{k1^+,k2^-}\frac{\xi_{k1}\xi_{k2}}{E_{k1}E_{k2}}\left(\hat{P}^-\gamma_{k2}^\dagger\gamma_{k2}\hat{P}^-\rho_s\hat{P}^+\gamma_{k1}^\dagger\gamma_{k1}\hat{P}^+ + \hat{P}^+\gamma_{k1}^\dagger\gamma_{k1}\hat{P}^+\rho_s\hat{P}^-\gamma_{k2}^\dagger\gamma_{k2}\hat{P}^-\right) \tag{3.3.6}$$

With the respective k-values in each subspace.
The derivation can be seen in the appendix C.2. The function $\kappa(\omega)$ is the Fourier transform of the bath correlator

$$\kappa(\omega) = \int_{-\infty}^{\infty} dt e^{i\omega t}F(t) \tag{3.3.7}$$

$$\kappa_0 = \lim_{\omega\to 0}\int_{-\infty}^{\infty} dt e^{i\omega t}F(t) = \frac{1}{2T_\phi} \tag{3.3.8}$$

With T_ϕ the pure dephasing time of a single spin (see 1.3).
Finally, the full Lindblad master equation takes the form

$$\frac{d\rho_s}{dt} = \hat{L}^+(\rho_s) + \hat{L}^-(\rho_s) + \hat{L}^0(\rho_s). \tag{3.3.9}$$

3.3.1 J=0 limit case

To verify the Lindblad master equation, lets have a look on the case of non interacting spins $J = 0$. With $\Delta_k = 2J\sin(\pi/Nk) = 0$ some of the terms in the Lindblad drop out

$$\begin{aligned}\frac{d\rho_s}{dt} &= \frac{2}{T_\phi}\sum_{k1,k2}\left(\gamma^\dagger_{k1}\gamma_{k1}\rho_s\gamma^\dagger_{k2}\gamma_{k2} - \frac{1}{2}\left\{\gamma^\dagger_{k1}\gamma_{k1}\gamma^\dagger_{k2}\gamma_{k2},\rho_s\right\}\right)\\ &= \frac{2}{T_\phi}\sum_{k1,k2}\left(\hat{n}_{k1}\rho_s\hat{n}_{k2} - \frac{1}{2}\left\{\hat{n}_{k1}\hat{n}_{k2},\rho_s\right\}\right).\end{aligned} \tag{3.3.10}$$

Note that here k_1 and k_2 are summed over all possible integer (of both subspaces) due to the terms from $\hat{L}_0(\rho_s)$.
For a general matrix element $\langle\{m_j\}|\,\rho_s\,|\{\tilde{m}_j\}\rangle$, where m_j is the occupation of the j-th site, we have

$$\begin{aligned}\frac{d\,\langle\{m_j\}|\,\rho_s\,|\tilde{m}_j\}\rangle}{dt} &= \frac{2}{T_\phi}\left(\sum_j m_j\right)\left(\sum_j \tilde{m}_j\right)\langle\{m_j\}|\,\rho_s\,|\tilde{m}_j\}\rangle\\ &\quad - \frac{1}{T_\phi}\left(\sum_j m_j^2 + \sum_j \tilde{m}_j^2\right)\langle\{m_j\}|\,\rho_s\,|\tilde{m}_j\}\rangle\\ &= -\frac{1}{T_\phi}\left(\sum_j m_j - \sum_j \tilde{m}_j\right)^2\langle\{m_j\}|\,\rho_s\,|\tilde{m}\rangle\ .\end{aligned} \tag{3.3.11}$$

Hence every subspace with the same number of fermionic occupation is a decoherence free subspace, whereas the decay of the matrix elements scales quadratically with the difference of the numbers of excitations $\sum_j m_j$ and $\sum_j \tilde{m}_j$.

3.3.2 Decoherence for t<J

For finite J $\delta_{E_{k1},E_{k2}}$ can be fulfilled for $k_1 = -k_2$ and $k_1 = k_2$, due to the degeneracy of the single particle spectrum. With $\Delta_k = -\Delta_{-k}$ the Lindblad operator $\hat{L}^\pm(\rho_s)$ has the form

$$\begin{aligned}\hat{L}^\pm = 4\kappa_0 &\sum_{k1^\pm,k2^\pm}\frac{\xi_{k1}\xi_{k2}}{E_{k1}E_{k2}}\left(\hat{P}^\pm\gamma^\dagger_{k1}\gamma_{k1}\hat{P}^\pm\rho_s\hat{P}^\pm\gamma^\dagger_{k2}\gamma_{k2}\hat{P}^\pm - \frac{1}{2}\left\{\hat{P}^\pm\gamma^\dagger_{k1}\gamma_{k1}\gamma^\dagger_{k2}\gamma_{k2}\hat{P}^\pm,\rho_s\right\}\right)\\ &+ 2\sum_{k1^\pm,k2^\pm}\kappa(2E_{k1})\frac{\Delta^2_{k1}}{E^2_{k1}}\left(\hat{P}^\pm\gamma_{-k1}\gamma_{k1}\hat{P}^\pm\rho_s\hat{P}^\pm\gamma^\dagger_{k1}\gamma^\dagger_{-k1}\hat{P}^\pm - \frac{1}{2}\left\{\hat{P}^\pm\gamma^\dagger_{k1}\gamma^\dagger_{k1}\gamma_{-k1}\gamma_{k1}\hat{P}^\pm,\rho_s\right\}\right)\\ &+ 2\sum_{k1^\pm,k2^\pm}\kappa(-2E_{k1})\frac{\Delta^2_{k1}}{E^2_{k1}}\left(\hat{P}^\pm\gamma^\dagger_{k1}\gamma_{-k1}\hat{P}^\pm\rho_s\hat{P}^\pm\gamma_{-k1}\gamma_{k1}\hat{P}^\pm - \frac{1}{2}\left\{\hat{P}^\pm\gamma_{-k1}\gamma_{k1}\gamma^\dagger_{k1}\gamma^\dagger_{-k1}\hat{P}^\pm,\rho_s\right\}\right).\end{aligned} \tag{3.3.12}$$

Thus the off diagonal element between the ground state $|GS^+\rangle$ (even parity) and the lowest state of the odd parity subspace $|GS^-\rangle$ (nearly degenerate to the ground state for $t < J$, see 2.1.5) can be expressed as

$$\begin{aligned}\frac{d\langle GS^+|\rho_s|GS^-\rangle}{dt} &= -\sum_{k1^+}\frac{\Delta_{k1}^2}{E_{k1}^2}\kappa(-2E_{k1})\langle GS^+|\gamma_{-k1}\gamma_{k1}\gamma_{k1}^\dagger\gamma_{-k1}^\dagger\rho_s|GS^-\rangle \\ &\quad -\sum_{k1^-}\frac{\Delta_{k1}^2}{E_{k1}^2}\kappa(-2E_{k1})\langle GS^+|\rho_s\gamma_{-k1}\gamma_{k1}\gamma_{k1}^\dagger\gamma_{-k1}^\dagger|GS^-\rangle \\ &= -\left(\sum_{k1^+}\frac{\Delta_{k1}^2}{E_{k1}^2}\kappa(-2E_{k1})+\sum_{k1^-}\frac{\Delta_{k1}^2}{E_{k1}^2}\kappa(-2E_{k1})\right)\langle GS^+|\rho_s|GS^-\rangle \\ &= -\Gamma_\pm\langle GS^+|\rho_s|GS^-\rangle\ . \end{aligned} \tag{3.3.13}$$

Hence the coherence between the two lowest states decays exponentially with the rate $\Gamma_\pm$ from eq.3.3.13.
With the spectral density $K(\omega)$ of the bath coupling, $\kappa(\omega)$ reads as

$$\kappa(\omega) = \begin{cases} K(\omega)(1+n_B(\omega)) & \text{for } \omega > 0 \\ K(\omega)n_B(-\omega) & \text{for } \omega < 0 \end{cases}. \tag{3.3.14}$$

For the ohmic case we have $K(\omega) = \eta\omega$ (η determines the coupling strength to the environment) and the bosonic distribution n_B

$$n_B(\omega) = \frac{1}{e^{\frac{\omega}{k_BT}}-1}. \tag{3.3.15}$$

For $k_BT << 2E_k$ (for every k), $n_B(E_k)$ can be approximated with e^{-2E_k/k_BT} and leads to an exponentially suppression of the decoherence rate $\Gamma_\pm$ at low temperature depicted in Fig.3.1.
Besides the decoherence rate scales almost linearly with the number of spins N (as the number of possible excitations the ground states can interact scales with N) as shown in Fig.3.2.
The rate does mainly depend on the gap energy (increases with decreasing t/J) between the lowest states and higher excited states, additionally the number of higher excited states (scales with N), the lowest two states can interact with, influences the total decoherence rate $\Gamma_\pm$ in the topological regime.
At higher temperature the influence of the gap energy is reduced as depicted in Fig.3.2.

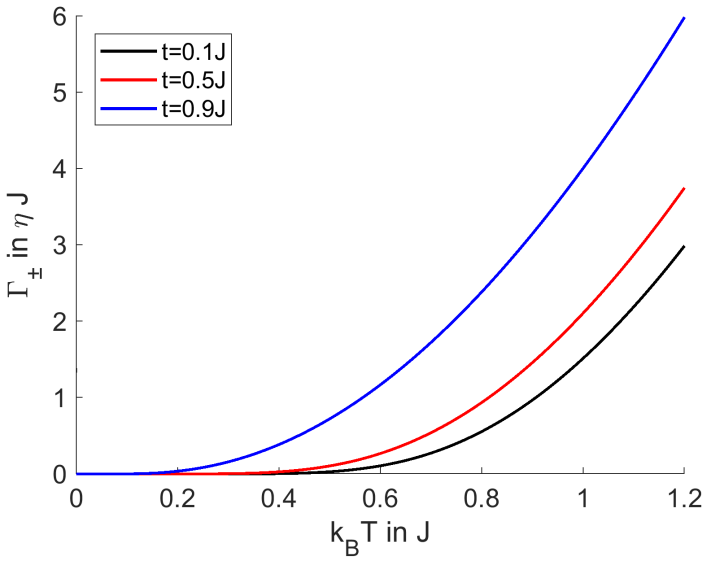

Figure 3.1: $\Gamma_\pm$ (eq.3.3.13) in units of ηJ for $N = 20$ and different ratio of t/J over the temperature $k_B T$.
As the gap energy to excitations is the largest for $t = 0.1J$ and smallest for $t = 0.9J$, the exponentially suppression of the decoherence rate starts for $t = 0.9J$ at lower temperature (at $k_B T \approx 0.6J$) in comparison to $t = 0.1J$ (here at $k_B T \approx J$). When the temperature is larger than the gap energy, there is a linear dependence of the decoherence rate on the temperature.

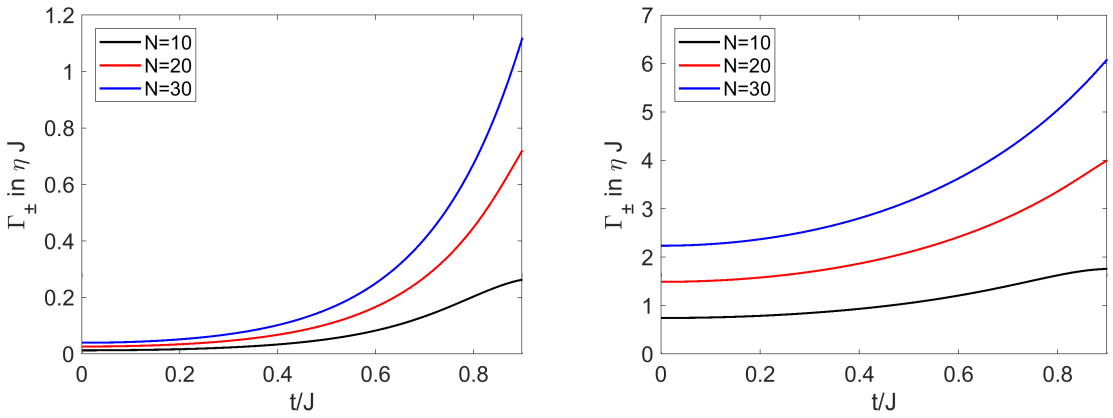

(a) $k_B T = 0.5J$ (b) $k_B T = J$

Figure 3.2: $\Gamma_\pm$ (eq.3.3.13) in units of ηJ for different numbers of spins N and temperature at $k_B T = 0.5J$ over the ratio t/J. The "almost" linear scaling with the number of spins can be seen in the whole parameter regime of $t < J$. The rate increases with decreasing gap energy (increasing t/J). At larger temperature the influence of the energy gap is reduced.

3.3.3 Decoherence for t>J

For this regime the same Lindblad equation as for $t < J$ is valid, but now the lowest energy state of the odd parity subspace $|GS^-\rangle = |GS^-_{(k=0)}\rangle$ corresponds to an excitation in the chain.
The coherence between the two states ($|GS^-_{(k=0)}\rangle$ and $|GS^+\rangle$), which have the energy difference of $E_{k=0}$ in this regime, reads

$$\begin{aligned}\frac{\langle GS^+|\,\rho\,|GS^-_{(k=0)}\rangle}{dt} &= -2\frac{\xi_0^2}{E_0^2}\kappa_0\,\langle GS^+|\,\rho\,|GS^-_{(k=0)}\rangle \\ &\quad - \left(\sum_{k1^+}\frac{\Delta_{k1}^2}{E_{k1}^2}\kappa(-2E_{k1}) + \sum_{k1^-}\frac{\Delta_{k1}^2}{E_{k1}^2}\kappa(-2E_{k1})\right)\langle GS^+|\,\rho\,|GS^-_{(k=0)}\rangle \\ &= -\left(2\kappa_0 + \Gamma_\pm\right)\langle GS^+|\,\rho\,|GS^-_{(k=0)}\rangle\ . \end{aligned} \tag{3.3.16}$$

Here we have additionally to the term $\Gamma_\pm$ (due to interaction with higher excited states) also a contribution of the single spin dephasing rate $2\kappa_0 = 1/T_\phi$.
Hence there will be an increase of $1/T_\phi$ from the topological regime $t < J$ to the trivial regime $t > J$, which is independent on the number of spins.
$\Gamma_\pm$ has the same properties as in the topological regime, as exponential suppression at low temperatures and scaling with the number of spins N, see Fig.3.3 and Fig.3.4.
For large t/J the decoherence rate tends to the case of non-interacting spins, as $\Gamma_\pm$ tends to zero and only the contribution of the single spin dephasing rate remains.

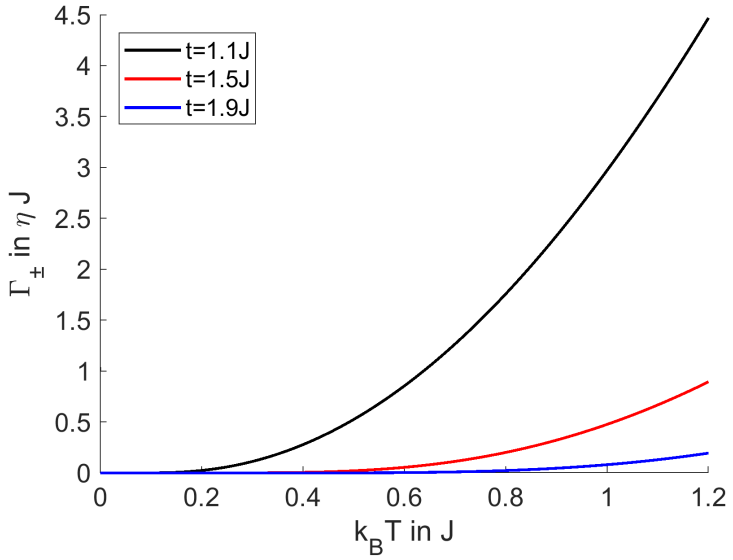

Figure 3.3: $\Gamma_\pm$ (eq.3.3.16) for different ratio t/J over the temperature for $N = 20$ spins. The exponential suppression starts for larger energy gaps (increased t/J) at larger temperature in comparison to smaller t/J with smaller energy gap.

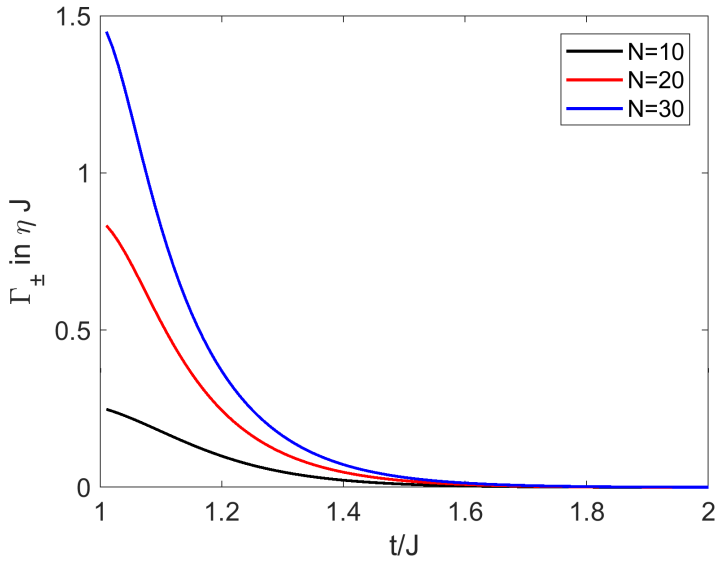

Figure 3.4: $\Gamma_\pm$ (eq.3.3.16) for different numbers of spins N at $k_BT = 0.5J$ over the ratio t/J. For large t/J $\Gamma_\pm$ tends to zero and is increased when the energy gap is small (close to $t = J$).

3.3.4 Energy relaxation

In the topological regime ($t < J$) the relaxation to the two parity ground states

$$\begin{aligned}\frac{d\left\langle GS^{\pm}\right|\rho\left|GS^{\pm}\right\rangle}{dt} &= 2\sum_{k_1^{\pm}}\frac{\Delta_{k1}^2}{E_{k1}^2}\kappa(4E_{k1})\left\langle k_1^{\pm},-k_1\right|^{\pm}\rho\left|k_1^{\pm},-k_1^{\pm}\right\rangle \\ &\quad - 2\sum_{k_1^{\pm}}\frac{\Delta_{k1}^2}{E_{k1}^2}\kappa(-4E_{k1})\left\langle GS^{\pm}\right|\rho\left|GS^{\pm}\right\rangle \end{aligned} \tag{3.3.17}$$

are only connected to specific states $|k^{\pm},-k^{\pm}\rangle$ with the same parity.
And for these excited states, we have

$$\begin{aligned}\frac{d\left\langle k^{\pm},-k^{\pm}\right|\rho\left|k^{\pm},-k^{\pm}\right\rangle}{dt} &= -2\frac{\Delta_k^2}{E_k^2}\kappa(4E_k)\left\langle k^{\pm},-k^{\pm}\right|\rho\left|k^{\pm},-k^{\pm}\right\rangle \\ &\quad + 2\frac{\Delta_k^2}{E_k^2}\kappa(-4E_{k1})\left\langle GS^{\pm}\right|\rho\left|GS^{\pm}\right\rangle \\ &\quad + 2\sum_{k_1^{\pm}\neq k,-k}\frac{\Delta_{k_1}^2}{E_{k_1}^2}\kappa(4E_{k_1})\left\langle k^{\pm},-k^{\pm},k_1^{\pm},-k_1^{\pm}\right|\rho\left|k^{\pm},-k^{\pm},k_1^{\pm},-k_1^{\pm}\right\rangle \\ &\quad - 2\sum_{k_1^{\pm}\neq k,-k}\frac{\Delta_{k_1}^2}{E_{k_1}^2}\kappa(-4E_{k_1})\left\langle k^{\pm},-k^{\pm}\right|\rho\left|k^{\pm},-k^{\pm}\right\rangle\ , \end{aligned} \tag{3.3.18}$$

which are connected to next higher excited states. At low temperature one can do the assumption that only the first excited states and ground state can be occupied, if not initially occupied, thus $\langle k,-k,k_1,-k_1|\,\rho\,|k,-k,k_1,-k_1\rangle \approx 0$ and
$\kappa(-2E_k)\,\langle k,-k,|\,\rho\,|k,-k\rangle \approx 0$ (since $\kappa(-2E_k)$) and $\langle k,-k,|\,\rho\,|k,-k\rangle$ is small at low

temperature, thus the product is negligible). Hence the Lindblad for the first excited state simplifies to

$$\frac{d\left\langle k^{\pm},-k^{\pm}\right|\rho\left|k^{\pm},-k^{\pm}\right\rangle}{dt} = -2\frac{\Delta_k^2}{E_k^2}\kappa(2E_k)\left\langle k^{\pm},-k^{\pm}\right|\rho\left|k^{\pm},-k^{\pm}\right\rangle + 2\frac{\Delta_k^2}{E_k^2}\kappa(-2E_{k1})\left\langle GS^{\pm}\right|\rho\left|GS^{\pm}\right\rangle . \tag{3.3.19}$$

At zero temperature the terms with $\kappa(-\omega)$ drop out, such that the relaxation rate r_k of a state $|k^{\pm},-k^{\pm}\rangle$ can be directly determined to

$$r_k = 2\frac{\Delta_k^2}{E_k^2}K(2E_k)\,, \tag{3.3.20}$$

plotted in Fig3.5. Note that all states $|k^{\pm},q^{\pm}\rangle$ with $k \neq -q$ cannot relax into a ground state with a global bath coupling.
For finite temperature we have coupled differential equations, which leads to different decay channels for each state, such that the relaxation rates can be determined numerically, see Fig.3.6. One can see that at temperature $k_BT < J$ the deviation of the rate r_k at zero temperature is small and the zero temperature rate can be used as an approximation.
The relaxation of the states tends to zero for increasing t/J, as the spin chain tends to the case of non-interacting spins, where all diagonal elements do not decay (no energy relaxation).

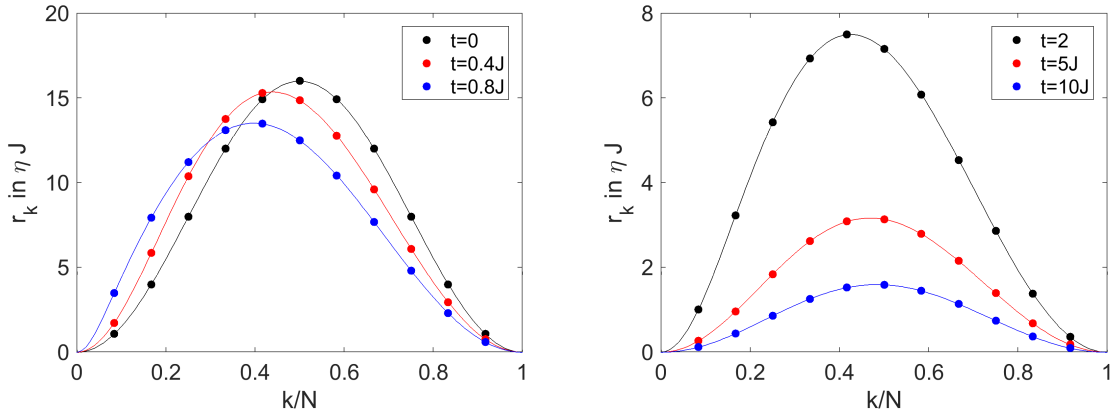

(a) $t < J$ (b) $t > J$

Figure 3.5: Energy relaxation rate r_k of a state $|k^{\pm},-k^{\pm}\rangle$ at zero temperature. k/N shows the position for the state $|k^{\pm},-k^{\pm}\rangle$ in a spin chain with N spins. The dots are an example for all states that relax to the groundstate for $N = 12$ spins. All states with even parity (and odd k^+) relax into $|GS^+\rangle$ and all states with odd parity (and even k^-) relax into $|GS^-\rangle$.

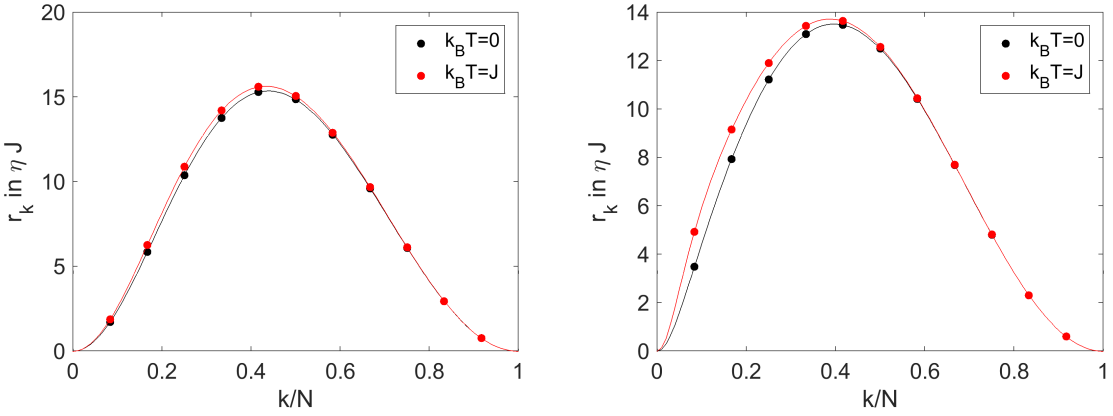

(a) $t = 0.4J$ (b) $t = 0.8J$

Figure 3.6: Energy relaxation rate r_k of the first excited states for (a) $t = 0.4J$ and (b) $t = 0.8J$. k/N shows the position for a state $|k^{\pm}, -k^{\pm}\rangle$ in a spin chain with N spins. The dots are an example for all states that relax to the groundstate for $N = 12$ spins. The deviation of r_k at finite temperature are small in comparison to the result at zero temperature.

3.3.5 Comparison to perturbation theory in the strong coupling regime

Consider the strong coupling regime, where $J >> t$, such that the transverse field can be seen as a perturbation H_p of the Hamiltonian

$$H = -J \sum_i \sigma_i^x \sigma_{i+1}^x \tag{3.3.21}$$

$$H_p = -t \sum \sigma_i^z \,, \tag{3.3.22}$$

and the coupling to the environment

$$H_I = \hat{B} \sum_i \sigma_i^z + H_B \,. \tag{3.3.23}$$

Starting from the limit $t = 0$, the spectrum of the Ising model has a simple form.
There are two ground states ($|u\rangle$ and $|d\rangle$) with all spins parallel along the x-direction, whereas the excited subspaces are formed by states corresponding to domain walls separating regions of parallel spins with different direction.
For instance, the first excited subspace contains only one pair of domains walls, see Fig.3.7, and has energy $4J$ in respect to the ground state with dimension (degeneracy) $N(N-1)$. In the first excited subspace, we characterize the states with two domain walls as $|n, m\rangle$ in which the first index refers to the position of the domain wall between n and $n+1$ where the spin component (along the x direction) changes from up to down, whereas the second index refers to the position of the domain wall between m and $m+1$, where the spin component (along the x direction) changes from down to up, see Fig. 3.7.
Notice that two states of inverted domain wall positions are different $|n, m\rangle \neq |m, n\rangle$.
For low temperature one can consider only the two ground states and the first excited

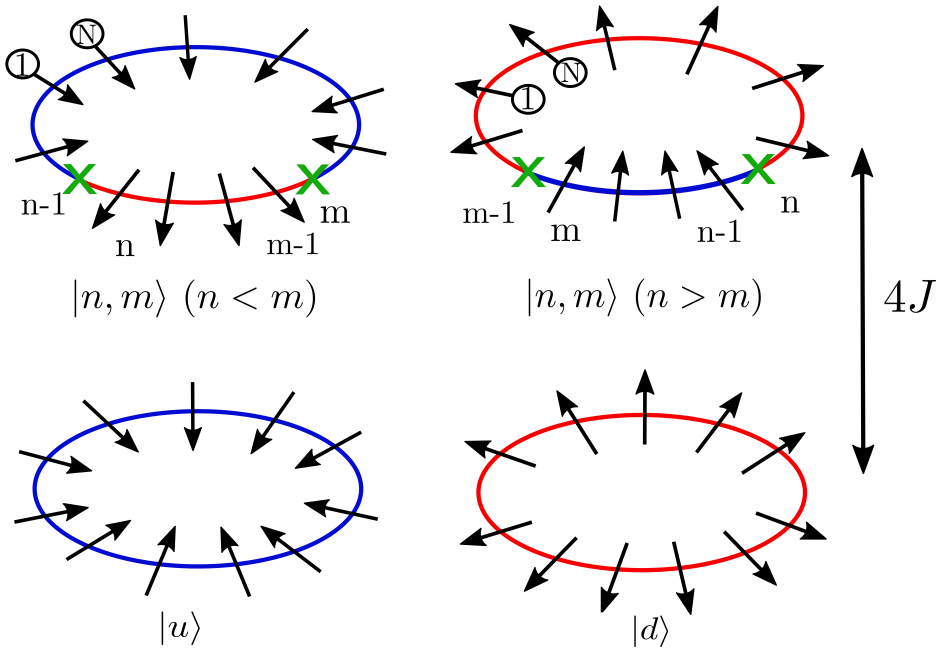

Figure 3.7: Schematic picture of the lowest states for $t = 0$. The two ground states $|u\rangle$ and $|d\rangle$ where all spins are aligned the x-direction. And the first excited subspace with two domain walls $|n, m\rangle$ at position n (down to up) and m (up to down).

states.
For small t one has find the real eigenstates Ψ with

$$\varepsilon\Psi = t\sum_i \sigma_i^z \Psi \tag{3.3.24}$$

$$\Psi = \sum_{n,m} f_{n,m}\,|n,m\rangle\ . \tag{3.3.25}$$

The perturbation operator acts as a hopping operator on the states with the two domain walls:

$$\sum_i \sigma_i^z\,|n,m\rangle = \sum_{s=-1,+1} |n+s,m\rangle + \sum_{s=-1,+1} |n,m+s\rangle \tag{3.3.26}$$

This leads to the following set of equations

$$t\left[f_{(n+1,m)} + f_{(n-1,m)} + f_{(n,m+1)} + f_{(n,m-1)}\right] = \varepsilon f_{(n,m)}\,, \tag{3.3.27}$$

for $|n-m| > 1$ and $|N+n-m| < 1$, whereas for $n = m+1$ we have

$$t\left[f_{(n+1,m)} + f_{(n,m-1)}\right] = \varepsilon f_{(n,m)}\,, \tag{3.3.28}$$

or for $n = m-1$ we have

$$t\left[f_{(n-1,m)} + f_{(n,m+1)}\right] = \varepsilon f_{(n,m)}\,. \tag{3.3.29}$$

Eq.3.3.28 and eq.3.3.29 are automatically satisfied if we set $f_{n,n} = 0$.
Thus the problem can be connected to the tight binding model with an effective lattice

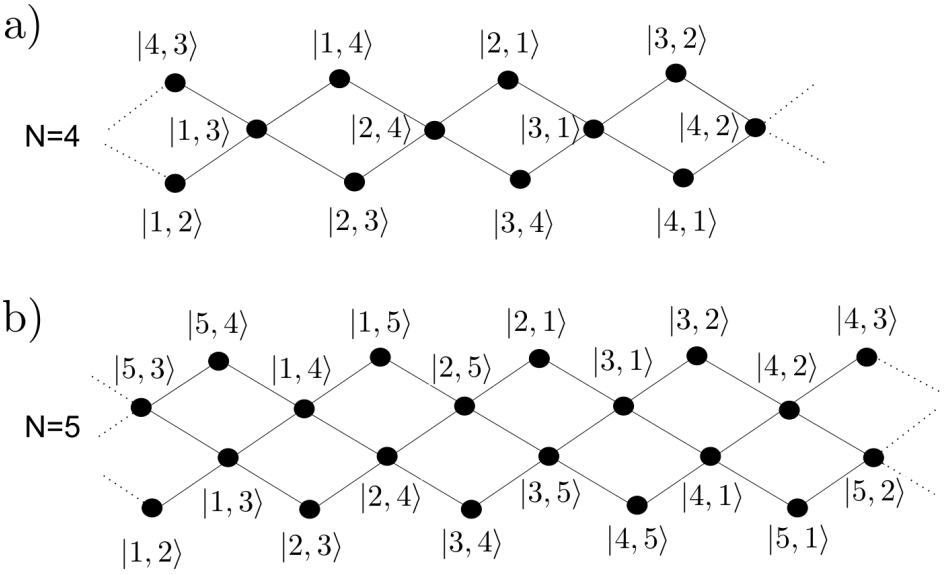

Figure 3.8: Effective lattice for (a) $N = 4$ and (b) $N = 5$ of the first excited subspace with the states $|n, m\rangle$ (dots) and the connection through the perturbation $\sum_i \sigma_i^z$ (lines) of these states.

as shown in Fig.3.8. The eigenstates can be expressed with the two new quantum numbers $q = 1, .., N$ and $k = 1, ..., N - 1$.

$$|k, q\rangle = \sum_{n,m=1}^{N} f_{(n,m)}(k, q) \, |n, m\rangle \tag{3.3.30}$$

with

$$f_{n,m} = \left[\theta(m - n) + \theta(n - m)e^{i\pi()k+q}\right] \frac{\sqrt{2}}{N} \sin(\frac{\pi}{N}k(m - n))e^{i\frac{\pi}{N}q(m+n)} \tag{3.3.31}$$

$$\varepsilon(k, q) = 2t \left[\cos\left(\pi(k - q)/N\right) + \cos\left(\pi(k + q)/N\right)\right] \tag{3.3.32}$$

The full derivation can be seen in the appendix C.3. Thus the Lindblad operators can be directly expressed via the projection on these new eigenstates:

$$\hat{A}(\omega_i) = \sum_{E_\alpha, E_\beta} \delta_{\omega_i, E_\alpha - E_\beta} \, \hat{\Pi}(E_\beta) \sum_i \sigma_i^z \hat{\Pi}(E_\alpha) \, . \tag{3.3.33}$$

with the projection operator $\hat{\Pi}$.
The projectors on the ground state subspace, with $\omega_i = 0$, has zero matrix element since $\sum_i \sigma_i^z$ can only flip one spin of the lattice. The projectors within the first excited subspace with the energy spacing $|\omega_i| = \varepsilon(k, q) - \varepsilon(k', q')$ give only a finite contribution for $\omega_i = 0$ ($\varepsilon(k, q) = \varepsilon(k', q')$) since the first excited subspace is formed by the eigenstates of the operator $\sum_i \sigma_i^z$ within this subspace, thus there is no connection between different excited states of the first excited subspace. Hence we obtain for the Lindblad operator acting only in one subspace

$$\hat{A}(\omega_i = 0) = \hat{A}_0 = \hat{A}_0^\dagger = \sum_{k,q} \frac{\varepsilon(k, q)}{t} \, |k, q\rangle \, \langle k, q| \tag{3.3.34}$$

The connection between the ground states with the first excited subspace is characterized by the energy spacing $|\omega_i| = 4J + \varepsilon(k,q)$. Since $\sum_i \sigma_i^z$ can flip one spin only, the interaction with the bath can create only domain walls of distance one by applying $\sum_i \sigma_i^z$ to one of the two ground state states (Fig. 3.7), i.e. $\sum_i \sigma_i^z$ has only non zero matrix element between the ground states and $|n,m\rangle$ with $|n-m| = 1, N$. In the effective tight-binding lattice representation (Fig. 3.8), these states are located on the borders of the effective lattice. The detailed calculation as done in the appendix C.4 shows that the Lindblad operator only connects excited states with $q = N$ to the ground states.

$$\hat{A}(\omega_i = E_k) = 2\sin\left(\frac{\pi k}{N}\right)|g_s\rangle\langle k,N| \tag{3.3.35}$$

$$\hat{A}(\omega_i = -E_k) = 2\sin\left(\frac{\pi k}{N}\right)|k,N\rangle\langle g_s| \ , \tag{3.3.36}$$

with $E_k = 4J + \varepsilon(k,N)$ and $s = e^{i\pi(k+N+1)}$.
The states $|g_\pm\rangle$ are a superposition, of the two classical ground states $|u\rangle$ and $|d\rangle$

$$|g_\pm\rangle = \frac{1}{\sqrt{2}}\left(|u\rangle \pm |d\rangle\right) \ . \tag{3.3.37}$$

Thus the the two ground states (even and odd superposition) have defined parity with the parity operator $\hat{P}$ defined as

$$\hat{P} = e^{i\pi\sum_i \sigma_i^z} = \prod_n \hat{\sigma}_n^z \, . \tag{3.3.38}$$

The total Lindblad for the system restricted on the ground state and the first excited states takes the form

$$\begin{aligned} d_t\rho =& \kappa(0)\left[\sum_{\substack{k,q\\k',q'}} \frac{\epsilon(k,q)\epsilon(k',q')}{t^2}|k,q\rangle\langle k,q|\rho|k',q'\rangle\langle k',q'| - \frac{1}{2}\sum_{k,q}\frac{\epsilon^2(k,q)}{t^2}\left\{|k,q\rangle\langle k,q|,\rho\right\}\right] \\ &+ 2\sum_k \kappa(-E_k)\sin^2\left(\frac{\pi}{N}k\right)\left[|k,N\rangle\langle g_k|\rho|g_k\rangle\langle k,N| - \frac{1}{2}\Big\{|g_k\rangle\langle g_k|,\rho\Big\}\right] \\ &+ 2\sum_k \kappa(E_k)\sin^2\left(\frac{\pi}{N}k\right)\left[|g_k\rangle\langle k,N|\rho|k,N\rangle\langle g_k| - \Big\{|k,N\rangle\langle k,N|,\rho\Big\}\right] \end{aligned} \tag{3.3.39}$$

Thus the coherence between the two parity ground states reads

$$\frac{d\langle g_+|\rho_s|g_-\rangle}{dt} = \sum_k \kappa(-E_k)\sin^2\left(\frac{\pi}{N}k\right) \ , \tag{3.3.40}$$

which features exponentially suppression for $k_bT << E_k$ and linear scaling with the number of spins.
For the energy relaxation we find at zero temperature for the state $|k,N\rangle$ to $|g_\pm\rangle$ that the rate is proportional to $r_k \propto \sin^2(k\pi/N)$. Thus the results shows the same behavior as for arbitrary t/J in the limit of small t, such that for $t/J \to 0$ the two models reproduce the same results. Notice that the states $|k,N\rangle$ in this model refer to the

states $|k,-k\rangle$ and the ground states $|g_{\pm}\rangle$ in this approach to the two parity ground states $|GS^{\pm}\rangle$ for arbitrary t/J (in the limit of $t/J \to 0$).

3.3.6 Overview

For a global coupling to the bath the decoherence is determined by the gap energy, as the interaction of the lowest states are always with excited states gapped by the energy $2E_k$, see Fig.3.9 for the topological regime and Fig.3.10 for the trivial regime. In the trivial regime there is an additional pure dephasing contribution of the single spin dephasing rate, as the two state $|GS^+\rangle$ and $|GS^-_{(k=0)}\rangle$ belong to different excitational subspaces, similar as in the case for non interacting spins.
In Fig.3.11 the total decoherence rate of $\langle GS^+|\,\rho_s\,|GS^-\rangle = e^{-\Gamma_{dec}t}\,\langle GS^+|\,\rho_s(0)\,|GS^-\rangle$ is shown, the decoherence rate is strongly suppressed at low temperature in the topological regime, whereas in the trivial regime the two states are not protected against dephasing, due to additional pure dephasing in this regime.

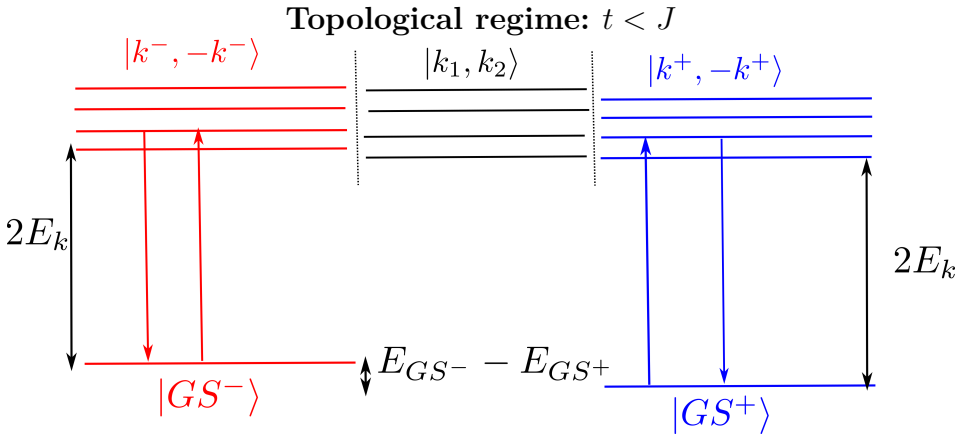

Figure 3.9: Even parity subspace in blue and odd parity subspace in red. In the topological regime both the ground state and the nearly degenerate lowest state of the odd parity can interact only with states $|k^{\pm},-k^{\pm}\rangle$ (with there respective parity) gapped by the energy $2E_k$. Hence the decoherence rate is fully determined by the gap energy $2E_k$ and the number of states the lowest states can interact.

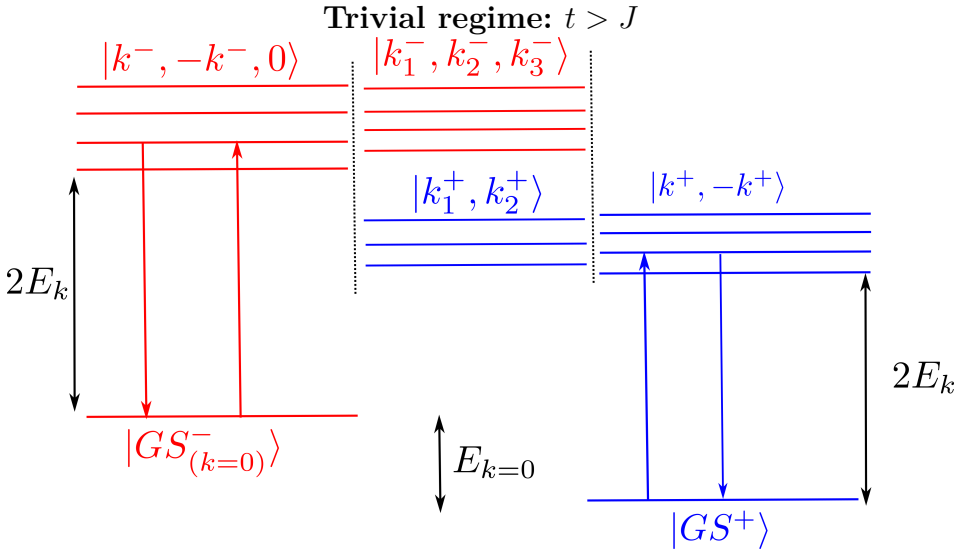

Figure 3.10: Even parity subspace in blue and odd parity subspace in red. In the trivial regime the ground state can interact only with states $|k, -k\rangle$ (with the respective parity) gapped by the energy $2E_k$. The lowest state of the odd parity subspace $|GS^-_{(k=0)}\rangle$ can only interact with states $|k^-, -k^-, 0\rangle$ gapped by the energy $2E_k$. Hence that decoherence rate is fully determined by the gap energy $2E_k$ and the numbers of higher excited states (scales with N) and the pure dephasing contribution in the trivial regime, see Fig.3.11.

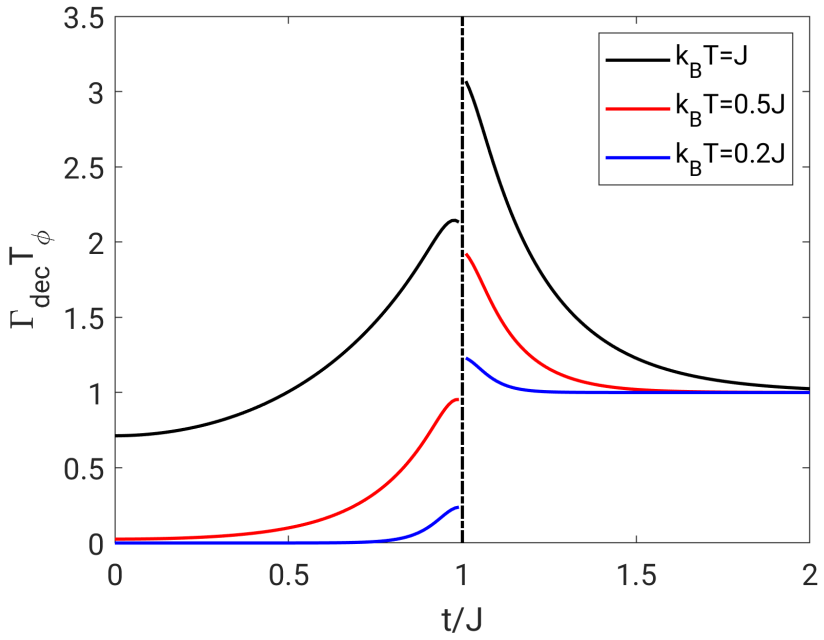

Figure 3.11: Decay rate $\Gamma_{dec} = \frac{\theta(t-J)}{T_\phi} + \Gamma_\pm$ of the coherence between the two lowest states $|GS^+\rangle$ and $|GS^-\rangle$ normalized with the single spin dephasing rate $\frac{1}{T_\phi} = \eta\pi k_B T$ (see 1.3) for $N = 40$ spins. At low temperature the dephasing rate can be strongly suppressed in the topological regime.

3.4 Local bath coupling

For local coupling to the environment every spin is coupled to a local bath, which is independent of the bathes coupled to other spins, such that the bath correlator is only nonzero for correlators from the same spin sites

$$F_{n_1,n_2}(t-t') = \delta_{n_1,n_2} F(t-t')\,. \tag{3.4.1}$$

Hence the terms in the master equation have the following form (here one part as an example):

$$\sum_{n_1,n_2} F_{n_1,n_2}(t-t')\sigma^z_{n_1}(t)\sigma^z_{n_2}(t')\rho_s(t) = F(t-t')\sum_{n_1}\sigma^z_{n_1}(t)\sigma^z_{n_1}(t')\rho_s(t)\,. \tag{3.4.2}$$

The full derivation of all terms in the Lindblad equation can be seen in the appendix C.5 leading to the following Lindblad super operators (neglecting the Lamb shift terms):

$$\begin{aligned}
\hat{L}^{\pm}(\rho_s) = \frac{4}{N}\sum_{k1^{\pm},k2^{\pm},k3^{\pm},k4^{\pm}} & (u_{k1}u_{k2}-v_{k1}v_{k2})(u_{k3}u_{k4}-v_{k3}v_{k4})\delta_{k_1-k_2,k_4-k_3}\delta_{E_{k1}-E_{k2},E_{k4}-E_{k3}} \\
&\left(\kappa(E_{k1}-E_{k2})\left(\hat{P}^{\pm}\gamma^{\dagger}_{k3}\gamma_{k4}\hat{P}^{\pm}\rho_s\hat{P}^{\pm}\gamma^{\dagger}_{k1}\gamma_{k2}\hat{P}^{\pm} - \frac{1}{2}\{\hat{P}^{\pm}\gamma^{\dagger}_{k1}\gamma_{k2}\gamma^{\dagger}_{k3}\gamma_{k4}\hat{P}^{\pm},\rho_s\}\right)\right) \\
&+\frac{4}{N}\sum_{k1^{\pm},k2^{\pm},k3^{\pm},k4^{\pm}} u_{k1}v_{k2}u_{k3}v_{k4}\delta_{k_1+k_2,k_4+k_3}\delta_{E_{k1}+E_{k2},E_{k4}+E_{k3}} \\
&\left(\kappa(E_{k1}+E_{k2})\left(\hat{P}^{\pm}\gamma_{k4}\gamma_{k3}\hat{P}^{\pm}\rho_s\hat{P}^{\pm}\gamma^{\dagger}_{k1}\gamma^{\dagger}_{k2}\hat{P}^{\pm} - \frac{1}{2}\{\hat{P}^{\pm}\gamma^{\dagger}_{k1}\gamma^{\dagger}_{k2}\gamma_{k4}\gamma_{k3}\hat{P}^{\pm},\rho_s\}\right)\right) \\
&+\frac{4}{N}\sum_{k1^{\pm},k2^{\pm},k3^{\pm},k4^{\pm}} u_{k1}v_{k2}u_{k3}v_{k4}\delta_{k_1+k_2,k_4+k_3}\delta_{E_{k1}+E_{k2},E_{k4}+E_{k3}} \\
&\left(\kappa(-E_{k1}-E_{k2})\left(\hat{P}^{\pm}\gamma^{\dagger}_{k3}\gamma^{\dagger}_{k4}\hat{P}^{\pm}\rho_s\hat{P}^{\pm}\gamma_{k2}\gamma_{k1}\hat{P}^{\pm} - \frac{1}{2}\{\hat{P}^{\pm}\gamma_{k2}\gamma_{k1}\gamma^{\dagger}_{k3}\gamma^{\dagger}_{k4}\hat{P}^{\pm},\rho_s\}\right)\right)
\end{aligned} \tag{3.4.3}$$

and from the terms mixing the parity, we have

$$\begin{aligned}
\hat{L}^{\pm\mp}(\rho_s) = \frac{4}{N}\sum_{k1^{\mp},k2^{\mp},k3^{\pm},k4^{\pm}} & (u_{k1}u_{k2}-v_{k1}v_{k2})(u_{k3}u_{k4}-v_{k3}v_{k4})\delta_{k_1-k_2,k_4-k_3}\delta_{E_{k1}-E_{k2},E_{k4}-E_{k3}} \\
&\kappa(E_{k1}-E_{k2})\left(\hat{P}^{\pm}\gamma^{\dagger}_{k3}\gamma_{k4}\hat{P}^{\pm}\rho_s\hat{P}^{\mp}\gamma^{\dagger}_{k1}\gamma_{k2}\hat{P}^{\mp}\right) \\
&+\frac{4}{N}\sum_{k1^{\mp},k2^{\mp},k3^{\pm},k4^{\pm}} u_{k1}v_{k2}u_{k3}v_{k4}\delta_{k_1+k_2,k_4+k_3}\delta_{E_{k1}+E_{k2},E_{k4}+E_{k3}} \\
&\kappa(E_{k1}+E_{k2})\left(\hat{P}^{\pm}\gamma_{k4}\gamma_{k3}\hat{P}^{\pm}\rho_s\hat{P}^{\mp}\gamma^{\dagger}_{k1}\gamma^{\dagger}_{k2}\hat{P}^{\mp}\right) \\
&+\frac{4}{N}\sum_{k1^{\mp},k2^{\mp},k3^{\pm},k4^{\pm}} u_{k1}v_{k2}u_{k3}v_{k4}\delta_{k_1+k_2,k_4+k_3}\delta_{E_{k1}+E_{k2},E_{k4}+E_{k3}} \\
&\kappa(-E_{k1}-E_{k2})\left(\hat{P}^{\pm}\gamma^{\dagger}_{k3}\gamma^{\dagger}_{k4}\hat{P}^{\pm}\rho_s\hat{P}^{\mp}\gamma_{k2}\gamma_{k1}\hat{P}^{\mp}\right)\,.
\end{aligned} \tag{3.4.4}$$

Resulting in the full Lindblad master equation

$$\frac{d\rho_s}{dt} = \hat{L}^{+}(\rho_s) + \hat{L}^{-}(\rho_s) + \hat{L}^{-+}(\rho_s) + \hat{L}^{+-}(\rho_s)\,. \tag{3.4.5}$$

Note that this is the most general Lindblad equation for arbitrary t/J and N, the δ-functions have to determined in principle for every configuration of those parameters.

3.4.1 J=0 limit case

For $J = 0$ all excitations have the same energy $E_k = 2t$, thus the δ-functions for the energy are always fulfilled. As $v_k^2 = 1/2(1 - \xi_k/E_k) = 0$ and $u_k^2 = 1$ many terms drop out in the master equation

$$\frac{d\rho_s}{dt} = \frac{2}{T_\phi} \sum_{k1,k2,k3,k4} \delta_{k_1-k_2,k_4-k_3} \left(\left(\gamma_{k3}^\dagger \gamma_{k4} \rho_s \gamma_{k1}^\dagger \gamma_{k2} - \frac{1}{2}\{\gamma_{k1}^\dagger \gamma_{k2} \gamma_{k3}^\dagger \gamma_{k4}, \rho_s\} \right) \right). \tag{3.4.6}$$

Notice that the sum is now over all possible k (of the even and odd subspace), due to the terms of $\hat{L}^{+-}$ and $\hat{L}^{-+}$.
All diagonal elements e.g. $\langle k|\,\rho_s\,|k\rangle$ with $|k\rangle = \gamma_k^\dagger\,|GS^+\rangle$ do not decay:

$$\begin{aligned}\frac{d\,\langle k|\,\rho_s\,|k\rangle}{dt} &= \frac{2}{NT_\phi} \sum_{k_1} \langle k|\,\gamma_k^\dagger \gamma_{k1} \rho_s \gamma_{k1}^\dagger \gamma_k\,|k\rangle \\ &\quad - \frac{1}{NT_\phi} \sum_{k_1} \langle k|\,\{\gamma_k^\dagger \gamma_{k1} \gamma_{k1}^\dagger \gamma_k, \rho_s\}\,|k\rangle = 0\end{aligned} \tag{3.4.7}$$

Besides the subspace with same number of excitations is not a decoherence free subspace anymore (as for the global bath with $J = 0$)

$$\begin{aligned}\frac{d\,\langle k|\,\rho_s\,|q\rangle}{dt} &= -\frac{1}{NT_\phi} \sum_{k_1} \langle k|\,\gamma_k^\dagger \gamma_{k1} \gamma_{k1}^\dagger \gamma_k \rho_s\,|q\rangle \\ &\quad - \frac{1}{NT_\phi} \sum_{k_1} \langle k|\,\rho_s \gamma_q^\dagger \gamma_{k1} \gamma_{k1}^\dagger \gamma_q\,|q\rangle \\ &= -\frac{2}{T_\phi}\,\langle k|\,\rho_s\,|q\rangle\ .\end{aligned} \tag{3.4.8}$$

And for the coherence between a fully excited state $|k_1, .., k_N\rangle = |\{k\}\rangle$ and the ground state we have

$$\begin{aligned}\frac{d\,\langle GS^+|\,\rho_s\,|\{k\}\rangle}{dt} &= -\frac{1}{NT_\phi} \kappa_0 \sum_{k_1 k_2} \langle k|\,\rho_s \gamma_{k2}^\dagger \gamma_{k2} \gamma_{k1}^\dagger \gamma_{k1}\,|\{k\}\rangle \\ &= -\frac{N}{T_\phi}\,\langle GS|\,\rho_s\,|\{k\}\rangle\ .\end{aligned} \tag{3.4.9}$$

One can see that it scales linearly with the difference in the excitations, such that for arbitrary states $|a\rangle$ and $|b\rangle$ we have

$$\frac{d\,\langle a|\,\rho_s\,|b\rangle}{dt} = -\frac{1}{T_\phi} \sum_{k \in (a \cup b) \setminus (a \cap b)} \langle a|\,\rho_s\,|b\rangle \tag{3.4.10}$$

a contribution of the single spin dephasing rate for each excitation (not excitation number as for the global case), which is only in one of these two arbitrary states.

3.4.2 Approximation: no accidental degeneracy

For finite J we have terms with

$$\delta_{k_1-k_2,k_4-k_3}\delta_{E_{k1}-E_{k2},E_{k4}-E_{k3}}\,, \tag{3.4.11}$$

these terms are always fulfilled (for arbitrary t/J and N) for $k_1 = k_2$ and $k_3 = k_4$ or for $k_1 = k_4$ and $k_2 = k_3$. But additional to these general solution there can be also solutions, which are valid for a special configuration of t/J and N. In the following we will focus only on these general solutions, which are valid for the whole parameter regime.
This means the derived result can differ a bit for special configurations of t/J and N, which have such a special solution (as here an additional term will appear in the Lindblad). But as it can be seen for $N = 10$ qubits in the appendix C.6, these additional solutions rarely happens (at least for an intermediate amount of qubits) and also have low influence on the result (N^2 general solution for the delta-functions with the same scaling prefactor).
For $N \to \infty$ these additional terms will of course happen more often (for more ratios of t/J), but also the influence of these terms should be small (due to the quadratically increasing amount of other terms).
In similar way, the relation

$$\delta_{k_1+k_2,k_4+k_3}\delta_{E_{k1}+E_{k2},E_{k4}+E_{k3}} \tag{3.4.12}$$

is generally fulfilled for the cases $k_1 = k_3$ and $k_2 = k_4$ or $k_2 = k_3$ and $k_1 = k_4$.

3.4.3 Decoherence for t<J

Using this approximation for the Lindblad operators we have

$$\begin{aligned}\hat{L}^{\pm}(\rho_s) = &\frac{4}{N}\sum_{k1^{\pm},k2^{\pm}}\frac{\xi_{k1}\xi_{k2}}{E_{k1}E_{k2}}\left(\kappa_0\left(\hat{P}^{\pm}\gamma_{k2}^{\dagger}\gamma_{k2}\hat{P}^{\pm}\rho_s\hat{P}^{\pm}\gamma_{k1}^{\dagger}\gamma_{k1}\hat{P}^{\pm}-\frac{1}{2}\{\hat{P}^{\pm}\gamma_{k1}^{\dagger}\gamma_{k1}\gamma_{k2}^{\dagger}\gamma_{k2}\hat{P}^{\pm},\rho_s\}\right)\right)\\
&+\frac{2}{N}\sum_{k1^{\pm}\neq k2^{\pm}}\frac{E_{k1}E_{k2}+\xi_{k1}\xi_{k2}-\Delta_{k1}\Delta_{k2}}{E_{k1}E_{k2}}\\
&\left(\kappa(E_{k1}-E_{k2})\left(\hat{P}^{\pm}\gamma_{k2}^{\dagger}\gamma_{k1}\hat{P}^{\pm}\rho_s\hat{P}^{\pm}\gamma_{k1}^{\dagger}\gamma_{k2}\hat{P}^{\pm}-\frac{1}{2}\{\hat{P}^{\pm}\gamma_{k1}^{\dagger}\gamma_{k2}\gamma_{k2}^{\dagger}\gamma_{k1}\hat{P}^{\pm},\rho_s\}\right)\right)\\
&+\frac{1}{N}\sum_{k1^{\pm},k2^{\pm}}\frac{E_{k1}E_{k2}+\xi_{k1}E_{k2}-\xi_{k2}E_{k1}-\xi_{k1}\xi_{k2}-\Delta_{k1}\Delta_{k2}}{E_{k1}E_{k2}}\\
&\left(\kappa(E_{k1}+E_{k2})\left(\hat{P}^{\pm}\gamma_{k2}\gamma_{k1}\hat{P}^{\pm}\rho_s\hat{P}^{\pm}\gamma_{k1}^{\dagger}\gamma_{k2}^{\dagger}\hat{P}^{\pm}-\frac{1}{2}\{\hat{P}^{\pm}\gamma_{k1}^{\dagger}\gamma_{k2}^{\dagger}\gamma_{k2}\gamma_{k1}\hat{P}^{\pm},\rho_s\}\right)\right)\\
&+\frac{1}{N}\sum_{k1^{\pm},k2^{\pm}}\frac{E_{k1}E_{k2}+\xi_{k1}E_{k2}-\xi_{k2}E_{k1}-\xi_{k1}\xi_{k2}-\Delta_{k1}\Delta_{k2}}{E_{k1}E_{k2}}\\
&\left(\kappa(-E_{k1}-E_{k2})\left(\hat{P}^{\pm}\gamma_{k1}^{\dagger}\gamma_{k2}^{\dagger}\hat{P}^{\pm}\rho_s\hat{P}^{\pm}\gamma_{k2}\gamma_{k1}\hat{P}^{\pm}-\frac{1}{2}\{\hat{P}^{\pm}\gamma_{k2}\gamma_{k1}\gamma_{k1}^{\dagger}\gamma_{k2}^{\dagger}\hat{P}^{\pm},\rho_s\}\right)\right),\end{aligned} \tag{3.4.13}$$

and from the mixing parity terms from the master equation, we have

$$\hat{L}^{\pm\mp}(\rho_s) = \frac{4}{N}\sum_{k1^{\mp},k2^{\pm}}\frac{\xi_{k1}\xi_{k2}}{E_{k1}E_{k2}}\kappa_0\left(\hat{P}^{\pm}\gamma_{k2}^{\dagger}\gamma_{k2}\hat{P}^{\pm}\rho_s\hat{P}^{\mp}\gamma_{k1}^{\dagger}\gamma_{k1}\hat{P}^{\mp}\right). \tag{3.4.14}$$

Thus the off diagonal element between the two lowest states reads as

$$\begin{aligned}\frac{d\langle GS^{+}|\rho_s|GS^{-}\rangle}{dt} &= -\left(\frac{1}{2N}\sum_{k1^{+}\neq k2^{+}}\kappa(-E_{k1}-E_{k2})\frac{E_{k1}E_{k2}-\xi_{k1}\xi_{k2}-\Delta_{k1}\Delta_{k2}}{E_{k1}E_{k2}}\right.\\
&\left.+\frac{1}{2N}\sum_{k1^{-}\neq k2^{-}}\kappa(-E_{k1}-E_{k2})\frac{E_{k1}E_{k2}-\xi_{k1}\xi_{k2}-\Delta_{k1}\Delta_{k2}}{E_{k1}E_{k2}}\right)\langle GS^{+}|\rho_s|GS^{-}\rangle\\
&= -\Gamma_{\pm}^{(l)}\langle GS^{+}|\rho_s|GS^{-}\rangle.\end{aligned} \tag{3.4.15}$$

Hence the coherence between the two parity ground states decay exponentially with the decoherence rate $\Gamma_{\pm}^{(l)}$.
One can see that for $k_BT < E_{k1}+E_{k2}$ the decoherence rate is exponentially suppressed, due to the reduced interaction with higher excited states as depicted in Fig.3.12(a). There is "almost" linear scaling with the number of spins N for $t < J$. Besides near the critical point the rate is increased, as the gap energy to excited states is smaller near $t = J$, leading to an increased interaction with excited states (see Fig.3.12(b)).

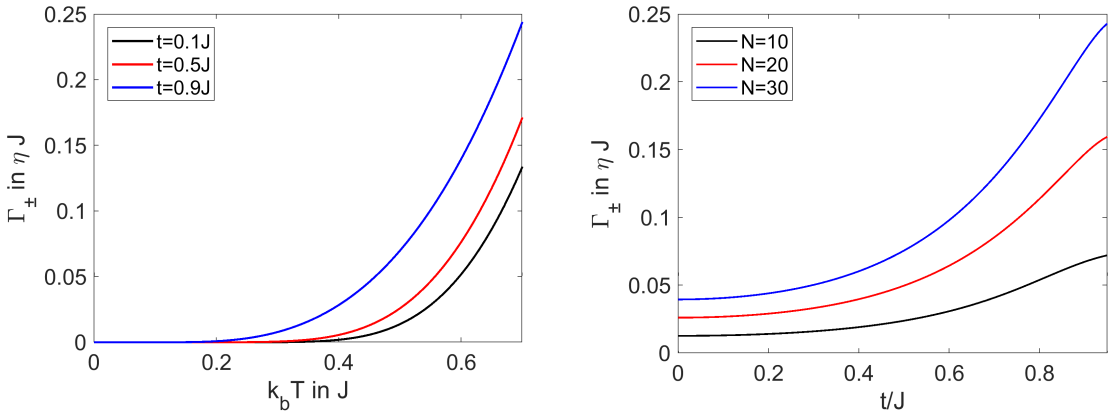

(a) $N = 10$ (b) $k_B T = 0.5J$

Figure 3.12: Decoherence rate $\Gamma_{\pm}^{(l)}$ (eq.3.4.15) over temperature (a) for $N = 10$ spins and $\Gamma_{\pm}^{(l)}$ over t/J (b) at $k_B T = 0.5J$. In (a) one can see exponentially suppressed behavior for temperatures lower than the gap. The suppression starts for larger gaps ($t/J = 0.1$) much earlier as for smaller gaps (e.g $t/J = 0.9$). In (b) one can see "almost" linear scaling of $\Gamma_{\pm}^{(l)}$ with the number of the spins N in the whole regime.

3.4.4 Decoherence for t>J

In this regime the lowest state in the odd parity subspace $|GS^-_{(k=0)}\rangle$ has the property $\gamma_0^\dagger\gamma_0 |GS^-_{(k=0)}\rangle = |GS^-_{(k=0)}\rangle$. The off diagonal element between the two lowest states reads

$$\begin{aligned}
\frac{d\langle GS^+|\rho_s|GS^-_{(k=0)}\rangle}{dt} = -\Bigg(&\frac{1}{2N}\sum_{k1^+\neq k2^+}\kappa(-E_{k1}-E_{k2})\frac{E_{k1}E_{k2}-\xi_{k1}\xi_{k2}-\Delta_{k1}\Delta_{k2}}{E_{k1}E_{k2}}\\
&+\frac{1}{2N}\sum_{k1^-\neq k2^-}\kappa(-E_{k1}-E_{k2})\frac{E_{k1}E_{k2}-\xi_{k1}\xi_{k2}-\Delta_{k1}\Delta_{k2}}{E_{k1}E_{k2}}\\
&+\frac{2}{N}\kappa_0+\underbrace{\frac{2}{N}\sum_{k1^-\neq 0}\kappa(E_{k=0}-E_{k1})\frac{E_{k=0}E_{k1}+\xi_{k=0}\xi_{k1}-\Delta_{k=0}\Delta_{k1}}{E_{k1}E_{k=0}}}_{\Gamma_l}\Bigg)\\
&\langle GS^+|\rho_s|GS^-_{(k=0)}\rangle\\
&=-\left(\Gamma_{\pm}^{(l)}+\frac{2\kappa_0}{N}+\Gamma_l\right)\langle GS^+|\rho_s|GS^-_{(k=0)}\rangle\ .
\end{aligned}\tag{3.4.16}$$

Here we have again the contribution $\Gamma_{\pm}^{(l)}$, due to the interaction to higher excited states (e.g $|GS^+\rangle$ with $|k_1^+, k_2^+\rangle$ or $|GS^-_{(k=0)}\rangle$ with $|k_1^-, k_2^-, 0\rangle$) gapped by the energy $E_{k1}+E_{k2}$. $\Gamma_{\pm}^{(l)}$ has the same properties as for $t < J$, as exponential suppression at low temperature and the scaling with N.
Hence there is an increase in the decoherence rate between the two lowest state in the trivial regime by $\frac{2\kappa_0}{N}+\Gamma_l$.
The pure dephasing contribution $\frac{2\kappa_0}{N}$ (because $|GS^+\rangle$ and $|GS^-_{(k=0)}\rangle$ belong to different excitational subspaces in the trivial regime) vanishes for larger N, and plays only a role when the number of spins is not too large (as it scales with $1/N$).
The last term Γ_l is due to the interaction of the state $|GS^-_{(k=0)}\rangle$ with states as

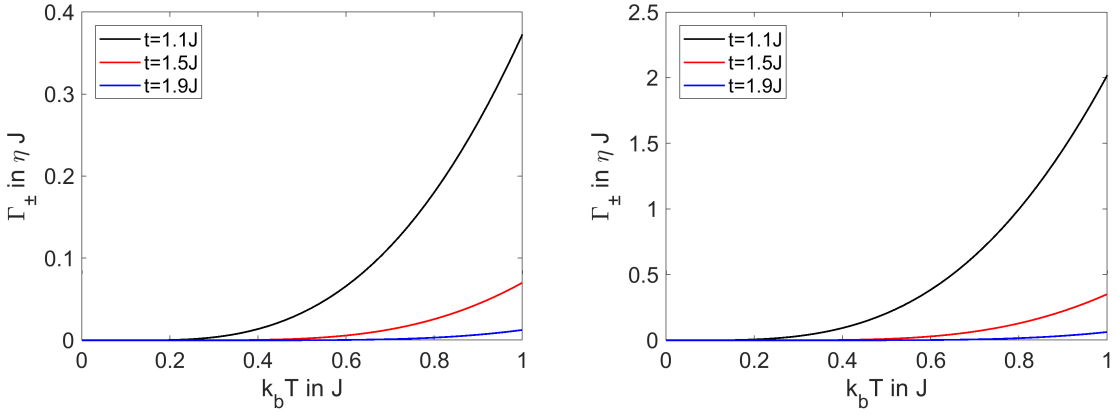

(a) $\Gamma_{\pm}^{(l)}$ for $N = 10$ (b) $\Gamma_{\pm}^{(l)}$ for $N = 50$

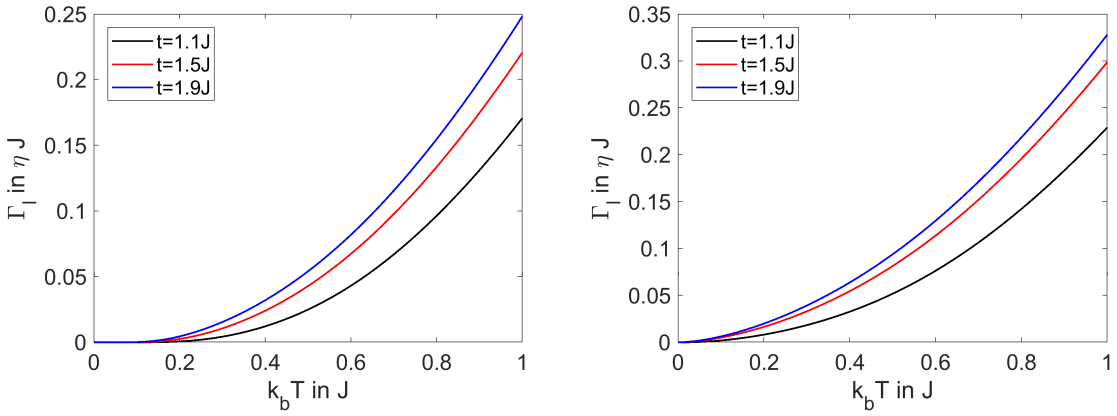

(c) Γ_l for $N = 10$ (d) Γ_l for $N = 50$

Figure 3.13: $\Gamma_{\pm}^{(l)}$ (eq.3.4.16) plotted over temperature for $N = 10$ (a) and $N = 50$ (b) spins, and Γ_l (eq.3.4.16) plotted over temperature for $N = 10$ (c) and $N = 50$ (d) spins. $\Gamma_{\pm}^{(l)}$ shows exponential suppression at temperature lower than the gap energy and besides "almost" linear scaling with N. Γ_l is increasing already at lower temperature. For larger N the rate Γ_l is increasing at lower temperature.

$\gamma_{k_1^-}^{\dagger}\gamma_{k=0}\,|GS_{(k=0)}^{-}\rangle = |k_1^-\rangle$, which have only slightly higher energy $E_{k_1} - E_{k=0}$. Thus Γ_l breaks the exponential suppression at temperature lower than the gap energy (of $\sim 2E_k$).
In Fig.3.13 one can see that Γ_l leads to an increased decoherence rate at very low temperature. With increasing N the energy difference of $|GS_{(k=0)}^{-}\rangle$ to the next higher state $|k = \pm 2\rangle$ decreases, such that Γ_l increases even at lower temperature (in comparison to smaller N).
In Fig.3.14 ($\Gamma_{\pm}^{(l)} + \Gamma_l$) are plotted over the ratio t/J. $\Gamma_{\pm}^{(l)}$ contributes only close to $t = J$ when the energy gap is small. In contrast, Γ_l contributes also at larger t/J, as the energy difference between $|GS_{(k=0)}^{-}\rangle$ and $|k_1\rangle$ does not increase with t/J (it even is slightly reduced for increasing t/J). This causes the non-monotonic behavior in Fig.3.14.

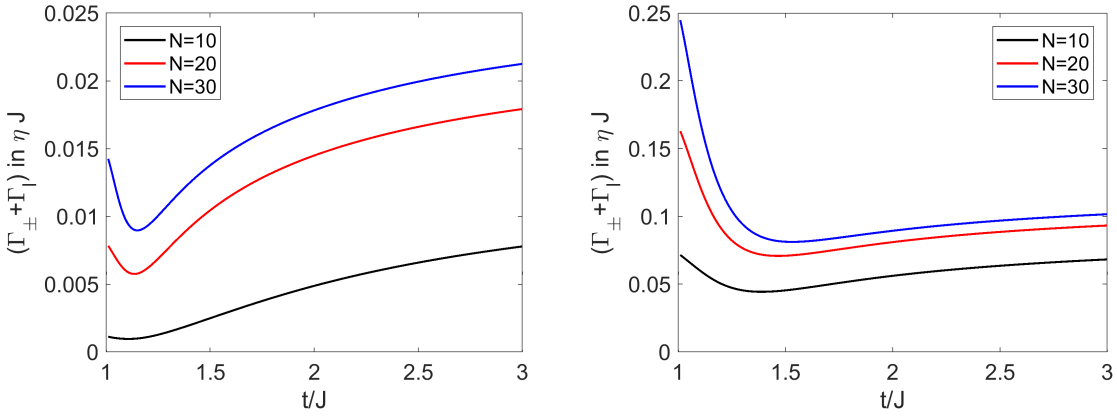

(a) $k_BT = 0.2J$

(b) $k_BT = 0.5J$

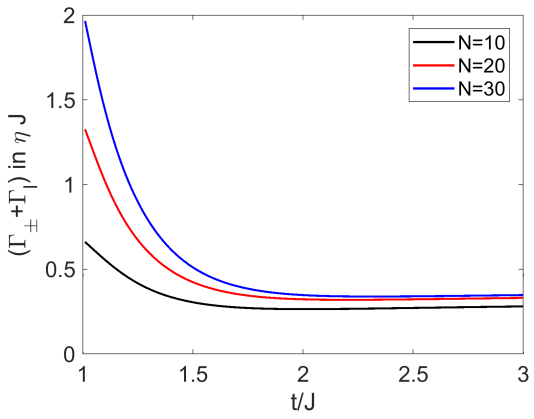

(c) $k_BT = J$

Figure 3.14: $\Gamma_{\pm}^{(l)}+\Gamma_l$ (eq.3.4.16) for different numbers of spins N and temperature at (a) $k_BT = 0.2J$, (b) $k_BT = 0.5J$ and (c) $k_BT = J$ over the ratio t/J. At all temperature the rate is increased near $t = J$, as the reduced gap energy leads to an increase in $\Gamma_{\pm}^{(l)}$. Besides at $k_BT = 0.2J$ the rate increases for increasing t/J, since the energy difference of $|GS^-\rangle$ to $|k_1\rangle$ decreases leading to a bigger contribution of Γ_s to the rate. For $t >> J$ the rate tends to a constant value depending on temperature and N.

3.4.5 Energy relaxation

For a local bath the excited states also interact with each other, and each state does relax to the ground state. In the topological regime ($t < J$) we have for both subspaces

$$\begin{aligned}\frac{d\langle GS^{\pm}|\,\rho\,|GS^{\pm}\rangle}{dt} = &\frac{1}{N}\sum_{k1^{\pm},k2^{\pm}}\frac{E_{k1}E_{k2}-\xi_{k1}\xi_{k2}-\Delta_{k1}\Delta_{k2}}{E_{k1}E_{k2}}\kappa(E_{k1}+E_{k2})\,\langle k_1^{\pm},k_2^{\pm}|\,\rho\,|k_1^{\pm},k_2^{\pm}\rangle\\ &-\frac{1}{N}\sum_{k1^{\pm},k2^{\pm}}\frac{E_{k1}E_{k2}-\xi_{k1}\xi_{k2}-\Delta_{k1}\Delta_{k2}}{E_{k1}E_{k2}}\kappa(-E_{k1}-E_{k2}))\,\langle GS^{\pm}|\,\rho\,|GS^{\pm}\rangle\ .\end{aligned} \tag{3.4.17}$$

And for the excited state for low temperatures $k_BT < 2E_k$, such that the interaction with higher excited states $|k_1,k_2,k_3,k_4\rangle$ can be neglected:

$$\begin{aligned}\frac{d\langle k_1^{\pm},k_2^{\pm}|\,\rho\,|k_1^{\pm},k_2^{\pm}\rangle}{dt} = &\frac{2}{N}\sum_{k3\neq k_2}\frac{E_{k_3}E_{k1}+\xi_{k_3}\xi_{k1}-\Delta_{k1}\Delta_{k_3}}{E_{k1}E_{k_3}}\kappa(E_{k3}-E_{k1})\,\langle k_3^{\pm},k_2^{\pm}|\,\rho\,|k_3^{\pm},k_2^{\pm}\rangle\\ &+\frac{2}{N}\sum_{k3\neq k_1}\frac{E_{k_3}E_{k2}+\xi_{k_3}\xi_{k2}-\Delta_{k2}\Delta_{k_3}}{E_{k2}E_{k_3}}\kappa(E_{k3}-E_{k2})\,\langle k_3^{\pm},k_1^{\pm}|\,\rho\,|k_3^{\pm},k_1^{\pm}\rangle\\ &-\frac{2}{N}\Bigg(\sum_{k_3}\frac{E_{k_3}E_{k1}+\xi_{k_3}\xi_{k1}-\Delta_{k1}\Delta_{k_3}}{E_{k1}E_{k_3}}\kappa(-E_{k3}+E_{k1}))\\ &+\sum_{k_3}\frac{E_{k_3}E_{k2}+\xi_{k_3}\xi_{k2}-\Delta_{k2}\Delta_{k_3}}{E_{k2}E_{k_3}}\kappa(-E_{k3}+E_{k2})\\ &+\kappa(E_{k1}+E_{k2})\frac{E_{k1}E_{k2}-\xi_{k1}\xi_{k2}-\Delta_{k1}\Delta_{k2}}{E_{k1}E_{k2}}\Bigg)\,\langle k_1^{\pm},k_2^{\pm}|\,\rho\,|k_1^{\pm},k_2^{\pm}\rangle\\ &+\frac{2}{N}\kappa(E_{k1}-E_{k2})\frac{E_{k1}E_{k2}-\xi_{k1}\xi_{k2}-\Delta_{k1}\Delta_{k2}}{E_{k1}E_{k2}}\,\langle GS^{\pm}|\,\rho\,|GS^{\pm}\rangle\ .\end{aligned} \tag{3.4.18}$$

The first four terms are due to the interaction with other excited states (with same parity) and the last two terms due to the interaction with the ground state.
The numerical determined relaxation rate r_{k_1,k_2} of a doubly excited state $|k_1^{\pm},k_2^{\pm}\rangle$ to the ground state with respective parity is plotted in Fig.3.15 and Fig.3.16.
For $t/J > 0.5$ the relaxation rate is determined by the excitation energy of the state, such that higher excited states have a larger relaxation rate, as they have more possible relaxation channels by decaying into lower excited states.
For $t/J < 0.5$ the relaxation via lower energetic states is reduced and states in the middle of the excitational band have a faster direct decay channel to the ground state (similar as for the global bath, where states $|k^{\pm},-k^{\pm}\rangle$ with $k/N \sim 0.5$ have larger relaxation rates).
At larger temperature everything is washed out, due to the finite temperature allowing also decay via higher energetic states, see Fig.3.16.

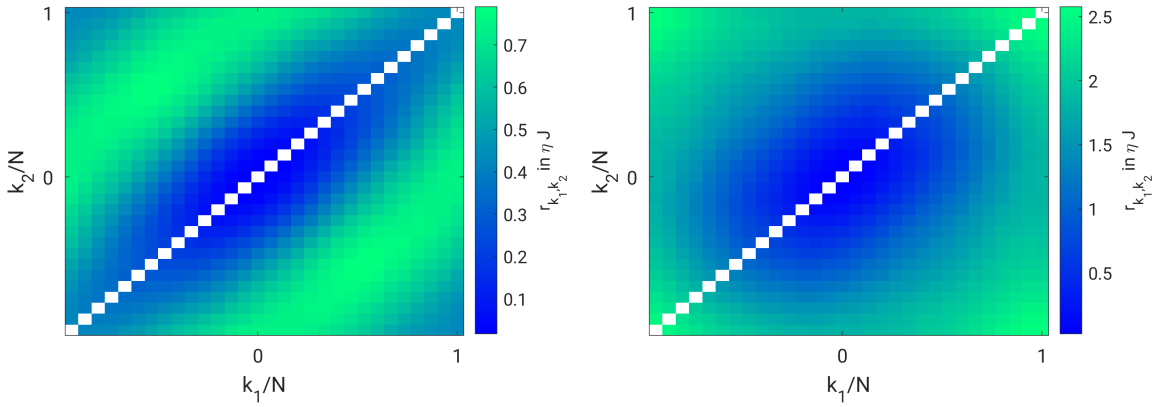

(a) $t = 0.1J$ (b) $t = 0.5J$

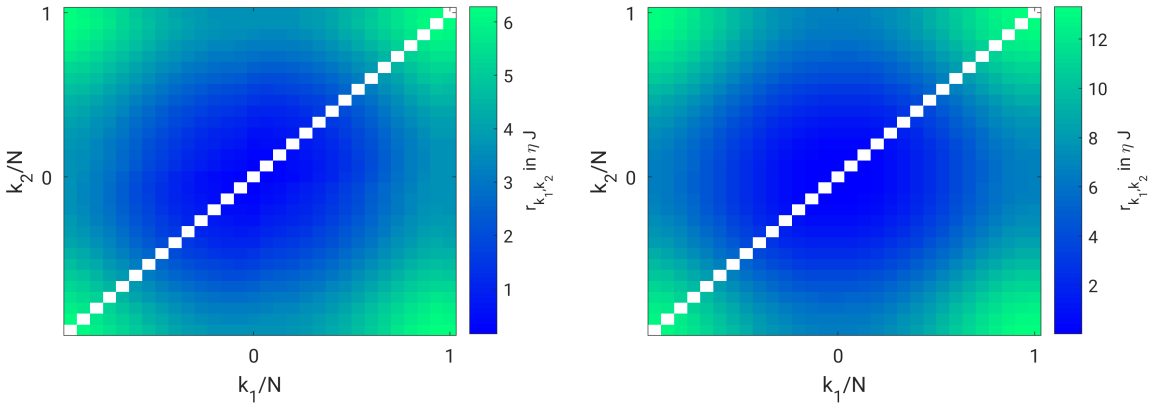

(c) $t = 0.9J$ (d) $t = 2J$

Figure 3.15: Relaxation rate of a state $|k_1, k_2\rangle$ for $N = 30$ spins. For larger t (e.g. $t = 0.9J$) the relaxation rate does mostly depend on the energy of the states, such that high energy states with large $|k|$ does relax faster as low energy states with small k (leading to the circle around the center). In contrary to the regime with small t, where the circle is squeezed, such that all state with lying in the middle of the excitation band have larger relaxation rates.

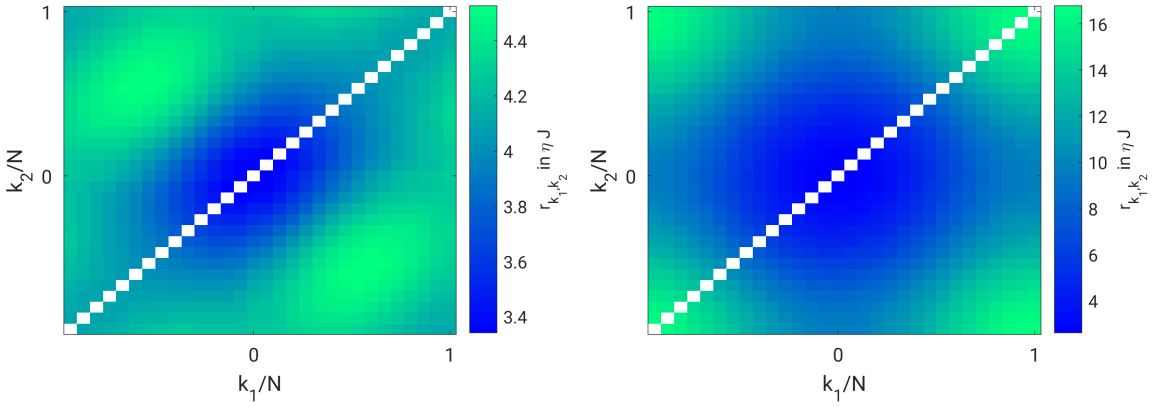

(a) $t = 0.1J$ (b) $t = 2J$

Figure 3.16: Relaxation rate of a state $|k_1, k_2\rangle$ at $k_B T = J$ for $N = 30$ spins. It has still the same shape as for zero temperature, but is washed out now at finite temperature.

In the trivial regime the lowest excitations in the odd parity subspace are $\gamma_{k_1^-}\left|GS^-_{(k=0)}\right\rangle = \left|k_1^-\right\rangle$. With $\kappa(E_k - E_0) >> \kappa(-E_{k1} - E_{k2})$ in the low temperature limit, we will focus on the interaction with the lowest excitations only

$$\begin{aligned}\frac{d\left\langle GS^-_{(k=0)}\right|\rho_s\left|GS^-_{(k=0)}\right\rangle}{dt} &= \frac{2}{N}\sum_{k1^-\neq 0}\frac{E_{k1}E_k+\xi_{k1}\xi_k-\Delta_{k1}\Delta_k}{E_{k1}E_k}\kappa(E_{k1}-E_k)\left\langle k_1^-\right|\rho_s\left|k_1^-\right\rangle \\ &\quad -\frac{2}{N}\sum_{k1^-\neq 0}\frac{E_{k1}E_{k=0}+\xi_{k1}\xi_{k=0}-\Delta_{k1}\Delta_{k=0}}{E_{k1}E_{k=0}}\kappa(E_{k=0}-E_{k1}) \\ &\quad \left\langle GS^-_{(k=0)}\right|\rho_s\left|GS^-_{(k=0)}\right\rangle\ . \end{aligned} \tag{3.4.19}$$

$$\begin{aligned}\frac{d\left\langle k^-\right|\rho_s\left|k^-\right\rangle}{dt} &= \frac{2}{N}\sum_{k1^-\neq k,0}\frac{E_{k1}E_k+\xi_{k1}\xi_k-\Delta_{k1}\Delta_k}{E_{k1}E_k}\kappa(E_{k1}-E_k)\left\langle k_1^-\right|\rho_s\left|k_1^-\right\rangle \\ &\quad -\frac{2}{N}\sum_{k1^-\neq k^-}\frac{E_{k1}E_k+\xi_{k1}\xi_k-\Delta_{k1}\Delta_k}{E_{k1}E_k}\kappa(E_k-E_{k1})\left\langle k^-\right|\rho_s\left|k^-\right\rangle \\ &\quad +\frac{2}{N}\frac{E_{k=0}E_k+\xi_{k=0}\xi_k-\Delta_{k=0}\Delta_k}{E_{k=0}E_k}\kappa(E_{k=0}-E_k)\left\langle GS^-_{(k=0)}\right|\rho_s\left|GS^-_{(k=0)}\right\rangle\ . \end{aligned} \tag{3.4.20}$$

Fig.3.17 depicts the numerical determined relaxation rate r_k of singly excited states $\left|k^-\right\rangle$ to $\left|GS^-_{(k=0)}\right\rangle$. The relaxation rate is fully determined by the excitation energy, as the higher excited states are also able to relax via lower energetic states.

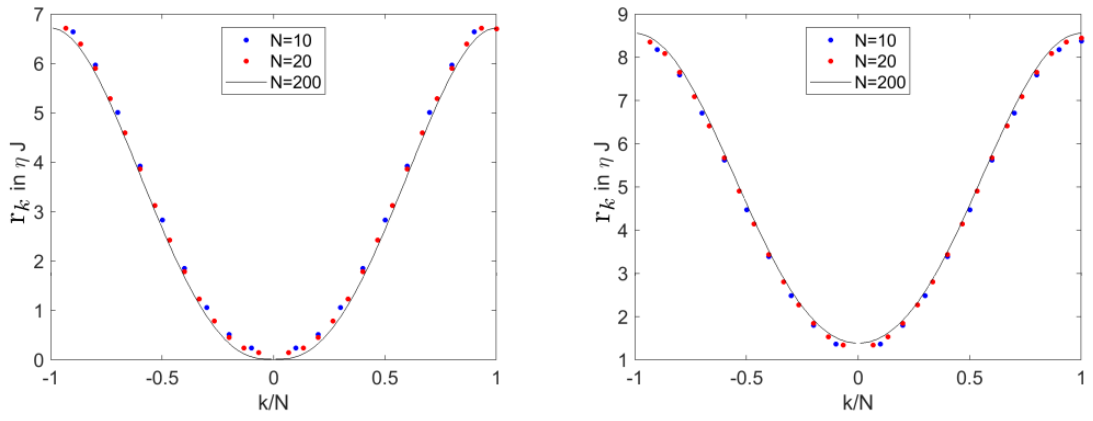

(a) $k_BT = 0$ (b) $k_BT = J$

Figure 3.17: Relaxation rate of the odd parity subspace of a state $\left|k^-\right\rangle$ for different number of spins at $t/J = 2$. The relaxation rate does not depend on N, higher energetic states do relax faster as states with low energy, as higher energy states can relax into more other lower lying states leading to an increased relaxation rate. At higher temperature the rates are increased.

3.4.6 Overview

For local coupling to the environment the decoherence is determined by the gap energy in the topological regime, as the interaction of the lowest states are always with states that are gapped with the gap energy $E_{gap} \sim 2E_k$, see Fig.3.18. For the trivial regime there is additionally to the interaction with the gapped states, also the interaction of $|GS^-_{(k=0)}\rangle$ with states $\gamma^\dagger_{k1^-}\gamma_{k=0}\,|GS^-_{(k=0)}\rangle = |k_1^-\rangle$ with energy difference $E_{k1} - E_{k=0} << E_{gap}$ smaller than the gap energy.
Hence we only have exponential suppression of the decoherence rate at $k_BT << E_{gap}$ in the topological regime, as the additional interaction in the trivial regime leads to an increased rate at low temperature.
In Fig.3.20 the total decoherence rate of $\langle GS^+|\,\rho_s\,|GS^-\rangle = e^{-\Gamma_{dec}t}\,\langle GS^+|\,\rho_s(0)\,|^-\rangle$ is shown, the decoherence rate is strongly suppressed at low temperature in the topological regime, whereas in the trivial regime the two states are not protected against dephasing, because interaction as well as the pure dephasing contribution are leading to an increase in the trivial regime.

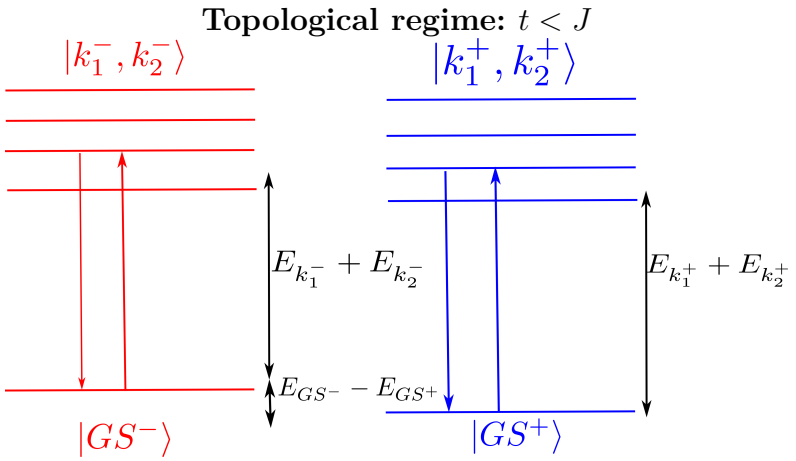

Figure 3.18: Even parity subspace in blue and odd parity subspace in red. In the topological regime the two (nearly degenerate) lowest states can interact only with states $|k, q\rangle$ (with the respective parity) gapped by the energy $E_{gap} = E_k + E_q$. Hence that decoherence rate is determined by the gap energy E_{gap} and the number of excited states the two lowest states can interact (scales with N).

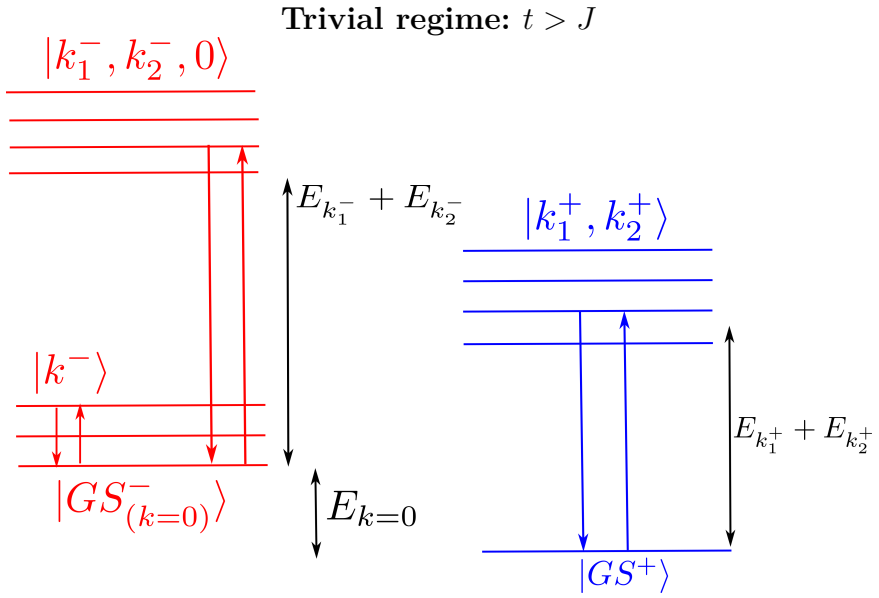

Figure 3.19: Even parity subspace in blue and odd parity subspace in red. In the trivial regime the lowest states can interact with states gapped by the energy $E_{gap} = E_{k1} + E_{k2}$. The lowest state of the odd subspace $|GS^-_{(k=0)}\rangle$ can also interact with slightly higher excited states $|k^-\rangle = \gamma_k^\dagger \gamma_{k=0} |GS^-_{(k=0)}\rangle$ with energy difference $E_k - E_0 << E_{gap}$.

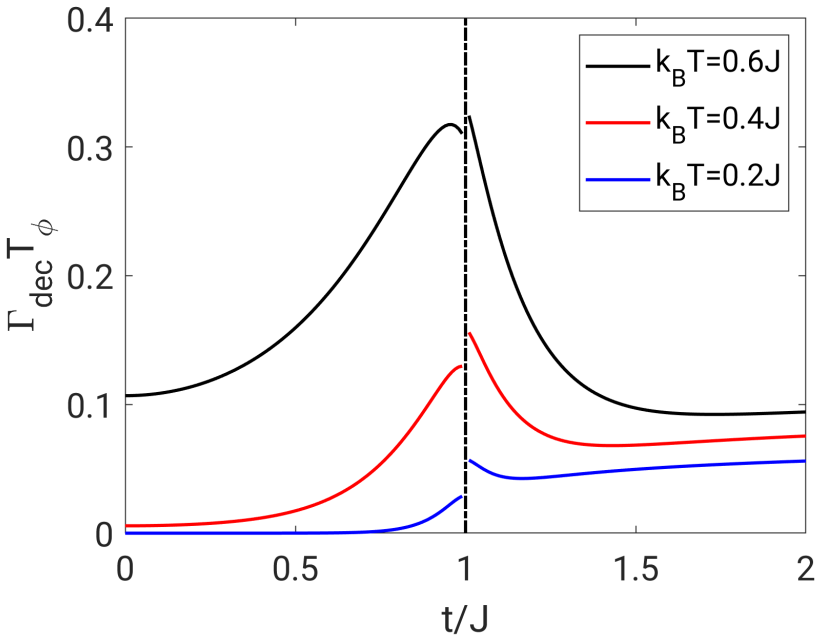

Figure 3.20: Decay rate $\Gamma_{dec} = \theta(t-J)\left(\frac{1}{NT_\phi} + \Gamma_l\right) + \Gamma_\pm^{(l)}$ of the coherence between the two lowest states $|GS^+\rangle$ and $|GS^-\rangle$ normalized with the single spin dephasing rate $\frac{1}{T_\phi} = \eta\pi k_B T$ (see 1.3) for $N = 40$ spins. At low temperature the dephasing rate can be strongly suppressed in the topological regime.

Chapter 4

Dissipation in the open Ising chain

For the open chain, the same interaction to the environment H_B is assumed

$$H = H_s + H_B + H_{int} \tag{4.0.1}$$

$$H_s = -t \sum_{i}^{N} \sigma_i^z - J \sum_{i}^{N-1} \sigma_i^x \sigma_{i+1}^x \tag{4.0.2}$$

$$H_{int} = \sum_{i=1}^{N} \sigma_i^z \hat{B}_i \,. \tag{4.0.3}$$

4.1 Transformation of the interaction

In the open chain there is no discrimination between the even and the odd parity subspace, thus using the Jordan-Wigner transformation and the transformation for diagonalizing the quadratic fermionic Hamiltonian (see 2.2.1) leads for the parity conserving coupling term to

$$\sigma_n^z = 1 - 2 \sum_{i,j} \left[\left(u_{in}^* u_{jn} - v_{jn} v_{in}^* \right) \gamma_i^\dagger \gamma_j + \left(v_{in} u_{jn} \gamma_i \gamma_j + h.c. \right) \right] , \tag{4.1.1}$$

whereas $i = 0, ..., N-1$, $u_{in} = u_{k_i,n}$, $v_{in} = v_{k_i,n}$ and $\gamma_i = \gamma_{k_i}$ as introduced in the notation in 2.2.3 for simplification ($i = 0$ the lowest excitation and $i = N-1$ the largest excitation in energy).
By using the time evolution of the eigenoperators γ_i and $\gamma_i^\dagger$ we find the time evolution of the interaction

$$\sigma_n^z(t) = 1 - 2 \sum_{i,j} \left[e^{i(E_i - E_j)t} \left(u_{in}^* u_{jn} - v_{jn} v_{in}^* \right) \gamma_i^\dagger \gamma_j + \left(e^{-i(E_j + E_i)t} v_{in} u_{jn} \gamma_i \gamma_j + h.c. \right) \right] . \tag{4.1.2}$$

4.2 Master equation

With the bath correlator $F_{n_1,n_2}(t-t')$, the Redfield master equation can be expressed in the compact form

$$\frac{d\rho_s}{dt} = -\int_{t_0}^{t} dt' \sum_{n_1,n_2} \Bigg(F_{n_1,n_2}(t-t')[\sigma^z_{n_1}(t), \sigma^z_{n_2}(t')\rho_s(t)] + F_{n_2,n_1}(t'-t)[\rho_s(t)\sigma^z_{n_2}(t'), \sigma^z_{n_1}(t)] \Bigg). \tag{4.2.1}$$

In the appendix D the complete Lindblad master equation is derived starting from the Redfield master equation. With the use of the Rotating Wave Approximation and omitting the Lamb shift terms, we arrive to

$$\begin{aligned}
\frac{d\rho_s}{dt} = \sum_{n1,n2} \Bigg(& 4 \sum_{i1,i2,j1,j2} A_{i1,j1,n1} A_{i2,j2,n2} \delta_{E_{i1}-E_{j1},E_{j2}-E_{i2}} \\
& \left(\kappa_{n1,n2}(E_{i1}-E_{j1}) \left(\gamma^\dagger_{i2}\gamma_{j2}\rho_s\gamma^\dagger_{i1}\gamma_{j1} - \frac{1}{2}\{\gamma^\dagger_{i1}\gamma_{j1}\gamma^\dagger_{i2}\gamma_{j2}, \rho_s\} \right) \right) \\
& + 4 \sum_{i1,i2,j1,j2} A_{i1,j1,n1} u_{j2,n2} v_{i2,n2} \delta_{E_{i1}-E_{j1},E_{i2}+E_{j2}} \\
& \left(\kappa_{n1,n2}(E_{i1}-E_{j1}) \left(\gamma_{i2}\gamma_{j2}\rho_s\gamma^\dagger_{i1}\gamma_{j1} - \frac{1}{2}\{\gamma^\dagger_{i1}\gamma_{j1}\gamma_{i2}\gamma_{j2}, \rho_s\} \right) \right) \\
& + 4 \sum_{i1,i2,j1,j2} A_{i1,j1,n1} u^*_{j2,n2} v^*_{i2,n2} \delta_{E_{i1}-E_{j1},-E_{i2}-E_{j2}} \\
& \left(\kappa_{n1,n2}(E_{i1}-E_{j1}) \left(\gamma^\dagger_{j2}\gamma^\dagger_{i2}\rho_s\gamma^\dagger_{i1}\gamma_{j1} - \frac{1}{2}\{\gamma^\dagger_{i1}\gamma_{j1}\gamma^\dagger_{j2}\gamma^\dagger_{i2}, \rho_s\} \right) \right) \\
& + 4 \sum_{i1,i2,j1,j2} u_{j1,n1} v_{i1,n2} A_{i2,j2,n2} \delta_{E_{i1}+E_{j1},E_{i2}-E_{j2}} \\
& \left(\kappa_{n1,n2}(-E_{i1}-E_{j1}) \left(\gamma^\dagger_{i2}\gamma_{j2}\rho_s\gamma_{i1}\gamma_{j1} - \frac{1}{2}\{\gamma_{i1}\gamma_{j1}\gamma^\dagger_{i2}\gamma_{j2}, \rho_s\} \right) \right) \\
& + 4 \sum_{i1,i2,j1,j2} u_{j1,n1} v_{i1,n1} u^*_{j2,n2} v^*_{i2,n2} \delta_{E_{i1}+E_{j1},E_{i2}+E_{j2}} \\
& \left(\kappa_{n1,n2}(-E_{i1}-E_{j1}) \left(\gamma^\dagger_{j2}\gamma^\dagger_{i2}\rho_s\gamma_{i1}\gamma_{j1} - \frac{1}{2}\{\gamma_{i1}\gamma_{j1}\gamma^\dagger_{j2}\gamma^\dagger_{i2}, \rho_s\} \right) \right) \\
& + 4 \sum_{i1,i2,j1,j2} u^*_{j1,n1} v^*_{i1,n1} u_{j2,n2} v_{i2,n2} \delta_{E_{i1}+E_{j1},E_{i2}+E_{j2}} \\
& \left(\kappa_{n1,n2}(E_{i1}+E_{j1}) \left(\gamma_{i2}\gamma_{j2}\rho_s\gamma^\dagger_{j1}\gamma^\dagger_{i1} - \frac{1}{2}\{\gamma^\dagger_{j1}\gamma^\dagger_{i1}\gamma_{i2}\gamma_{j2}, \rho_s\} \right) \right) \\
& + 4 \sum_{i1,i2,j1,j2} u^*_{j1,n1} v^*_{i1,n1} A_{i2,j2,n2} \delta_{E_{i1}+E_{j1},E_{j2}-E_{i2}} \\
& \left(\kappa_{n1,n2}(E_{i1}+E_{j1}) \left(\gamma^\dagger_{i2}\gamma_{j2}\rho_s\gamma^\dagger_{j1}\gamma^\dagger_{i1} - \frac{1}{2}\{\gamma^\dagger_{j1}\gamma^\dagger_{i1}\gamma^\dagger_{i2}\gamma_{j2}, \rho_s\} \right) \right) \Bigg),
\end{aligned} \tag{4.2.2}$$

with $A_{i,j,n} = v_{jn}v^*_{in} - u^*_{in}u_{jn}$ and $\kappa_{n1,n2}(\omega) = \int_{-\infty}^{\infty} dt e^{i\omega t} F_{n_1,n_2}(t)$ the Fourier transform of the bath correlator.

4.3 Global bath coupling

For a global bath the correlator of the bath does not depend on the spin sites, such that for ohmic spectral density $K(\omega) = \eta\omega$, we have

$$\kappa_{n1,n2}(\omega) = \kappa(\omega) = K(\omega)\left[\theta(\omega)(1 + n_B(\omega)) + \theta(-\omega)n_B(-\omega))\right] \tag{4.3.1}$$

With the bosonic distribution function $n_B(\omega)$.

4.3.1 Decoherence

The off diagonal element between the two lowest states $|GS\rangle$ (even parity) and $|0\rangle = \gamma_0^\dagger |GS\rangle$ (odd parity), which is nearly degenerate with the ground state in the topological regime (see 2.2.2), reads in the whole parameter regime as

$$\begin{aligned}
\frac{d\langle GS|\rho_s|0\rangle}{dt} = \sum_{n1,n2}\Bigg(& -2\sum_{i1,i2} A_{0,i1,n1}A_{i1,0,n2}\kappa(E_0 - E_{i1})\langle GS|\rho_s|0\rangle \\
& + 4\sum_{i1,i2,j1} A_{i1,0,n1}u_{j1,n2}v_{i2,n2}\delta_{E_{i1}-E_0,E_{i2}+E_{j1}}\kappa(E_{i1} - E_0)\langle i_2, j_1|\rho_s|i_1\rangle \\
& - 2\sum_{i1,j1} u_{j1,n1}v_{i1,n1}(u^*_{j1,n2}v^*_{i1,n2} - u^*_{i1,n2}v^*_{j1,n2})\kappa(-E_{i1} - E_{j1})\langle GS|\rho_s|0\rangle \\
& - 2\sum_{i1,j1\neq 0} u_{j1,n1}v_{i1,n1}(u^*_{j1,n2}v^*_{i1,n2} - u^*_{i1,n2}v^*_{j1,n2})\kappa(-E_{i1} - E_{j1})\langle GS|\rho_s|0\rangle \\
& + 4\sum_{i1,i2,j1,j2} u^*_{j1,n1}v^*_{i1,n1}u_{j2,n2}v_{i2,n2}\delta_{E_{i1}+E_{j1},E_{i2}+E_{j2}} \\
& \kappa(E_{i1} + E_{j1})\langle GS|\gamma_{i2}\gamma_{j2}\rho_s\gamma^\dagger_{j1}\gamma^\dagger_{i1}|0\rangle\Bigg).
\end{aligned} \tag{4.3.2}$$

with $|i\rangle = \gamma_i^\dagger |GS\rangle$ (with i=0,..,N-1) as discussed in 2.2.3.
At low temperature $\kappa(E_{i1}+E_{j1}) > \kappa(E_i - E_0) >> \kappa(E_0 - E_{j1}) > \kappa(-E_{k1} - E_{j1})$, thus in the steady state solution $\langle GS|\rho_s|0\rangle_s >> \langle i_2, j_2|\rho_s|i_1\rangle_s > \langle GS|\gamma_{i2}\gamma_{j2}\rho_s\gamma^\dagger_{j1}\gamma^\dagger_{i1}|0\rangle_s \approx 0$. Therefore one can assume $\langle i_2, j_2|\rho_s|i_1\rangle(t) \approx 0$ and $\langle GS|\gamma_{i2}\gamma_{j2}\rho_s\gamma^\dagger_{j1}\gamma^\dagger_{i1}|0\rangle(t) \approx 0$ if

the initial value of these matrix elements are zero. Hence at low temperature the off diagonal element between the two lowest states reads

$$\begin{aligned}
\frac{d\langle GS|\rho_s|0\rangle}{dt} &= \sum_{n1,n2}\Bigg(-2\sum_{i1}A_{0,i1,n1}A_{i1,0,n2}\kappa(E_0-E_{i1}) \\
&\quad -2\sum_{i1,j1}u_{j1,n1}v_{i1,n1}(u^*_{j1,n2}v^*_{i1,n2}-u^*_{i1,n2}v^*_{j1,n2})\kappa(-E_{i1}-E_{j1}) \\
&\quad -2\sum_{i1,j1\neq 0}u_{j1,n1}v_{i1,n1}(u^*_{j1,n2}v^*_{i1,n2}-u^*_{i1,n2}v^*_{j1,n2})\kappa(-E_{i1}-E_{j1})\Bigg)\langle GS|\rho_s|0\rangle \\
&= \Bigg(-2\underbrace{\sum_{n1,n2}A_{0,0,n1}A_{0,0,n2}}_{G}\kappa_0-\underbrace{2\sum_{n1,n2}\sum_{i1\neq 0}A_{0,i1,n1}A_{i1,0,n2}\kappa(E_0-E_{i1})}_{\Gamma_s} \\
&\quad -2\sum_{n1,n2}\sum_{i1,j1}u_{j1,n1}v_{i1,n1}(u^*_{j1,n2}v^*_{i1,n2}-u^*_{i1,n2}v^*_{j1,n2})\kappa(-E_{i1}-E_{j1}) \\
&\quad \underbrace{-2\sum_{n1,n2}\sum_{i1,j1\neq 0}u_{j1,n1}v_{i1,n1}(u^*_{j1,n2}v^*_{i1,n2}-u^*_{i1,n2}v^*_{j1,n2})\kappa(-E_{i1}-E_{j1})}_{\Gamma_d}\Bigg)\langle GS|\rho_s|0\rangle \\
&= -\left(2G\kappa_0+\Gamma_s+\Gamma_d\right)\langle GS|\rho_s|0\rangle\,, \qquad (4.3.3)
\end{aligned}$$

with the expressions

$$\begin{aligned}
u_{in} &= \frac{1}{2}\left(\phi_{k_i n}+\psi_{k_i n}\right) = c\left(s_{k_i}\sin(k_i n)+\sin(k_i(N+1-n))\right) \\
v_{in} &= \frac{1}{2}\left(\phi_{k_i n}+\psi_{k_i n}\right) = c\left(\sin(k_i(N+1-n))-s_{k_i}\sin(k_i n)\right) \\
G &= \sum_{n1,n2}A_{0,0,n1}A_{0,0,n2} = \left(\sum_{n1}\phi_{k_0,n1}\psi_{k_0,n1}\right)^2\,, \qquad (4.3.4)
\end{aligned}$$

where c is the normalization constant, such that $\sum_n |\phi_n|^2 = 1$.
Thus the coherence of the two lowest states decays exponentially with the prefactor in eq.4.3.3 as decay rate.
First lets have a look on the function G, which describes the global overlap between ϕ_{k_0} and ψ_{k_0}. In the topological regime these represent the localized solution with only small overlap. Hence the pure dephasing contribution of the single spin dephasing rate $2\kappa_0 = 1/T_\phi$ drops out for $(t/J)^N \to 0$, see Fig.4.1. In the trivial regime there is an increase by the single spin dephasing rate, as $G \sim 1$ (no localized solution anymore).
Besides there is Γ_s contributing to the decoherence rate, due to the interaction of $|0\rangle$ with $\gamma_i^\dagger\gamma_0|0\rangle = |i\rangle$ with energy difference $E_i - E_0$. This interaction contribution can be exponentially suppressed for $k_BT << E_i - E_0$, see Fig.4.2(a).
The last term in the decoherence rate Γ_d is due to the interaction of the two lowest states with higher excited states (e.g. $|GS\rangle$ with $\gamma_{i1}^\dagger\gamma_{i2}^\dagger|GS\rangle = |i_1, i_2\rangle$) with energy difference of $E_{i1} + E_{i2}$ and can be suppressed as well at low temperature, see Fig.4.2(b).
Due to the reduced gap energy to higher excited states near the critical point $\Gamma_s + \Gamma_d$ is increased at this point, see Fig.4.3.
At low temperature (e.g. $k_BT = 0.3J$) the decoherence rate does not scale with N (plotted in Fig.4.3(a)) for $t << J$.

Besides for $t >> J$ the rate Γ_s tends to zero for global bath coupling, indicating also suppressed interaction of $|0\rangle$ with $|i\rangle$ in the trivial regime (see also next chapter).

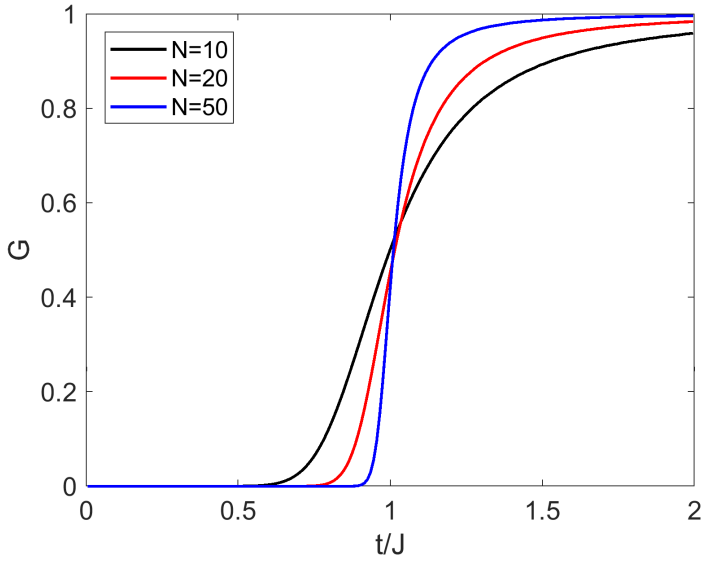

Figure 4.1: G (eq.4.3.4) plotted over t/J for different numbers of spins. The function describes the overlap of the localized solutions in the topological regime (scales with $(t/J)^N$), where G tends to zero. In the trivial regime it tends to 1 (no localized solution anymore).

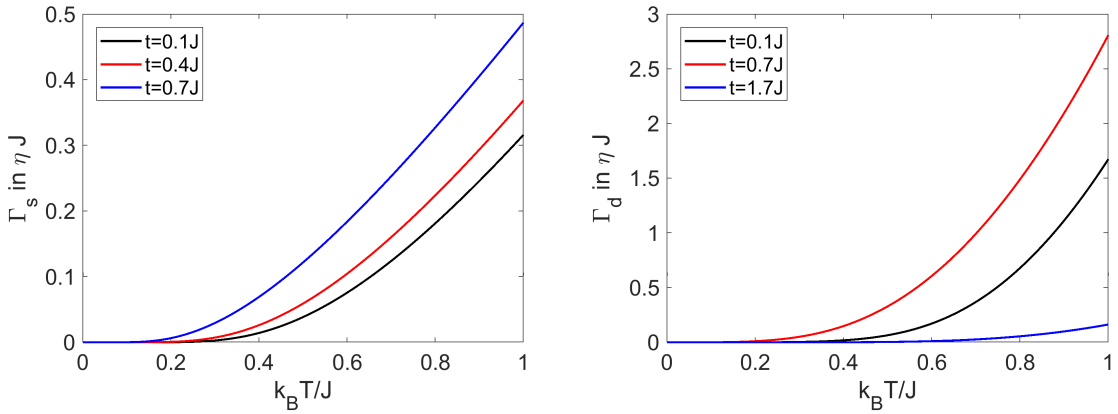

(a) Γ_s (b) Γ_d

Figure 4.2: Γ_s and Γ_d (eq.4.3.3) plotted over the temperature for $N = 20$. Γ_d is suppressed for $k_BT << E_{i1} + E_{i2}$ and Γ_s for $k_BT << E_i - E_0 < E_{i1} + E_{i2}$.

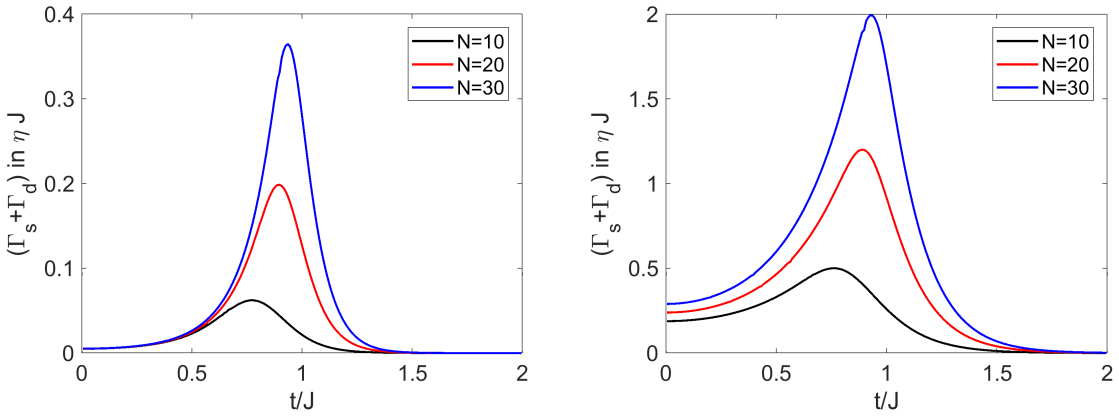

(a) $k_BT = 0.3J$ (b) $k_BT = 0.6J$

Figure 4.3: $\Gamma_s + \Gamma_d$ (eq.4.3.3) at $k_BT = 0.3J$ (a) and $k_BT = 0.6J$ (b) plotted over t/J. At low temperature $\Gamma_s + \Gamma_d$ do not scale with N for small t/J. Close to $t = J$ the rate $(\Gamma_s + \Gamma_d)$ is increased and scales strongly with N. Whereas for large t/J the rate $(\Gamma_s + \Gamma_d)$ tends to zero.

4.3.2 Energy relaxation

Here we will focus on the relaxation of the lowest possible excitation for each subspace. Such that for the even parity subspace the states $|i_1, i_2\rangle$ (which relax to $|GS\rangle$) will be analyzed.
The connection to higher excited states will be neglected as for low temperature their steady state solution will be approximately zero, thus if not initially occupied they can be approximated by zero occupation

$$\begin{aligned}\frac{d\langle GS|\rho_s|GS\rangle}{dt} = -4\sum_{n1,n2}\sum_{i1,i2,j1,j2} & u_{j1,n1}v_{i1,n1}(u^*_{j1,n2}v^*_{i1,n2} - u^*_{i1,n2}v^*_{j1,n2}) \\ & \kappa(-E_{i1} - E_{j1})\langle GS|\rho_s|GS\rangle \\ & + 4\sum_{n1,n2}\sum_{i1} u^*_{j1,n1}v^*_{i1,n1}(u_{j1,n2}v_{i1,n2} - u_{i1,n2}v_{j1,n2}) \\ & \kappa(E_{i1} + E_{j1})\langle i_1, j_1|\rho_s|i_1, j_1\rangle \ . \end{aligned} \tag{4.3.5}$$

Neglecting the interaction with higher excited states the equation for the lowest excitations with even parity reads

$$\begin{aligned}\frac{d\left\langle i_1,j_1\right|\rho_s\left|i_1,j_1\right\rangle}{dt} = \sum_{n1,n2}\Bigg(&4\sum_{i2\neq j_1}A_{i2,i1,n1}A_{i1,i2,n2}\kappa(E_{i2}-E_{i1})\left\langle j_1,i_2\right|\rho_s\left|j_1,i_2\right\rangle\\ &+4\sum_{i2\neq i_1}A_{i2,j1,n1}A_{j1,i2,n2}\kappa(E_{i2}-E_{j1})\left\langle i_1,i_2\right|\rho_s\left|i_1,i_2\right\rangle\\ &-4\sum_{i2\neq i_1}A_{j1,i2,n1}A_{i2,j1,n2}\kappa(E_{j1}-E_{i2})\left\langle i_1,j_1\right|\rho_s\left|i_1,j_1\right\rangle\\ &-4\sum_{i2\neq j_1}A_{i1,i2,n1}A_{i2,i1,n2}\kappa(E_{i1}-E_{i2})\left\langle i_1,j_1\right|\rho_s\left|i_1,j_1\right\rangle\\ &+8u_{i1,n1}v_{j1,n1}(u^*_{i1,n2}v^*_{j1,n2}-u^*_{j1,n2}v^*_{i1,n2})\kappa(-E_{i1}-E_{j1})\left\langle GS\right|\rho_s\left|GS\right\rangle\\ &-8u_{i1,n1}v_{j1,n1}(u^*_{i1,n2}v^*_{j1,n2}-u^*_{j1,n2}v^*_{i1,n2})\kappa(E_{i1}+E_{j1})\left\langle i_1,j_1\right|\rho_s\left|i_1,j_1\right\rangle\Bigg).\end{aligned} \tag{4.3.6}$$

And for the odd parity sector we have for the lowest excitations (neglecting interaction with higher excited states for low temperature, as $\kappa(-E_i) >> \kappa(-E_{i1}-E_{i2})$):

$$\begin{aligned}\frac{d\left\langle i\right|\rho_s\left|i\right\rangle}{dt} = \sum_{n1,n2}\Bigg(&4\sum_{j1}A_{j,i,n1}A_{i,j,n2}\kappa(E_j-E_i)\left\langle j\right|\rho_s\left|j\right\rangle\\ &-4\sum_{j}A_{i,j,n1}A_{j,i,n2}\kappa(E_i-E_j)\left\langle i\right|\rho_s\left|i\right\rangle\Bigg),\end{aligned} \tag{4.3.7}$$

with the notation that $i,j=0,...N-1$ with increasing energy of the referring state as introduced in 2.2.3 (e.g. the state $|0\rangle$ has the lowest energy).
The numerical results of the relaxation rate r_{i_1,i_2} of a state $|i_1,i_2\rangle$ to the ground state $|GS\rangle$ is plotted in Fig.4.4, and the numerical result for the relaxation rate r_i of a state $|i\rangle$ to $|0\rangle$ is plotted in Fig.4.5.
The relaxation is similar as for the closed chain, where only states with the excitation $|k,-k\rangle$ (two degenerate excitation k and $-k$) can relax to $|GS\rangle$ (such that the total pseudo-momentum k is conserved). This is similar for the open chain such that states with $|i,i+1\rangle$ (two excitations with nearly the same energy) have some finite relaxation rate, and for all other states it is strongly suppressed (see Fig.4.4).
Besides there is an additional symmetry in the interaction for a global bath coupling. E.g. in the topological regime there are also the states $|0,i\rangle=\gamma_0^\dagger\gamma_i\left|GS\right\rangle$, which have finite relaxation rates for $i=odd$ and no relaxation to $|GS\rangle$ for $i=even$. The reason for that is the symmetry of the wave functions $(u_i(n))$ in respect to $n\leftrightarrow N+1-n$ (which only appears for the open chain with two ends).
If you e.g. assume a symmetric mode $u_s(n)=u_s(N+1-n)$ and the antisymmetric mode $u_a(n)=-u_a(N+1-n)$ (in respect to the fermionic occupation $\hat{n}_n$) the global overlap guided by the global bath is always zero $\sum_n u_s(n)u_a(n)=0$.
Hence only interaction between states with the same symmetry in respect to the two ends of the chain is possible, which is depicted in Fig.4.4 in the "checkerboard" like pattern.
The same behavior can be also seen in the odd parity subspace (see Fig.4.5), where only $|i=even\rangle$ states can relax to the zero mode $|0\rangle$, due to the symmetry reasons in

respect of the ends of the chain. Here one can also see that in the trivial regime the interaction/relaxation is strongly suppressed for single excited states $|i\rangle$ to $|0\rangle$.

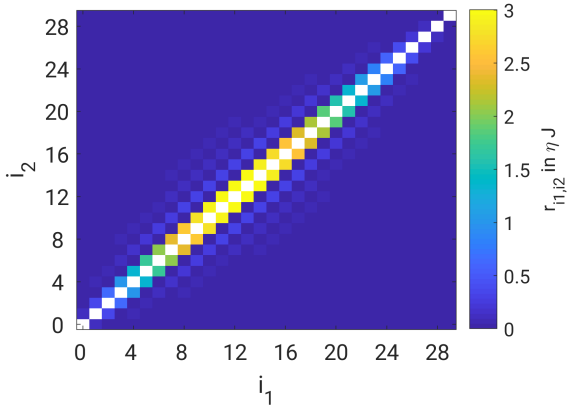

(a) $t/J = 2$

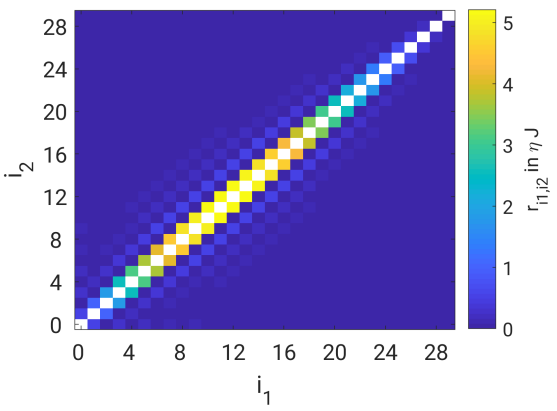

(b) $t/J = 0.9$

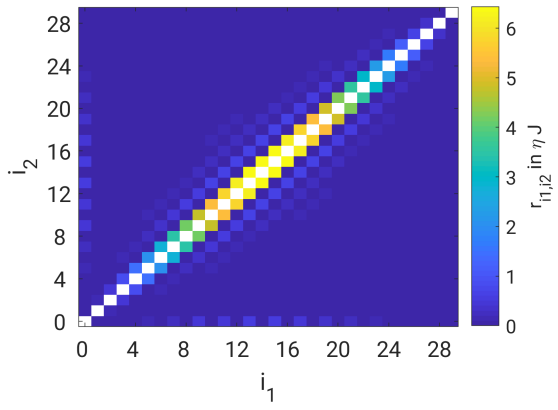

(c) $t/J = 0.1$

Figure 4.4: Comparison of the energy relaxation r_{i_1,i_2} of a state $|i_1, i_2\rangle$ to $|GS\rangle$ (where i is the index, such that $i = 0$ is the lowest excitation and $i = N-1$ the largest excitation in energy) for $N = 30$ spins at zero temperature for different ratio t/J. For most states the relaxation process is strongly suppressed, only the relaxation for $|i, i+1\rangle$ is not suppressed. Besides one can see that only certain states (e.g. $|i = odd, 0\rangle$) have finite relaxation rates, due to symmetry reasons (see text).

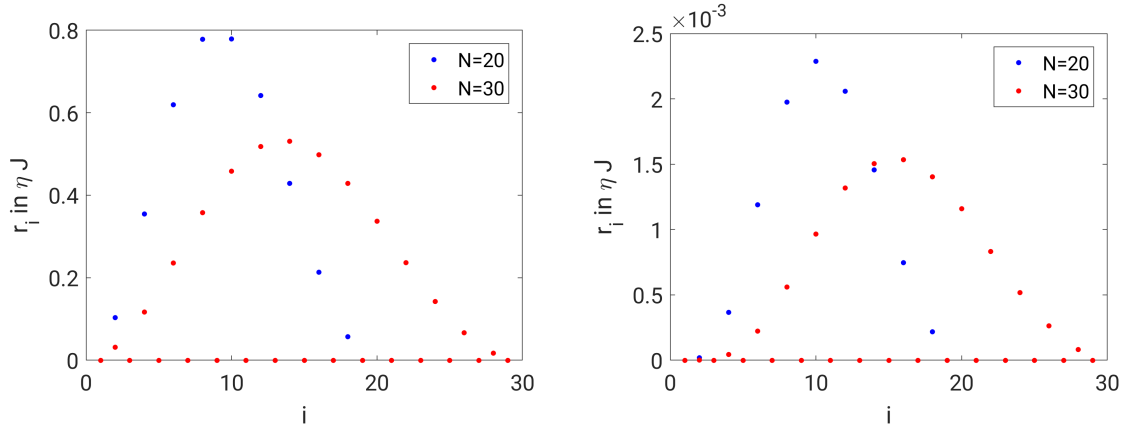

(a) $t/J = 0.1$ (b) $t/J = 2$

Figure 4.5: Energy relaxation rate r_i of the odd subspace for the lowest excitation $|i\rangle$ to $|0\rangle$ at different ratio t/J. One can see that the relaxation is strongly suppressed in the trivial regime, the relaxation rate is several magnitudes lower as in the topological regime. States which have symmetric $u_{i=even}(n)$ in respect to the ends of the chain can relax to the state $|0\rangle$. Other modes with anti symmetric $u_{i=odd}(n)$ have zero global overlap with $|0\rangle$ and thus cannot relax to this state.

4.3.3 Overview

For global coupling to the environment there is interaction to higher excited states with energy difference $E_{i1} + E_{i2}$ (e.g. $|GS\rangle$ with $|i_1, i_2\rangle$) in the whole parameter regime. The interaction is (mainly) with states $|i, i+1\rangle$ for $|GS\rangle$ in the trivial regime, as the interaction with other states is negligible for $t > J$ (see 4.3.2).
Besides there is also interaction to states with a singly excited states in the topological regime as depicted in Fig.4.6 with energy difference $\sim E_i$. Due to the global coupling there is a symmetry restricted interaction (in respect to the two ends of the chain, see 4.3.2).
For the trivial regime there is additionally to the interaction with excited states also a pure dephasing contribution to the decoherence rate.
In Fig.4.8 the total decoherence rate of $\langle GS| \rho_s |0\rangle = e^{-\Gamma_{dec} t} \langle GS| \rho_s(0) |0\rangle$ is shown, the decoherence rate is strongly suppressed at low temperature in the topological regime, whereas in the trivial regime the two states are not protected against dephasing, due to additional pure dephasing in this regime.

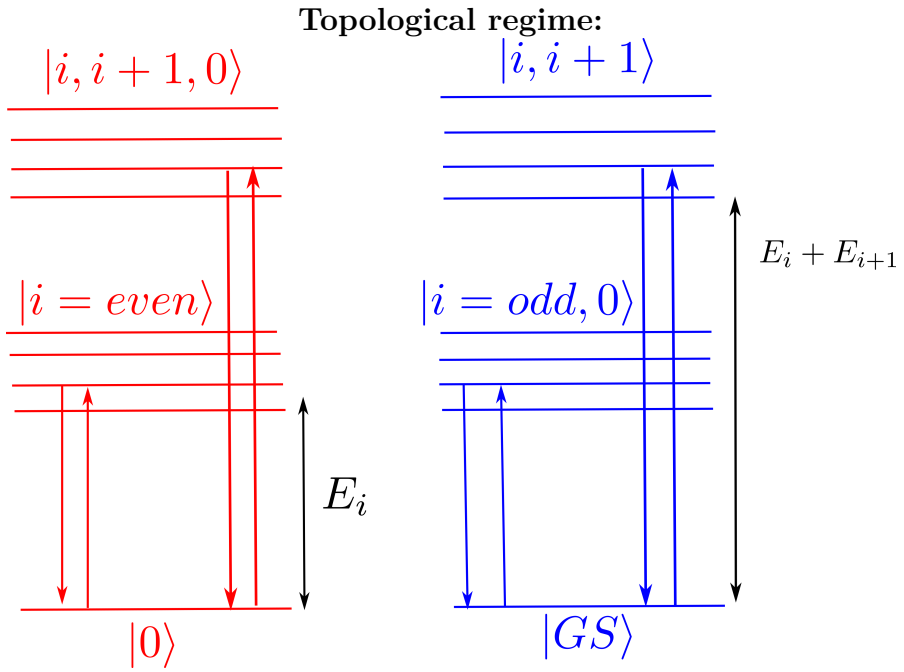

Figure 4.6: In the topological regime both ground states can interact with states with a single finite energy mode and energy difference $\sim E_i$ and states gapped by the energy $E_i + E_{i+1}$.

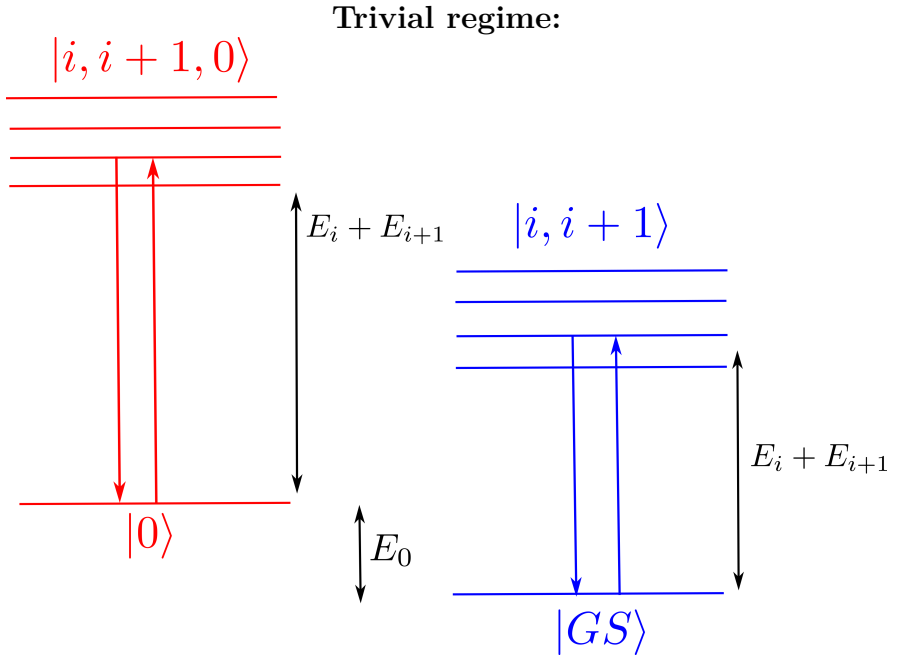

Figure 4.7: In the trivial regime the lowest states can interact with states gapped by the energy $E_i + E_{i+1}$. Besides the lowest states do not belong to the same excitational subspace anymore, as $|0\rangle$ is now a finite energy state.

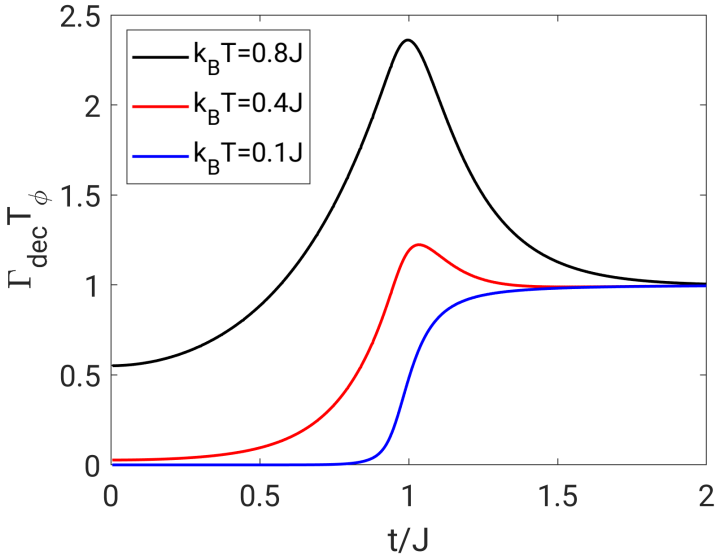

Figure 4.8: Decay rate $\Gamma_{dec} = \frac{G}{T_\phi} + \Gamma_s + \Gamma_d$ (eq.4.3.3) of the coherence between the two lowest states $|GS\rangle$ and $|0\rangle$ normalized with the single spin dephasing rate $\frac{1}{T_\phi} = \eta \pi k_B T$ (see 1.3) for $N = 40$ spins. At low temperature the dephasing rate can be strongly suppressed in the topological regime.

4.4 Local bath coupling

When each spin is locally coupled to a bosonic bath, the symmetrized noise correlator is only nonzero at the same spin sites

$$\kappa_{n1,n2}(\omega) = \delta_{n1,n2}\kappa(\omega)\,. \tag{4.4.1}$$

Hence we have to insert in the Lindblad equation the additional $\delta_{n1,n2}$ terms (in eq.4.3.3).

4.4.1 Decoherence

At low temperature the same approximation as for the global bath can be done, hence the off diagonal element between the two lowest states in the low temperature approximation reads

$$\begin{aligned}\frac{d\,\langle GS|\,\rho_s\,|0\rangle}{dt} = \Bigg(& \underbrace{-2\sum_{n1} A_{0,0,n1}A_{0,0,n1}}_{G^{(l)}}\,\kappa_0 \underbrace{-2\sum_{n1}\sum_{i1\neq 0} A_{0,i1,n1}A_{i1,0,n1}\kappa(E_0-E_{i1})}_{\Gamma_s^{(l)}} \\ & -2\sum_{n1}\sum_{i1,j1} u_{j1,n1}v_{i1,n1}(u^*_{j1,n1}v^*_{i1,n1}-u^*_{i1,n1}v^*_{j1,n1})\kappa(-E_{i1}-E_{j1}) \\ & \underbrace{-2\sum_{n1,n2}\sum_{i1,j1\neq 0} u_{j1,n1}v_{i1,n1}(u^*_{j1,n1}v^*_{i1,n1}-u^*_{i1,n1}v^*_{j1,n1})\kappa(-E_{i1}-E_{j1})}_{\Gamma_d^{(l)}}\Bigg)\,\langle GS|\,\rho_s\,|0\rangle \\ = & -\left(2G^{(l)}\kappa_0+\Gamma_s^{(l)}+\Gamma_d^{(l)}\right)\langle GS|\,\rho_s\,|0\rangle\,.\end{aligned} \tag{4.4.2}$$

with

$$G^{(l)} = \sum_{n1} A_{0,0,n1}A_{0,0,n1} = \sum_n \phi^2_{k_0,n}\psi^2_{k_0,n}\,. \tag{4.4.3}$$

The pure dephasing term $G^{(l)}\kappa_0$ is only nonzero in the trivial phase as depicted in Fig.4.9, as the local overlap $G^{(l)}$ of the localized solutions are zero in the topological regime. In the trivial regime $G^{(l)}$ tends to a constant value depending on N (no localized solutions anymore), leading to a pure dephasing contribution to the total decoherence rate in the trivial regime.
Besides there is $\Gamma_s^{(l)}$ contributing to the decoherence rate, due to interaction of $|0\rangle$ with $\gamma_i^\dagger\gamma_0\,|0\rangle = |i\rangle$ with energy difference $E_i - E_0$, see Fig.4.10(a). For $t < J$ we have $E_0 \approx 0$ and the interaction is gapped by the energy E_i, leading to a suppressed interaction at low temperature. In the trivial regime $E_i - E_0 << E_i$ (as $E_0 \sim E_i$) leading to an increased interaction even at low temperature.
The last term in the decoherence rate $\Gamma_d^{(l)}$ is due to the interaction of the two lowest states with higher excited states(e.g. $|GS\rangle$ with $|i_1, i_2\rangle$) with energy difference of $E_{i1} + E_{i2}$. Hence it is suppressed for $k_BT << E_{i1} + E_{i2}$.
Due to the reduced gap energy to higher excited states at $t = J$, $\Gamma_s^{(l)} + \Gamma_d^{(l)}$ is increased near the critical point (see Fig.4.11). For $t > J$ the gap energy to higher excited states (e.g. $|GS\rangle$ with $|i_1, i_2\rangle$) increases, leading to a decreased rate of $\Gamma_d^{(l)}$. On the other hand the energy difference of $|0\rangle$ with $|i\rangle$ is decreased for $t > J$ (as $|0\rangle$ becomes a finite energy

state in this regime) leading also to an enhanced rate $\Gamma_s^{(l)}$. The interplay of those two different interactions leads to a non-monotonic behavior shown in Fig.4.11.
Besides at low temperature (e.g. $k_BT = 0.3J$ as depicted in Fig.4.11(a)) the decoherence rate does not scale with N for $t << J$.

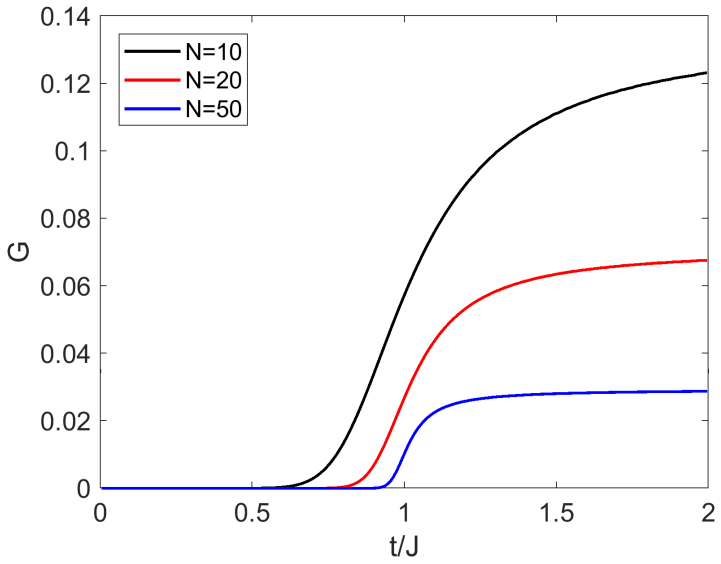

Figure 4.9: $G^{(l)}$ (eq.4.4.3) plotted over t/J for different numbers of spins. The function describes the overlap of the occupation probability of the localized solutions in the topological regime (scales with $(t/J)^N$), where G tends to zero. In the trivial regime it tends to a finite value depending on N (no localized solution anymore).

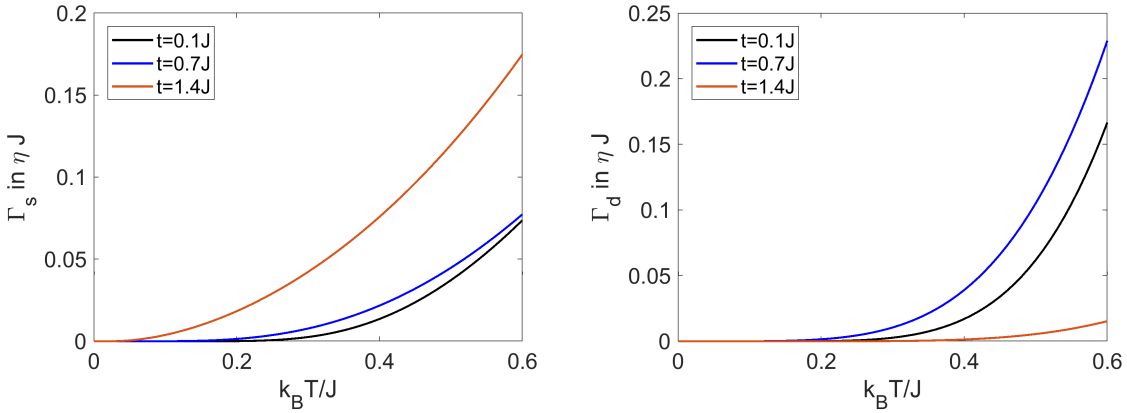

(a) $\Gamma_s^{(l)}$ (b) $\Gamma_d^{(l)}$

Figure 4.10: $\Gamma_s^{(l)}$ and $\Gamma_d^{(l)}$ (eq.4.4.2) plotted over the temperature for $N = 20$. $\Gamma_d^{(l)}$ is suppressed for $k_BT << E_{i1} + E_{i2}$ and Γ_d for $k_BT << E_i - E_0$.

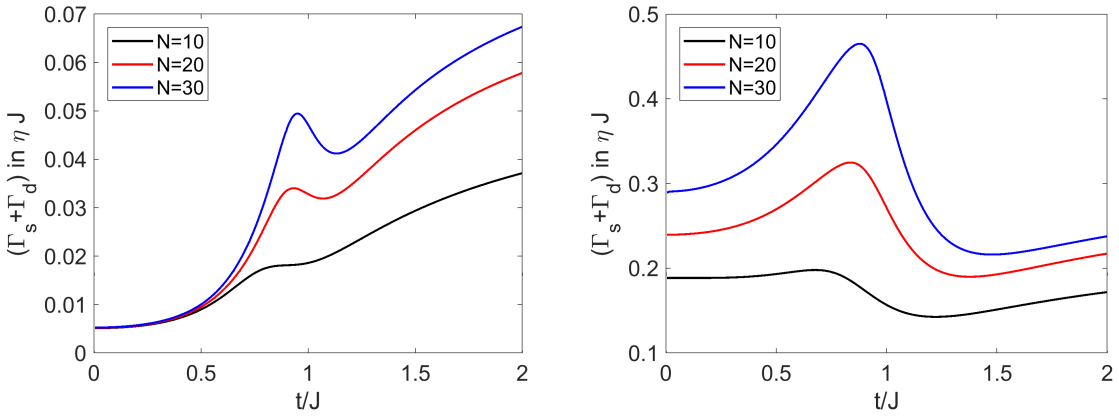

(a) $k_BT = 0.3J$ (b) $k_BT = 0.6J$

Figure 4.11: $\Gamma_s^{(l)} + \Gamma_d^{(l)}$ (eq.4.4.2) at $k_BT = 0.3J$ (a) and $k_BT = 0.6J$ (b) plotted over t/J. At low temperature $\Gamma_s^{(l)} + \Gamma_d^{(l)}$ do not scale with N for small t/J. Close to $t = J$ $\Gamma_s + \Gamma_d$ is increased and scales strongly with N.

4.4.2 Energy relaxation

Here we will focus on the relaxation of the lowest possible excitation for each subspace. Such that in the even parity subspace the relaxation of the states $|i_1, i_2\rangle$,which relax to $|GS\rangle$, will be determined. The connection to higher excited states will be neglected, as for low temperature their steady state solution will be ≈ 0, thus if not initially occupied, they can be approximated with 0

$$\begin{aligned}\frac{d\langle GS|\rho_s|GS\rangle}{dt} = -4\sum_{n1}\sum_{i1,i2,j1,j2} & u_{j1,n1}v_{i1,n1}(u^*_{j1,n1}v^*_{i1,n1} - u^*_{i1,n1}v^*_{j1,n1}) \\ & \kappa(-E_{i1} - E_{j1})\langle GS|\rho_s|GS\rangle \\ & + 4\sum_{n1,n2}\sum_{i1} u^*_{j1,n1}v^*_{i1,n1}(u_{j1,n1}v_{i1,n1} - u_{i1,n1}v_{j1,n1}) \\ & \kappa(E_{i1} + E_{j1})\langle i_1, j_1|\rho_s|i_1, j_1\rangle \end{aligned} \tag{4.4.4}$$

Neglecting the interaction with higher excited states the equation for the lowest excitations with even parity reads

$$\begin{aligned}\frac{d\left\langle i_a,i_b\right|\rho_s\left|i_a,i_b\right\rangle}{dt} = \sum_{n1}\Bigg(&4\sum_{i1\neq i_b} A_{i1,i_a,n1}A_{i_a,i1,n2}\kappa(E_{i1}-E_{i_a})\left\langle i_b,i_1\right|\rho_s\left|i_b,i_1\right\rangle\\ &+4\sum_{i1\neq i_a} A_{i1,i_b,n1}A_{i_b,i1,n1}\kappa(E_{i1}-E_{i_b})\left\langle i_a,i_1\right|\rho_s\left|i_a,i_1\right\rangle\\ &-4\sum_{j1\neq i_a} A_{i_b,j1,n1}A_{j1,i_b,n1}\kappa(E_{i_b}-E_{j1})\left\langle i_a,i_b\right|\rho_s\left|i_a,i_b\right\rangle\\ &-4\sum_{j1\neq i_b} A_{i_a,j1,n1}A_{j1,i_a,n1}\kappa(E_{i_a}-E_{j1})\left\langle i_a,i_b\right|\rho_s\left|i_a,i_b\right\rangle\\ &+8u_{i_a,n1}v_{i_b,n1}(u^*_{i_a,n1}v^*_{i_b,n1}-u^*_{i_b,n1}v^*_{i_a,n1})\kappa(-E_{i_a}-E_{i_b})\left\langle GS\right|\rho_s\left|GS\right\rangle\\ &-8u_{i_a,n1}v_{i_b,n1}(u^*_{i_a,n1}v^*_{i_b,n1}-u^*_{i_b,n1}v^*_{i_a,n1})\kappa(E_{i_a}+E_{i_b})\left\langle i_a,i_b\right|\rho_s\left|i_a,i_b\right\rangle\Bigg).\end{aligned} \tag{4.4.5}$$

And for the odd parity sector we have for the lowest excitations (neglecting interaction with higher excited states for low temperature, as $\kappa(-E_i) >> \kappa(-E_{i1}-E_{i2})$):

$$\begin{aligned}\frac{d\left\langle i\right|\rho_s\left|i\right\rangle}{dt} = \sum_{n1}\Bigg(&4\sum_j A_{j,i,n1}A_{i,j,n1}\kappa(E_j-E_i)\left\langle j\right|\rho_s\left|j\right\rangle\\ &-4\sum_j A_{i,j,n1}A_{j,i,n1}\kappa(E_i-E_j)\left\langle i\right|\rho_s\left|i\right\rangle\Bigg).\end{aligned} \tag{4.4.6}$$

The numerical results of the relaxation rate r_{i_1,i_2} of a state $|i_1,i_2\rangle$ to the ground state $|GS\rangle$ is plotted in Fig.4.12, and the numerical determined relaxation rates r_i of a state $|i\rangle$ to $|0\rangle$ is plotted in Fig.4.13.
We can see that all states have finite relaxation rates to the lowest states (with the same parity). One can see that in the trivial regime the states with higher energy decaying more rapidly, as they have more possible decay channels (due to the decay via lower lying states). In the topological regime the direct decay from a state to the ground state gets more dominant, such that states $|k_i\rangle$ with $i \approx N/2$ (lying in the middle of the excitational band) have larger decay rates.

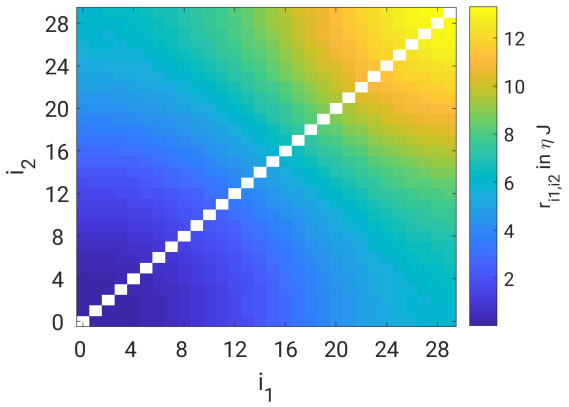

(a) $t/J = 2$

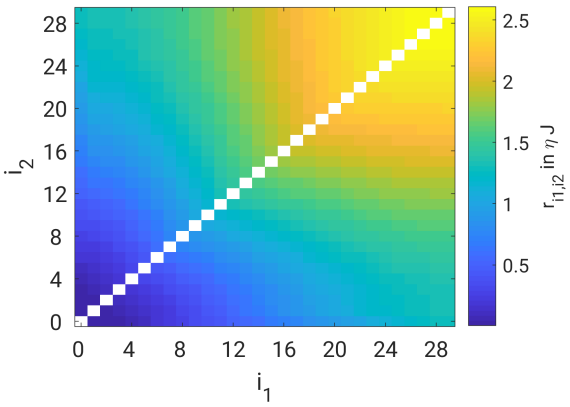

(b) $t/J = 0.5$

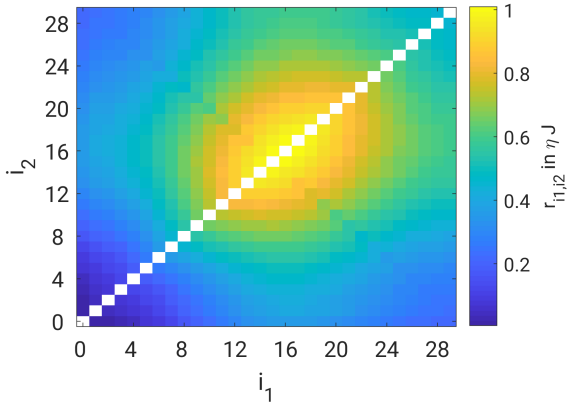

(c) $t/J = 0.1$

Figure 4.12: Comparison of the energy relaxation rate $r_{i1,i2}$ of a state $|i_1, i_2\rangle$ (where i is the index, such that $i = 0$ is the lowest excitation and $i = N - 1$ the largest excitation in energy) to the ground state $|GS\rangle$ for $N = 30$ spins at zero temperature for different ratio t/J. In the trivial regime the higher energetic excitation are relaxing more rapidly as the lower excitations. In the topological regime with $t/J = 0.1$ there is not a simple relation between the energy of the state and the rate anymore. The rate tends to be larger for states, which are in the middle of the excitational band $i \simeq N/2$.

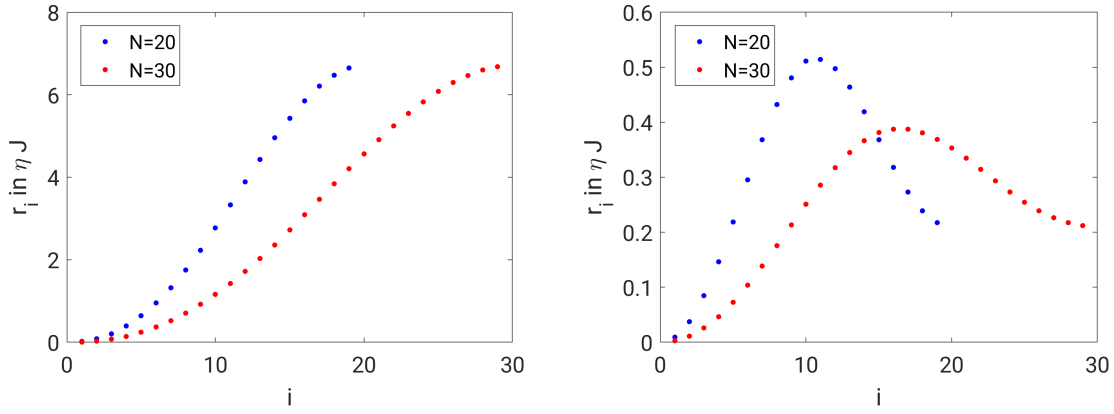

(a) $t/J = 2$ (b) $t/J = 0.1$

Figure 4.13: Energy relaxation at zero temperature of the odd subspace for the lowest excitation $|i\rangle$ to $|0\rangle$ at different ratio t/J. In the trivial regime the states with larger energy do relax faster, as they have more decay channels (through lower states). In the topological regime the states with $i \simeq N/2$ have increased rates.

4.4.3 Overview

In the topological regime the decoherence is determined by the interaction with the singly excited states gapped by E_i and the doubly excited states gapped by $E_{i1}+E_{i2}$, see Fig.4.14. In the trivial regime there is additionally to the interaction with the gapped states, also the interaction of $|0\rangle$ with $|i\rangle$, leading to an increased decoherence rate even at low temperature due to the small energy difference of $E_i - E_0$. Besides there is also a pure dephasing contribution in the trivial regime to the total decoherence rate.
In Fig.4.16 the total decoherence rate of $\langle GS|\, \rho_s\, |0\rangle = e^{-\Gamma_{dec} t}\, \langle GS|\, \rho_s(0)\, |0\rangle$ is shown, the decoherence rate is strongly suppressed at low temperature in the topological regime, whereas in the trivial regime the two states are not protected against dephasing, because interaction as well as the pure dephasing contribution are leading to an increase in the trivial regime.

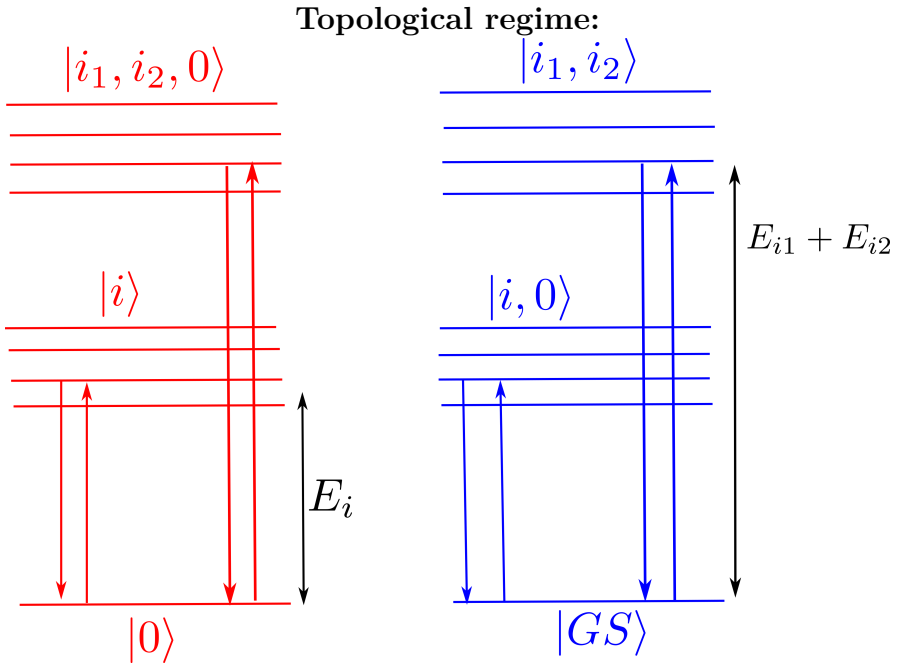

Figure 4.14: In the topological regime both ground states can interact with states gapped by E_i and with states that are gapped by the energy $E_{i1} + E_{i2}$.

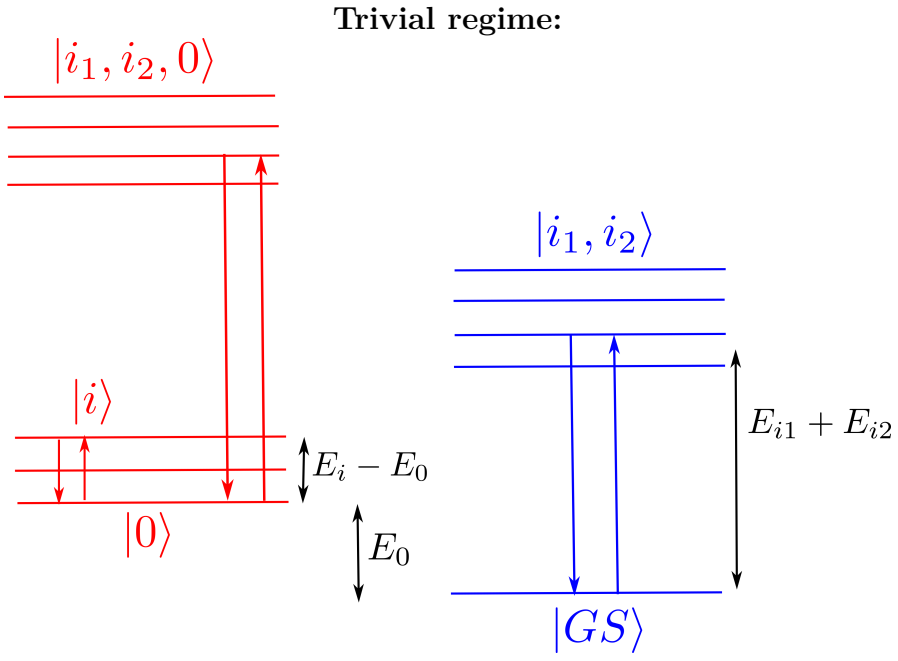

Figure 4.15: In the trivial regime the lowest states can interact with states gapped by the energy $E_{i1} + E_{i2}$. The lowest excitation $|0\rangle$ can also interact with other singly excited states with energy difference $E_i - E_0 << E_{i1} + E_{i2}$.

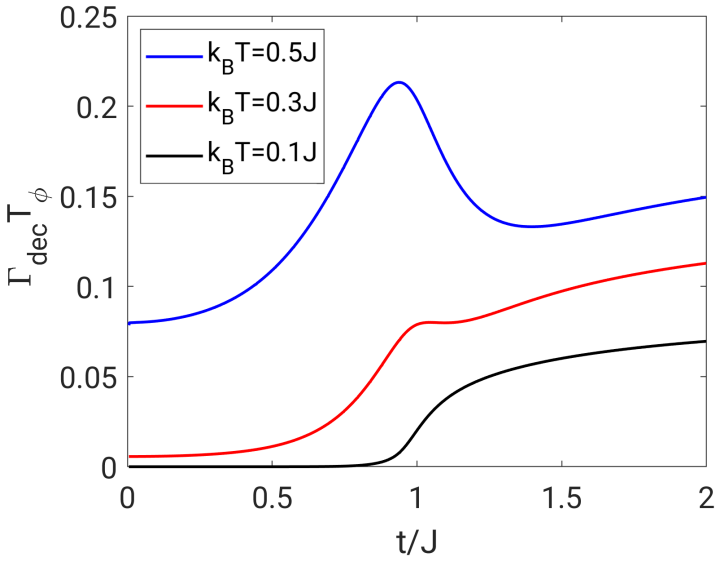

Figure 4.16: Decay rate $\Gamma_{dec} = \frac{G^{(l)}}{T_\phi} + \Gamma_s^{(l)} + \Gamma_d^{(l)}$ (eq.4.4.2) of the coherence between the two lowest states $|GS\rangle$ and $|0\rangle$ normalized with the single spin dephasing rate $\frac{1}{T_\phi} = \eta\pi k_B T$ (see 1.3) for $N = 40$ spins. At low temperature the dephasing rate can be strongly suppressed in the topological regime.

Conclusion

We evaluated the dynamics of the lowest states in the transverse Ising model with single site dephasing, which is a realistic assumption for the dissipation for specific qubits/spins (as discussed in 1.2). The ground states of the spin chain shows robustness against the single site dephasing in the topological regime for temperature lower than the gap energy, as the ground states are isolated to the lowest excitations and for $k_BT \to 0$ the decoherence rate can be completely suppressed for the two topological states, such that they can be used for topological quantum computation with long coherence time. This robustness against dephasing holds for open or closed chains and also for global and local correlation of the bath. In the trivial regime there will be an increase of the decoherence rate due to a pure dephasing contribution. For local bath correlation, there is also an increase in the trivial regime due to the interaction of the lowest odd parity state with other singly excited states. Hence there are two qualitatively different types of behaviour of the decoherence in the two phases of the spin chain.
One main difference in the topological regime between open and closed chains is that there can also be interaction with excited states gapped by E_i in the open chain, which is approximately half the gap energy as in the closed chain (where the lowest excitations are gapped by $E_{k1} + E_{k2}$).
Another difference is also that there is an (almost) linear scaling on N of the decoherence rate for the closed chain in the whole topological regime, whereas in the open chain there can be also constant behavior in N of the decoherence rate at low temperature (see Fig.4.3 and Fig.4.11).
Generally, the robustness of the ground states in the topological regime holds for any bath coupling which conserves the parity as the gap energy suppresses interaction of the ground states with excited states for low temperature. This means the topological ground states are also robust against fluctuations in J and t, as fluctuations in these terms conserve the parity.
However, energy relaxation of the single spins/qubits would break the parity conservation hence also allowing interaction between the two lowest states and thus also break the suppressed interaction for temperature below the gap energy. Thus the robustness of the ground states is only against dephasing of the single spins. For a more general model one would also need to implement the energy relaxation of the single spins to extend the model also for chains with spins that are in the regime of $T_1 \sim T_2$ or for times which are in the range of the energy relaxation time T_1.

Bibliography

[1] S. Sachdev and A. Young. Low temperature relaxational dynamics of the ising chain in a transverse field. *Physical Review Letters*, 78(11):2220, 1997.

[2] W. Zurek, U. Dorner, and P. Zoller. Dynamics of a quantum phase transition. *Physical Review Letters*, 95(10):105701, 2005.

[3] M Greiter, V. Schnells, and R. Thomale. The 1d ising model and the topological phase of the kitaev chain. *Annals of Physics*, 351:1026–1033, 2014.

[4] A. Kitaev. Unpaired majorana fermions in quantum wires. *Physics-Uspekhi*, 44(10S):131, 2001.

[5] G. Wendin. Quantum information processing with superconducting circuits: a review. *Reports on Progress in Physics*, 80(10):106001, 2017.

[6] S. Lloyd. Universal quantum simulators. *Science*, 273(5278):1073–1078, 1996.

[7] E. Lieb, T. Schultz, and D. Mattis. Two soluble models of an antiferromagnetic chain. *Annals of Physics*, 16(3):407–466, 1961.

[8] S. Katsura. Statistical mechanics of the anisotropic linear heisenberg model. *Physical Review Letters*, 127(5):1508, 1962.

[9] B. McCoy. Spin correlation functions of the x- y model. *Physical Review Letters*, 173(2):531, 1968.

[10] P. Pfeuty. The one-dimensional ising model with a transverse field. *Annals of Physics*, 57(1):79–90, 1970.

[11] S. Suzuki, J. Inoue, and B. Chakrabarti. *Quantum Ising phases and transitions in transverse Ising models*, volume 862. Springer, 2012.

[12] A. Osterloh, L. Amico, G. Falci, and R. Fazio. Scaling of entanglement close to a quantum phase transition. *Nature*, 416(6881):608, 2002.

[13] L. Amico, R. Fazio, A. Osterloh, and V. Vedral. Entanglement in many-body systems. *Reviews of Modern Physics*, 80(2):517, 2008.

[14] P. Calabrese, F. Essler, and M. Fagotti. Quantum quench in the transverse-field ising chain. *Physical Review Letters*, 106(22):227203, 2011.

[15] J. Caux and F. Essler. Time evolution of local observables after quenching to an integrable model. *Physical Review Letters*, 110(25):257203, 2013.

[16] M. Heyl, A. Polkovnikov, and S. Kehrein. Dynamical quantum phase transitions in the transverse-field ising model. *Physical Review Letters*, 110(13):135704, 2013.

[17] J. Dziarmaga. Dynamics of a quantum phase transition: Exact solution of the quantum ising model. *Physical Review Letters*, 95(24):245701, 2005.

[18] H. Quan, Z. Song, X. Liu, P. Zanardi, and C. Sun. Decay of loschmidt echo enhanced by quantum criticality. *Physical Review Letters*, 96(14):140604, 2006.

[19] G. Zhang and Z. Song. Topological characterization of extended quantum ising models. *Physical Review Letters*, 115(17):177204, 2015.

[20] G. Zhang, C. Li, and Z. Song. Majorana charges, winding numbers and chern numbers in quantum ising models. *Scientific reports*, 7(1):8176, 2017.

[21] X. Zhao, J. Yu, J. He, Q. Cheng, Y. Liang, and S. Kou. The simulation of non-abelian statistics of majorana fermions in ising chain with z 2 symmetry. *Modern Physics Letters B*, 31(11):1750123, 2017.

[22] J. Alicea, Y. Oreg, G. Refael, F. Von Oppen, and M. Fisher. Non-abelian statistics and topological quantum information processing in 1d wire networks. *Nature Physics*, 7(5):412, 2011.

[23] H. Labuhn, D. Barredo, S. Ravets, S. De Léséleuc, T. Macrì, T. Lahaye, and A. Browaeys. Tunable two-dimensional arrays of single rydberg atoms for realizing quantum ising models. *Nature*, 534(7609):667, 2016.

[24] A. Friedenauer, H. Schmitz, J. Glueckert, D. Porras, and T. Schätz. Simulating a quantum magnet with trapped ions. *Nature Physics*, 4(10):757, 2008.

[25] R. Islam, E. Edwards, K. Kim, S. Korenblit, C. Noh, H. Carmichael, G. Lin, L. Duan, C. Joseph Wang, J. Freericks, et al. Onset of a quantum phase transition with a trapped ion quantum simulator. *Nature communications*, 2:377, 2011.

[26] J. Simon, W. Bakr, R. Ma, M. Tai, P. Preiss, and M. Greiner. Quantum simulation of antiferromagnetic spin chains in an optical lattice. *Nature*, 472(7343):307, 2011.

[27] Y. Salathé, M. Mondal, M. Oppliger, J. Heinsoo, P. Kurpiers, A. Potočnik, A. Mezzacapo, U. Las Heras, L. Lamata, E. Solano, et al. Digital quantum simulation of spin models with circuit quantum electrodynamics. *Physical Review X*, 5(2):021027, 2015.

[28] P. McMahon, A. Marandi, Y. Haribara, R. Hamerly, C. Langrock, S. Tamate, T. Inagaki, H. Takesue, S. Utsunomiya, K. Aihara, et al. A fully programmable 100-spin coherent ising machine with all-to-all connections. *Science*, 354(6312):614–617, 2016.

[29] Z. Li, H. Zhou, C. Ju, H. Chen, W. Zheng, D. Lu, X. Rong, C. Duan, X. Peng, and J. Du. Experimental realization of a compressed quantum simulation of a 32-spin ising chain. *Physical Review Letters*, 112(22):220501, 2014.

[30] P. Werner, M. Troyer, and S. Sachdev. Quantum spin chains with site dissipation. *Journal of the Physical Society of Japan*, 74(Suppl):67–70, 2005.

[31] P. Werner, K. Völker, M. Troyer, and S. Chakravarty. Phase diagram and critical exponents of a dissipative ising spin chain in a transverse magnetic field. *Physical Review Letters*, 94(4):047201, 2005.

[32] G. Goldstein, C. Aron, and C. Chamon. Driven-dissipative ising model: Mean-field solution. *Physical Review B*, 92(17):174418, 2015.

[33] C. Bardyn, M. Baranov, C. Kraus, E. Rico, A. İmamoğlu, P. Zoller, and S. Diehl. Topology by dissipation. *New Journal of Physics*, 15(8):085001, 2013.

[34] H.-P. Breuer and F. Petruccione. *The theory of open quantum systems*. Oxford University Press on Demand, 2002.

[35] C. Rigetti, J. Gambetta, S. Poletto, B. Plourde, J. Chow, A. Córcoles, J. Smolin, S. Merkel, J. Rozen, G. Keefe, et al. Superconducting qubit in a waveguide cavity with a coherence time approaching 0.1 ms. *Physical Review B*, 86(10):100506, 2012.

[36] I. Chiorescu, Y. Nakamura, C. Harmans, and J. Mooij. Coherent quantum dynamics of a superconducting flux qubit. *Science*, 299(5614):1869–1871, 2003.

[37] M. Franz and L. Molenkamp. *Topological Insulators*, volume 6. Elsevier, 2013.

[38] M. Berry. Classical adiabatic angles and quantal adiabatic phase. *Journal of Physics A: Mathematical and General*, 18(1):15, 1985.

[39] D. Xiao, M. Chang, and Q. Niu. Berry phase effects on electronic properties. *Reviews of Modern Physics*, 82(3):1959, 2010.

[40] M. Xiao. Theory of transformation for the diagonalization of quadratic hamiltonians. *arXiv preprint arXiv:0908.0787*, 2009.

Appendix

A Pure dephasing rate

$$\begin{aligned}\Gamma_0(t) &= \eta\int_0^\infty d\omega e^{-\omega/\Omega}\frac{1-\cos(\omega t)}{\omega}\coth\left(\frac{\omega}{2k_BT}\right)\\ &= \eta\int_0^\infty d\omega e^{-\omega/\Omega}\frac{1-\cos(\omega t)}{\omega}+\eta\int_0^\infty d\omega e^{-\omega/\Omega}\frac{1-\cos(\omega t)}{\omega}\left(\coth\left(\frac{\omega}{2k_BT}\right)-1\right)\\ &= \frac{\eta}{2}\ln\left(1+\Omega^2t^2\right)+\eta\int_0^\infty d\omega e^{-\omega/\Omega}\frac{1-\cos(\omega t)}{\omega}\left(\coth\left(\frac{\omega}{2k_BT}\right)-1\right)\\ &= \frac{\eta}{2}\ln\left(1+\Omega^2t^2\right)+k_BT\eta\int_0^t dt'\int_0^\infty dx e^{-k_BTx/\Omega}\sin\left(k_BTxt'\right)\left(\coth\left(\frac{x}{2}\right)-1\right)\end{aligned} \tag{A.1}$$

for $k_BT << \Omega$ we have

$$\begin{aligned}&k_BT\eta\int_0^t dt'\int_0^\infty dx e^{-k_BTx/\Omega}\sin\left(k_BTxt'\right)\left(\coth\left(\frac{x}{2}\right)-1\right)\\ &\approx k_BT\eta\int_0^t dt'\int_0^\infty dx\sin\left(k_BTxt'\right)\left(\coth\left(x/2\right)-1\right)\\ &= \eta\ln\left(\frac{\sinh(\pi k_BTt)}{\pi k_BTt}\right).\end{aligned} \tag{A.2}$$

By using the integral

$$\int_0^\infty dx\sin(\alpha x)\left(coth(x/2)-1\right)=\pi\coth(\pi\alpha)-\frac{1}{\alpha}. \tag{A.3}$$

B Ising chain

B.1 Properties of the non-local phase

With the non-local phase of the Jordan-Wigner transformation

$$\begin{aligned}\hat{\nu}_n=\prod_{m=1}^{n-1}\left(e^{i\frac{\pi}{2}(1-\sigma_m^z)}\right)=\left(e^{i\frac{\pi}{2}}\right)^{n-1}\prod_{m=1}^{n-1}\left(e^{-i\frac{\pi}{2}\sigma_m^z}\right)=i^{n-1}\prod_{m=1}^{n-1}\left(-i\sigma_m^z\sin\left(\frac{\pi}{2}\right)\right)\\ =i^{n-1}\left(-i\right)^{n-1}\prod_{m=1}^{n-1}\sigma_m^z=\prod_{m=1}^{n-1}\sigma_m^z=\prod_{m=1}^{n-1}\left(1-2\hat{n}_m\right)\end{aligned} \tag{B.1}$$

it follows

$$\hat{\nu}_n^\dagger=\prod_{m=1}^{n-1}\left(e^{-i\frac{\pi}{2}(1-\sigma_m^z)}\right)=\prod_{m=1}^{n-1}\sigma_m^z=\prod_{m=1}^{n-1}\left(e^{i\frac{\pi}{2}(1-\sigma_m^z)}\right)=\hat{\nu}_n. \tag{B.2}$$

B.2 Jordan-Wigner transformation

For the number operator we have

$$\hat{n}_n=\hat{c}_n^\dagger\hat{c}_n=\sigma_n^-\sigma_n^+=\frac{1-\sigma_n^z}{2}. \tag{B.3}$$

Transformation of the nearest neighbor interaction:

$$\begin{aligned}
\sigma_n^x\sigma_{n+1}^x &= \left(\sigma_i^+ + \sigma_i^-\right)\left(\sigma_{i+1}^+ + \sigma_{i+1}^-\right) = \left(\hat{c}_n + \hat{c}_n^\dagger\right)\left(\hat{c}_{n+1} + \hat{c}_{n+1}^\dagger\right)\hat{\nu}_n^\dagger\hat{\nu}_{n+1} \\
&= \left(\hat{c}_n + \hat{c}_n^\dagger\right)\left(\hat{c}_{n+1} + \hat{c}_{n+1}^\dagger\right)\underbrace{\hat{\nu}_n^\dagger\hat{\nu}_n}_{1}\left(1-2\hat{n}_n\right) \\
&= \left(\hat{c}_n\left(1-2\hat{n}_n\right) + \hat{c}_n^\dagger\left(1-2\hat{n}_n\right)\right)\left(\hat{c}_{n+1} + \hat{c}_{n+1}^\dagger\right) \\
&= \left(\hat{c}_n\left(1-2\left(1-\hat{c}_n\hat{c}_n^\dagger\right)\right) + \hat{c}_n^\dagger\left(1-\hat{c}_n^\dagger\hat{c}_n\right)\right)\left(\hat{c}_{n+1} + \hat{c}_{n+1}^\dagger\right) \\
&= \left(-\hat{c}_n + \hat{c}_n^\dagger\right)\left(\hat{c}_{n+1} + \hat{c}_{n+1}^\dagger\right) \\
&= \hat{c}_n^\dagger\hat{c}_{n+1}^\dagger + \hat{c}_{n+1}\hat{c}_n + \hat{c}_n^\dagger\hat{c}_{n+1} + \hat{c}_{n+1}^\dagger\hat{c}_n
\end{aligned} \tag{B.4}$$

And the boundary term transforms to

$$\begin{aligned}
\sigma_N^x\sigma_1^x &= \hat{\nu}_N\left(\hat{c}_N + \hat{c}_N^\dagger\right)\left(\hat{c}_1\hat{c}_1^\dagger\right) \\
&= \prod_{m=1}^{N-1}\left(1-2\hat{n}_m\right)\underbrace{\left(1-2\hat{n}_N\right)\left(1-2\hat{n}_N\right)}_{=\sigma_N^z\sigma_N^z=1}\left(\hat{c}_N + \hat{c}_N^\dagger\right)\left(\hat{c}_1\hat{c}_1^\dagger\right) \\
&= \prod_{m=1}^{N}\left(1-2\hat{n}_m\right)\left(1-2\hat{n}_N\right)\left(\hat{c}_N + \hat{c}_N^\dagger\right)\left(\hat{c}_1\hat{c}_1^\dagger\right) \\
&= -\prod_{m=1}^{N}\left(1-2\hat{n}_m\right)\left(\hat{c}_N^\dagger\hat{c}_1^\dagger + \hat{c}_1\hat{c}_N + \hat{c}_N^\dagger\hat{c}_1 + \hat{c}_1^\dagger\hat{c}_N\right).
\end{aligned} \tag{B.5}$$

B.3 Fourier transformation of the even subspace

The first interaction terms can be transformed to

$$\begin{aligned}
&\sum_{n=1}^{N}\hat{c}_n^\dagger\hat{c}_{n+1} = \sum_{n=1}^{N-1}\hat{c}_n^\dagger\hat{c}_{n+1} - \hat{c}_N^\dagger\hat{c}_1 \\
&= \sum_{n=1}^{N-1}\frac{1}{N}\left(\sum_{k_0,k_1}\left(e^{-i\frac{\pi n k_0}{N}}e^{i\frac{\pi(n+1)k_1}{N}}\right)\hat{c}_{k_0}^\dagger\hat{c}_{k_1}\right) - \frac{1}{N}\sum_{k_0,k_1}\left(e^{-i\frac{\pi N k_0}{N}}e^{i\frac{\pi k_1}{N}}\right)\hat{c}_{k_0}^\dagger\hat{c}_{k_1} \\
&= \sum_{k_0,k_1}\hat{c}_{k_0}^\dagger\hat{c}_{k_1}\frac{e^{i\frac{\pi}{N}k_1}}{N}\left(\left(\sum_{n=1}^{N-1}e^{i\frac{\pi}{N}n(k_1-k_0)}\right) - \underbrace{e^{-i\pi k_0}}_{=-1}\right) \\
&= \sum_{k_0,k_1}\hat{c}_{k_0}^\dagger\hat{c}_{k_1}e^{i\frac{\pi}{N}k_1}\delta_{k_0,k_1} \\
&= \sum_{k_0}\hat{c}_{k_0}^\dagger\hat{c}_{k_0}e^{i\frac{\pi}{N}k_0} \\
&\to \sum_{n=1}^{N}\left(\hat{c}_n^\dagger\hat{c}_{n+1} + h.c.\right) = \sum_{k_0}\hat{c}_{k_0}^\dagger\hat{c}_{k_0}2\cos\left(\frac{\pi}{N}k_0\right).
\end{aligned} \tag{B.6}$$

Here was used that for $k_1 = k_0$

$$\frac{1}{N}\left(\sum_{n=1}^{N-1}\left(e^{i\frac{\pi}{N}n(k_1-k_0)}\right) + 1\right) = 1\,, \tag{B.7}$$

and for $k_1 \neq k_0$

$$\begin{aligned}
&\frac{1}{N}\left(\sum_{n=1}^{N-1}\left(e^{i\frac{\pi}{N}n(k_1-k_0)}\right)+1\right) = \frac{1}{N}\left(\sum_{n=0}^{N-1} e^{i\frac{\pi}{N}n(k_1-k_0)}\right) \\
&= \frac{1}{N}\left(\frac{1-e^{i\pi(k_1-k_0)}}{1-e^{i\frac{\pi}{N}(k_1-k_0)}}\right) = 0\,. \qquad \text{(B.8)}
\end{aligned}$$

The last step is true, since $k_1 - k_0$ has to be an even integer (difference between two odd values).
In that way also the second interaction term transforms to

$$\begin{aligned}
&\sum_{n=1}^{N}\hat{c}_n\hat{c}_{n+1} = \sum_{n=1}^{N-1}\hat{c}_n\hat{c}_{n+1} - \hat{c}_N\hat{c}_1 \\
&= \sum_{k_0,k_1}\hat{c}_{k_0}\hat{c}_{k_1}e^{-i\frac{\pi}{2}}e^{i\frac{\pi}{N}k_0}\frac{1}{N}\left(\sum_{n=1}^{N-1}e^{i\frac{\pi}{N}n(k_0+k_1)} - \underbrace{e^{i\pi k_1}}_{=-1}\right) \\
&= \sum_{k_0,k_1}\hat{c}_{k_0}\hat{c}_{k_1}e^{-i\frac{\pi}{2}}e^{i\frac{\pi}{N}k_0}\delta_{k_0,-k_1} \\
&= \sum_{k_0}\hat{c}_{k_0}\hat{c}_{-k_0}e^{-i\frac{\pi}{2}}e^{i\frac{\pi}{N}k_0} \\
&= e^{-i\frac{\pi}{2}}\sum_{k_0}\left(\cos\left(\frac{\pi}{N}k_0\right)\hat{c}_{k_0}\hat{c}_{-k_0} + i\sin\left(\frac{\pi}{N}k_0\right)\hat{c}_{k_0}\hat{c}_{-k_0}\right) \\
&= -e^{-i\frac{\pi}{2}}\sum_{k_0}\left(\cos\left(\frac{\pi}{N}k_0\right)\hat{c}_{k_0}\hat{c}_{-k_0} - i\sin\left(\frac{\pi}{N}k_0\right)\hat{c}_{k_0}\hat{c}_{-k_0}\right) \\
&= e^{-i\frac{\pi}{2}}\cdot\sum_{k_0} i\sin\left(\frac{\pi}{N}k_0\right)\hat{c}_{k_0}\hat{c}_{-k_0} \\
&= \sum_{k_0}\sin\left(\frac{\pi}{N}k_0\right)\hat{c}_{k_0}\hat{c}_{-k_0} \\
&\to \sum_{n=1}^{N}\hat{c}_n\hat{c}_{n+1} + h.c. = \sum_{k_0}\sin\left(\frac{\pi}{N}k_0\right)\left(\hat{c}_{k_0}\hat{c}_{-k_0} + \hat{c}^\dagger_{-k_0}\hat{c}^\dagger_{k_0}\right)\,. \qquad \text{(B.9)}
\end{aligned}$$

The kinetic term transforms to

$$\begin{aligned}
\hat{N} = \sum_{n=1}^{N}\hat{c}^\dagger_n\hat{c}_n &= \sum_{k_0,k_1}\underbrace{\left(\frac{1}{N}\sum_{n=1}^{N}e^{i\frac{\pi}{N}n(k_0-k_1)}\right)}_{\delta_{k_0,k_1}}\hat{c}^\dagger_{k_0}\hat{c}_{k_1} \\
&= \sum_{k_0}\hat{c}^\dagger_{k_0}\hat{c}_{k_0}\,. \qquad \text{(B.10)}
\end{aligned}$$

This leads for the even parity subspace Hamiltonian

$$H^+ = -tN + \sum_{k_0}\left[\left(2t - 2J\cos\left(\frac{\pi}{N}k_0\right)\right)\hat{c}^\dagger_{k_0}\hat{c}_{k_0} - J\sin\left(\frac{\pi}{N}k_0\right)\left(\hat{c}_{k_0}\hat{c}_{-k_0} + \hat{c}^\dagger_{-k_0}\hat{c}^\dagger_{k_0}\right)\right]\,. \qquad \text{(B.11)}$$

B.4 Bogoliubov transformation

$$\begin{aligned}
H &= -Nt + \sum_k \left(2\xi_k \hat{c}_k^\dagger \hat{c}_k + \Delta_k \left(\hat{c}_k \hat{c}_{-k} + \hat{c}_{-k}^\dagger \hat{c}_k^\dagger\right)\right) \\
&= -Nt + \left(\sum_k \xi_k \hat{c}_k^\dagger \hat{c}_k + \sum_k \xi_k \left(1 - \hat{c}_k \hat{c}_k^\dagger\right)\right) + \sum_k \Delta_k \left(\hat{c}_k^\dagger \hat{c}_{-k}^\dagger + \hat{c}_{-k} \hat{c}_k\right) \\
&= -Nt + \sum_k \xi_k + \left(\sum_k \xi_k \hat{c}_k^\dagger \hat{c}_k - \sum_k \xi_{-k} \hat{c}_{-k} \hat{c}_{-k}^\dagger\right) + \sum_k \Delta_k \left(\hat{c}_k^\dagger \hat{c}_{-k}^\dagger + \hat{c}_{-k} \hat{c}_k\right) \\
&= -Nt + \sum_k \xi_k + \sum_k \begin{pmatrix} \hat{c}_k^\dagger & \hat{c}_{-k} \end{pmatrix} \begin{pmatrix} \xi_k & \Delta_k \\ \Delta_k & -\xi_k \end{pmatrix} \begin{pmatrix} \hat{c}_k \\ \hat{c}_{-k}^\dagger \end{pmatrix}
\end{aligned} \tag{B.12}$$

To diagonalize this Hamiltonian a Bogoliubov transformation is applied with

$$\hat{c}_k = u_k \hat{\gamma}_k + v_k \hat{\gamma}_{-k}^\dagger \tag{B.13}$$

$$\hat{c}_{-k}^\dagger = -v_k \hat{\gamma}_k + u_k \hat{\gamma}_{-k}^\dagger \tag{B.14}$$

Here is $u_k^2 + v_k^2 = 1$, $u_k^2 = \frac{1}{2}\left(1 + \frac{\xi_k}{E_k}\right)$ and $v_k^2 = \frac{1}{2}\left(1 - \frac{\xi_k}{E_k}\right)$. This leads to a diagonalized Hamiltonian with the new quasiparticle operators $\hat{\gamma}_k$

$$\begin{aligned}
H &= -Nt + \sum_k \xi_k + \sum_k \begin{pmatrix} \hat{\gamma}_k^\dagger & \hat{\gamma}_k \end{pmatrix} \begin{pmatrix} E_k & 0 \\ 0 & -E_k \end{pmatrix} \begin{pmatrix} \hat{\gamma}_k \\ \hat{\gamma}_k^\dagger \end{pmatrix} \\
&= -Nt + \sum_k \xi_k + \sum_k E_k (\hat{\gamma}_k^\dagger \hat{\gamma}_k - \underbrace{\hat{\gamma}_k \hat{\gamma}_k^\dagger}_{1 - \hat{\gamma}_k^\dagger \hat{\gamma}_k}) \\
&= -Nt + \sum_k (\xi_k - E_k) + \sum_k 2E_k (\hat{\gamma}_k^\dagger \hat{\gamma}_k).
\end{aligned} \tag{B.15}$$

B.5 General transformation for a quadratic Hamiltonian

Consider a quadratic fermionic Hamiltonian in the following form (Δ_{ij} is assumed to be real)

$$\begin{aligned}
&\sum_{i,j} \left[t_{ij} \hat{a}_i^\dagger \hat{a}_j + \frac{1}{2}\Delta_{ij} \hat{a}_i^\dagger \hat{a}_j^\dagger + \frac{1}{2}\Delta_{ij} \hat{a}_j \hat{a}_i\right] \\
&= \frac{1}{2} \sum_{i,j} \begin{pmatrix} \hat{c}_i^\dagger & \hat{c}_j \end{pmatrix}^T \begin{pmatrix} t_{ij} & \Delta_{ij} \\ \Delta_{ji} & -t_{ij} \end{pmatrix} \begin{pmatrix} \hat{c}^\dagger \\ \hat{c} \end{pmatrix} \\
&= \frac{1}{2} \begin{pmatrix} \hat{c}^\dagger & \hat{c} \end{pmatrix}^T \begin{pmatrix} \bar{\bar{T}} & \bar{\bar{\Delta}} \\ \bar{\bar{\Delta}}^\dagger & -\bar{\bar{T}} \end{pmatrix} \begin{pmatrix} \hat{c}^\dagger \\ \hat{c} \end{pmatrix}.
\end{aligned} \tag{B.16}$$

One can introduce the transformation ([40])

$$\gamma_k = \sum_i \left(u_{ki} \hat{a}_i + v_{ki} \hat{a}_i^\dagger\right) \tag{B.17}$$

$$\gamma_k^\dagger = \sum_i \left(u_{ki}^* \hat{a}_i^\dagger + v_{ki}^* \hat{a}_i\right), \tag{B.18}$$

to diagonalize the Hamiltonian to

$$H' = \sum_k E_k \gamma_k^\dagger \gamma_k + E_0 \,. \tag{B.19}$$

The transformation is then determined by

$$\begin{aligned} \left[\gamma_\nu, H'\right] &= E_\nu \gamma_\nu = E_\nu \sum_i \left(u_{\nu i}\hat{a}_i + v_{\nu i}\hat{a}_i^\dagger\right) \\ &= \left[\sum_i \left(u_{\nu i}\hat{a}_i + v_{\nu i}\hat{a}_i^\dagger\right), H\right] . \end{aligned} \tag{B.20}$$

With the commutators

$$\left[\hat{a}_i, \hat{a}_j^\dagger \hat{a}_k\right] = \delta_{ij}\hat{a}_k \tag{B.21}$$

$$\left[\hat{a}_i^\dagger, \hat{a}_j^\dagger \hat{a}_k\right] = -\delta_{ki}\hat{a}_j^\dagger \tag{B.22}$$

$$[\hat{a}_i, \hat{a}_j \hat{a}_k] = \left[\hat{a}_i^\dagger, \hat{a}_j^\dagger \hat{a}_k^\dagger\right] = 0 \tag{B.23}$$

$$\left[\hat{a}_i, \hat{a}_j^\dagger \hat{a}_k^\dagger\right] = \delta_{ij}\hat{a}_k^\dagger - \delta_{ik}\hat{a}_j^\dagger \tag{B.24}$$

$$\left[\hat{a}_i^\dagger, \hat{a}_k \hat{a}_j\right] = \delta_{ik}\hat{a}_j - \delta_{ij}\hat{a}_k \,, \tag{B.25}$$

one can determine the commutator (B.20)

$$\begin{aligned} &E_\nu \sum_i \left(u_{\nu i}\hat{a}_i + v_{\nu i}\hat{a}_i^\dagger\right) = \left[\sum_i \left(u_{\nu i}\hat{a}_i + v_{\nu i}\hat{a}_i^\dagger\right), H\right] \\ &= \sum_{ijk} \left[u_{\nu i}\left(t_{jk}\delta_{ij}\hat{a}_k + \frac{1}{2}\Delta_{jk}\left(\delta_{ij}\hat{a}_k^\dagger - \delta_{ik}\hat{a}_j^\dagger\right)\right) + v_{\nu i}\left(t_{jk}(-\delta_{ki})\hat{a}_j^\dagger + \frac{1}{2}\Delta_{jk}\left(\delta_{ik}\hat{a}_j - \delta_{ij}\hat{a}_k\right)\right)\right] . \end{aligned} \tag{B.26}$$

By comparing the terms which contains $\hat{a}$ and the terms which contain $\hat{a}^\dagger$ one gets two equations

$$\sum_{ik} u_{\nu i} t_{ik}\hat{a}_k + \frac{1}{2}\sum_{ij} v_{\nu i}\Delta_{ji}\hat{a}_j - \frac{1}{2}\sum_{ik} v_{\nu i}\Delta_{ik}\hat{a}_k = E_\nu \sum_i u_{\nu i}\hat{a}_i \tag{B.27}$$

$$\sum_{ik} -v_{\nu i} t_{ji}\hat{a}_j^\dagger + \frac{1}{2}\sum_{ik} u_{\nu i}\Delta_{ik}\hat{a}_k^\dagger - \frac{1}{2}\sum_{ij} u_{\nu i}\Delta_{ji}\hat{a}_j^\dagger = E_\nu \sum_i v_{\nu i}\hat{a}_i^\dagger \,. \tag{B.28}$$

These two equations can be split up into $2N$ equations by comparing every term which contains the same $\hat{a}_i$ or $\hat{a}_i^\dagger$

$$\sum_p \left(u_{\nu p}t_{pi} + \frac{1}{2}v_{\nu p}\Delta_{ip} - \frac{1}{2}v_{\nu p}\Delta_{pi}\right)\hat{a}_i = E_\nu u_{\nu i}\hat{a}_i \tag{B.29}$$

$$\sum_p \left(-v_{\nu p}t_{ip} + \frac{1}{2}u_{\nu p}\Delta_{pi} - \frac{1}{2}u_{\nu p}\Delta_{ip}\right)\hat{a}_i^\dagger = E_\nu v_{\nu i}\hat{a}_i^\dagger \,. \tag{B.30}$$

As $\Delta_{ij} = -\Delta_{ji}$ (assuming Δ_{ij} is real) and $t_{ij} = t_{ji}$ it follows

$$\sum_p \left(t_{ip} u_{\nu p} + \Delta_{ip} v_{\nu p}\right) = E_\nu u_{\nu i} \tag{B.31}$$

$$\sum_p \left(-t_{ip} v_{\nu p} - \Delta_{ip} u_{\nu p}\right) = E_\nu v_{\nu i}\,. \tag{B.32}$$

For fixed ν it can be expressed in a compact form

$$\bar{\bar{T}}\vec{u} + \bar{\bar{\Delta}}\vec{v} = E\vec{u} \tag{B.33}$$

$$-\bar{\bar{T}}\vec{v} - \bar{\bar{\Delta}}\vec{u} = E\vec{v} \tag{B.34}$$

with

$$\vec{u}^{(\nu)} = \begin{pmatrix} u_1^{(\nu)} \\ \vdots \\ u_N^{(\nu)} \end{pmatrix}$$

$$\vec{v}^{(\nu)} = \begin{pmatrix} v_1^{(\nu)} \\ \vdots \\ v_N^{(\nu)} \end{pmatrix}$$

$$\left(\bar{\bar{T}}\right)_{pi} = t_{pi}$$

$$\left(\bar{\bar{\Delta}}\right)_{pi} = \Delta_{pi}\,.$$

And with $\vec{\phi} = \vec{u} - \vec{v}$ and $\vec{\psi} = \vec{u} + \vec{v}$ we have

$$E\vec{\psi} = \left(\bar{\bar{T}} - \bar{\bar{\Delta}}\right)\vec{\phi} \tag{B.35}$$

$$E\vec{\phi} = \left(\bar{\bar{T}} + \bar{\bar{\Delta}}\right)\vec{\psi}\,. \tag{B.36}$$

This transformation can be also used to derive the transformation for the closed chain (as done previously with the Fourier and Bogoliubov transformation) and can be seen in the appendix.B.7.

B.6 Back transformation

Consider

$$\hat{a}_n = \sum_k u_{kn}\gamma_k + v_{kn}^*\gamma_k^\dagger \tag{B.37}$$

$$\hat{a}_n^\dagger = \sum_k u_{kn}^*\gamma_k^\dagger + v_{kn}\gamma_k\,, \tag{B.38}$$

hence the commutator can be expressed as

$$\begin{aligned}[\hat{a}_n, H] &= \sum_{ij} \delta_{ni} t_{ij} \hat{a}_j + \frac{1}{2}\Delta_{ij}\left(\delta_{ni}\hat{a}_j^\dagger - \delta_{nj}\hat{a}_i^\dagger\right) \\ &= \sum_j t_{nj}\hat{a}_j + \frac{1}{2}\left(\Delta_{nj}\hat{a}_j^\dagger - \Delta_{jn}\hat{a}_j^\dagger\right) \\ &= \sum_j \sum_k t_{nj}\left(u_{kj}\gamma_k + v_{kj}^*\gamma_k^\dagger\right) + \frac{1}{2}\left(\Delta_{nj}\left(u_{kj}^*\gamma_k^\dagger + v_{kj}\gamma_k\right) - \Delta_{jn}\left(u_{kj}^*\gamma_k^\dagger + v_{kj}\gamma_k\right)\right)\end{aligned} \tag{B.39}$$

$$\begin{aligned}[\hat{a}_n, H] &= [\sum_k u_{kn}\gamma_k + v_{kn}^*\gamma_k^\dagger, H] \\ &= \sum_k E_k u_{kn}\gamma_k - E_k v_{kn}^*\gamma_k^\dagger\,.\end{aligned} \tag{B.40}$$

Comparing the terms with γ_k and $\gamma_k^\dagger$ leads to the following equations

$$E_k u_{kn} = \sum_j t_{nj}u_{kj} + \Delta_{nj}v_{kj} \tag{B.41}$$

$$-E_k v_{kn}^* = \sum_j t_{nj}v_{kj}^* + \Delta_{nj}u_{kj}^*\,. \tag{B.42}$$

This yields the condition for the back transformation

$$E_k\vec{u} = \bar{\bar{T}}\vec{u} + \bar{\bar{\Delta}}\vec{v} \tag{B.43}$$

$$E_k\vec{v} = -\bar{\bar{T}}\vec{v} - \bar{\bar{\Delta}}\vec{u}\,, \tag{B.44}$$

such that we have the same condition as for the transformation.

B.7 Closed Boundary condition with general transformation

For the closed boundary condition the Hamiltonian reads as

$$H = -t\left(\sum_{n=1}^{N} 1 - 2\hat{n}_n\right) - J\left(\sum_{n=1}^{N-1}\left(\left(\hat{c}_n^\dagger\hat{c}_{n+1} + \hat{c}_{n+1}\hat{c}_n + h.c.\right) - \hat{P}\left(\hat{c}_N^\dagger\hat{c}_1 + \hat{c}_1\hat{c}_N + h.c.\right)\right)\right) \tag{B.45}$$

Here is $\hat{P} = \prod_{m=1}^{N}(1 - 2\hat{n}_m)$.
The total Hamiltonian is not quadratic and can not be diagonalized in total. But since the parity operator $\hat{P}$ is $+1$ in the even parity subspace and -1 in the odd parity subspace, the Hamiltonians of the odd and even subspace are quadratic and can be diagonalized

$$\begin{aligned}H^\pm &= \hat{P}^\pm(-t)\left(\sum_{n=1}^{N} 1 - 2\hat{n}_n\right) - J\left(\sum_{n=1}^{N-1}\left(\left(\hat{c}_n^\dagger\hat{c}_{n+1} + \hat{c}_{n+1}\hat{c}_n + h.c.\right) \mp \left(\hat{c}_N^\dagger\hat{c}_1 + \hat{c}_1\hat{c}_N + h.c.\right)\right)\right)\hat{P}^\pm \\ &= \hat{P}^\pm\left(\sum_{i,j}\left[t_{ij}\hat{a}_i^\dagger\hat{a}_j + \frac{1}{2}\Delta_{ij}\hat{a}_i^\dagger\hat{a}_j^\dagger + \frac{1}{2}\Delta_{ij}\hat{a}_j\hat{a}_i\right] - Nt\right)\hat{P}^\pm\end{aligned} \tag{B.46}$$

With the following matrices

$$\bar{\bar{T}}^{\pm} = \begin{pmatrix} 2t & -J & 0 & ... & & \pm J \\ -J & 2t & -J & 0 & ... & \\ 0 & -J & 2t & -J & 0 & ... \\ \vdots & \ddots & \ddots & \ddots & \ddots & \ddots \\ \pm J & & & & & \end{pmatrix}$$

$$\bar{\bar{\Delta}}^{\pm} = \begin{pmatrix} 0 & -J & 0 & ... & & \mp J \\ J & 0 & -J & 0 & ... & \\ 0 & J & 0 & -J & 0 & ... \\ \vdots & \ddots & \ddots & \ddots & \ddots & \ddots \\ \pm J & & & & & \end{pmatrix}$$

we can determine the transformation by

$$E^{\pm}\vec{\psi}^{\pm} = 2 \underbrace{\begin{pmatrix} t & 0 & 0 & ... & & \pm J \\ -J & t & 0 & 0 & ... & \\ 0 & -J & t & 0 & 0 & ... \\ \vdots & \ddots & \ddots & \ddots & \ddots & \ddots \end{pmatrix}}_{A^{\pm}} \vec{\phi}^{\pm} \tag{B.47}$$

$$E^{\pm}\vec{\phi}^{\pm} = 2 \underbrace{\begin{pmatrix} t & -J & 0 & ... & & \\ 0 & t & -J & 0 & ... & \\ 0 & 0 & t & -J & 0 & ... \\ \vdots & \ddots & \ddots & \ddots & \ddots & \ddots \\ \pm J & & & & & \end{pmatrix}}_{B^{\pm}} \vec{\psi}^{\pm} \tag{B.48}$$

$$(E^{\pm})^2\vec{\psi} = A^{\pm}B^{\pm}\vec{\psi} \tag{B.49}$$

$$(E^{\pm})^2\vec{\phi} = B^{\pm}A^{\pm}\vec{\phi} \tag{B.50}$$

With

$$A^{\pm}B^{\pm} = 4 \begin{pmatrix} t^2+J^2 & -Jt & 0 & ... & & \pm Jt \\ -Jt & t^2+J^2 & -Jt & 0 & ... & \\ 0 & -Jt & t^2+J^2 & -Jt & 0 & ... \\ \vdots & \ddots & \ddots & \ddots & \ddots & \ddots \\ \pm Jt & & & & & \end{pmatrix} = B^{\pm}A^{\pm} \tag{B.51}$$

Thus the equation for the transformation is for the even parity subspace

$$E^2\psi_n = (t^2+J^2)\psi_n - Jt(\psi_{n-1}+\psi_{n+1}) \tag{B.52}$$

$$E^2\phi_n = (t^2+J^2)\phi_n - Jt(\phi_{n-1}+\phi_{n+1}) \tag{B.53}$$

With the boundary condition $\psi_{N+1} = -\psi_1$, $\psi_0 = -\psi_N$ and $\phi_{N+1} = -\phi_1$, $\phi_0 = -\phi_N$.
And the equation for the transformation of the odd parity subspace:

$$E^2\psi_n = 4(t^2 + J^2)\psi_n - 4Jt(\psi_{n-1} + \psi_{n+1}) \tag{B.54}$$
$$E^2\phi_n = 4(t^2 + J^2)\phi_n - 4Jt(\phi_{n-1} + \phi_{n+1}) \tag{B.55}$$

With the boundary condition $\psi_{N+1} = \psi_1$, $\psi_0 = \psi_N$ and $\phi_{N+1} = \phi_1$, $\phi_0 = \phi_N$.
Using the Ansatz

$$\phi_n \propto e^{ikn} \tag{B.56}$$
$$\psi_n \propto e^{ikn} \tag{B.57}$$

we find that

$$\begin{aligned} \frac{1}{4}E^2 &= (t^2 + J^2) - Jt(e^{-ik} + e^{ik}) \\ \rightarrow \frac{1}{4}E^2 &= t^2 + J^2 - 2Jt\cos(k)\,. \end{aligned} \tag{B.58}$$

And from the boundary conditions it follows that

$$\begin{aligned} e^{ik(N+1)} &= \mp e^{ik} \\ 1 &= \mp e^{ikN} \\ \rightarrow k &= \begin{cases} \frac{(2l-1)\pi}{N} & H^+ \\ \frac{2l\pi}{N} & H^- \end{cases}. \end{aligned} \tag{B.59}$$

With $l = 0, 1, 2, 3, ..., N-1$ (By shifting $l' = N/2 - l$ one obtains the same condition for k as derived before).
Moreover the following condition has to be fullfilled (which determines the phase)

$$\begin{aligned} E\vec{\psi} &= A\vec{\phi} \\ \rightarrow E\psi_n &= 2t\phi_n - 2J\phi_{n-1} \\ E\psi_n &= \left(2t - 2Je^{-ik}\right)\phi_n \end{aligned} \tag{B.60}$$

$$\begin{aligned} E\vec{\phi} &= B\vec{\psi} \\ \rightarrow E\phi_n &= 2t\psi_n - 2J\psi_{n+1} \\ E\phi_n &= \left(2t - 2Je^{ik}\right)\psi_n \end{aligned} \tag{B.61}$$

Inserting E yields

$$\psi_n = \frac{t - Je^{-ik}}{\sqrt{t^2 + J^2 - 2Jt\cos(k)}}\phi_n$$
$$\psi_n = \frac{t - J\cos(k) - J\sin(k)}{\sqrt{(t - Je^{ik})(t - Je{-}ik)}}\phi_n$$
$$\psi_n = \left(\frac{\xi_k}{E_k} - i\frac{\Delta_k}{E_k}\right)\phi_n$$
$$\psi_n = e^{-i\theta_k}\phi_n \tag{B.62}$$
$$\phi_n = \frac{t - Je^{ik}}{\sqrt{t^2 + J^2 - 2Jt\cos(k)}}\psi_n$$
$$\phi_n = e^{i\theta_k}\psi_n\,. \tag{B.63}$$

With $\xi_k = 2(t - J\cos(k))$ and $\Delta_k = 2J\sin(k)$.
Thus the transformation can be expressed as

$$u_n^l = \cos(\theta_k/2)e^{ik_l n} \tag{B.64}$$
$$v_n^l = e^{-i\frac{\pi}{2}}\sin(\theta_k/2)e^{ik_l n}\,. \tag{B.65}$$

By multiplying both solution ϕ_n and ψ_n with a phase of $e^{i\frac{\pi}{4}}$ (does not change the relation between them, thus all above equations are still valid) one comes to the result of

$$u_n^l = e^{i\frac{\pi}{4}}\cos(\theta_k/2)e^{ik_l n} \tag{B.66}$$
$$v_n^l = e^{-i\frac{\pi}{4}}\sin(\theta_k/2)e^{ik_l n}\,. \tag{B.67}$$

Normalizing $\sum_n |u_n|^2 + |v_n|^2$ leads to an additional factor of $\sqrt{1/N}$, such that the full transformation can be expressed as (which is the same as the Fourier transformation and the Bogoliubov transformation from the chapter before)

$$\gamma_k = \frac{1}{\sqrt{N}}\sum_n e^{-i\frac{\pi}{4}}e^{ik_l n}\cos(\theta_k/2)\hat{c}_n + e^{+i\frac{\pi}{4}}e^{ik_l n}\sin(\theta_k/2)\hat{c}_n^\dagger\,. \tag{B.68}$$

With the condition for the even parity subspace that $k_l = (2l-1)\frac{\pi}{N}$, and $k_l = (2l)\frac{\pi}{N}$ for the odd parity subspace (as derived before).

B.8 Deriving the single particle spectrum and the condition for the k-values for the open chain

The two equations for the transformation are

$$\rightarrow\frac{E}{2t}\psi_n = \phi_n - \lambda\phi_{n-1} \tag{B.69}$$
$$\rightarrow\frac{E}{2t}\phi_n = \psi_n - \lambda\psi_{n+1}\,. \tag{B.70}$$

Inserting the Ansatz of

$$\psi_n \propto \sin(k(N+1-n)) \tag{B.71}$$
$$\phi_n \propto \sin(kn) \tag{B.72}$$

leads for ϕ_n for $1 \leq n \leq N-1$ to

$$\sin(kn) - \lambda \sin(k(n-1)) = -\frac{E}{2t}\sin(k(N+1-n))$$
$$\Big(1 - \lambda\cos(k) - \frac{E}{2t}\cos(k(N+1))\Big)\sin(kn) = -\Big(\lambda\sin(k) + \frac{E}{2t}\sin(k(N+1))\Big)\cos(kn)$$
$$\to 1 - \lambda\cos(k) - \frac{E}{2t}\cos(k(N+1)) = 0 \tag{B.73}$$
$$\to \lambda\sin(k) + \frac{E}{2t}\sin(k(N+1)) = 0\,. \tag{B.74}$$

By combining the last two equations one can get two different conditions

$$-\tan(k(N+1)) = \frac{\lambda\sin(k)}{1-\lambda\cos(k)} \tag{B.75}$$
$$1 + \lambda^2 - 2\lambda\cos(k) = \Big(\frac{E}{2t}\Big)^2\,. \tag{B.76}$$

Inserting the Ansatz for ψ_n for $2 \leq n \leq N$ leads to

$$-\sin(k(N+1-n)) + \lambda\sin(k(N+1-n-1)) = \frac{E}{2t}\sin(kn)$$
$$\Big(\cos(k(N+1)) - \lambda\cos(k(N)) - \frac{E}{2t}\Big)\sin(kn) = \Big(\sin(k(N+1)) - \lambda\sin(k(N))\Big)\cos(kn)$$
$$\to \cos(k(N+1)) - \lambda\cos(k(N)) - \frac{E}{2t} = 0 \tag{B.77}$$
$$\to \sin(k(N+1)) - \lambda\sin(k(N)) = 0 \tag{B.78}$$

By multiplying (B.77) with $\cos(k(N+1))$ and (B.78) with $\sin(k(N+1))$ this yields

$$\cos^2(k(N+1))\Big(1-\lambda\cos(k)\Big) - \lambda\sin(k(N+1))\cos(k(N+1))\sin(k) = \frac{E}{2t}\cos(k(N+1))$$
$$\sin^2(k(N+1))\Big(1-\lambda\cos(k)\Big) + \lambda\sin(k(N+1))\cos(k(N+1))\sin(k) = 0$$
$$\to 1 - \lambda\cos(k) - \frac{E}{2t}\cos(k(N+1)) = 0\,. \tag{B.79}$$

By multiplying (B.77) with $\sin(k(N+1))$ and (B.78) with $-\cos(k(N+1))$ this yields

$$\sin(k(N+1))\cos(k(N+1))\Big(1-\lambda\cos(k)\Big) - \lambda\sin^2(k(N+1))\sin(k) = \frac{E}{2t}\sin(k(N+1))$$
$$-\sin(k(N+1))\cos(k(N+1))(1-\lambda\cos(k)) - \lambda\cos^2(k(N+1))\sin(k) = 0$$
$$\to \frac{E}{2t}\sin(k(N+1)) + \lambda\sin(k) = 0\,. \tag{B.80}$$

Combining eq.B.79 with eq.B.80 leads again to the condition B.75.
The Boundary equation for $n = 1$ and $n = N$ are automatically fulfilled by the condition that $\phi_0 = 0$, $\psi_{N+1} = 0$ and fulfilling eq.B.69 and eq.B.70 (these conditions

combined results in the boundary equation).
The Boundary equation reads as

$$\frac{E}{2t} = \frac{\sin(k)}{\sin(kN)}\,. \tag{B.81}$$

Additionally we want always positive energy, which is here not necessarily fulfilled. Thus one can add an additional term into the Ansatz (note that all the previous calculations are still valid with this additional term)

$$s_k = sign\left(\frac{\sin(k)}{\sin(kN)}\right) \tag{B.82}$$

$$\phi_n \propto s_k \sin(kn) \tag{B.83}$$

$$\rightarrow \frac{E}{2t} = s_k \frac{\sin(k)}{\sin(kN)} \geq 0\,, \tag{B.84}$$

to have always positive energy.

B.9 Localized state

The energy of these localized states are:

$$E = 2\sqrt{t^2 + J^2 + 2tJ\cos(iq)} = 2\sqrt{t^2 + J^2 + 2tJ\cosh(q)} \tag{B.85}$$

And have to fulfill the condition

$$\begin{aligned}
-\tan((N+1)iq) &= \frac{\lambda\sin(iq)}{1-\lambda\cos(iq)} \\
-\tanh(q) &= \frac{\lambda\sinh(q)}{1-\lambda\cosh(q)} \\
\coth((N+1)q) &= \frac{\lambda\cosh(q)-1}{\lambda\sinh(q)} \\
\lambda\cosh(q) &= 1 + \lambda\sinh(q) + \lambda\sinh(q)\left(\coth((N+1)q) - 1\right) \\
\frac{\lambda}{2}\left(e^{q} + e^{-q}\right) &= 1 + \frac{\lambda}{2}\left(e^{q} - e^{-q}\right) + \lambda\sinh(q)\left(\frac{e^{(N+1)q} + e^{-(N+1)q}}{e^{(N+1)q} - e^{-(N+1)q}} - 1\right) \\
\lambda e^{-q} &= 1 + \frac{\lambda}{2}\left(e^{q} - e^{-q}\right)\left(\frac{e^{(N+1)q} + e^{-(N+1)q} - \left(e^{(N+1)q} - e^{-(N+1)q}\right)}{e^{(N+1)q} - e^{-(N+1)q}}\right) \\
\lambda e^{-q} &= 1 + \frac{\lambda}{2}\left(e^{q} - e^{-q}\right)\left(\frac{e^{-q(N+1)}}{e^{(N+1)q} - e^{-(N+1)q}}\right) \\
\lambda e^{-q} &= 1 + \lambda\left(e^{q} - e^{-q}\right)e^{-2q(N+1)}\left(\frac{1}{1-e^{-2q(N+1)}}\right)\,.
\end{aligned} \tag{B.86}$$

Expansion in the limit of $Nq >> 1$ to first order:

$$\begin{aligned}
\lambda e^{-q} &= 1 + \lambda \left(e^{q} - e^{-q}\right) e^{-2q(N+1)} \\
e^{-q} &= \frac{1}{\lambda} + \epsilon \\
e^{q} &= \frac{1}{1/\lambda + \epsilon} = \frac{\lambda}{1+\lambda\epsilon} \approx \lambda(1-\lambda\epsilon) \\
\rightarrow \lambda(\frac{1}{\lambda} + \epsilon) &\approx 1 + \lambda \left(\lambda - \lambda^2\epsilon - \frac{1}{\lambda} - \epsilon\right) \left(\frac{1}{\lambda} + \epsilon\right)^{2(N+1)} \\
\epsilon &\approx \left(\lambda - \lambda^2\epsilon - \frac{1}{\lambda} - \epsilon\right) \left(\frac{1}{\lambda} + \epsilon\right)^{2(N+1)} \\
\epsilon &\approx \left(\frac{\lambda^2-1}{\lambda} - \epsilon(1+\lambda^2)\right) \left(\left(\frac{1}{\lambda}\right)^{2(N+1)} + \frac{2(N+1)}{\lambda^{2N+1}}\epsilon\right) \\
\rightarrow \epsilon &= \frac{\lambda^2-1}{\lambda}\left(\frac{1}{\lambda}\right)^{2(N+1)} + \frac{\lambda^2-1}{\lambda}\frac{2(N+1)\epsilon}{\lambda^{2N+1}} - \epsilon(1+\lambda^2)\left(\frac{1}{\lambda}\right)^{2(N+1)} \\
\epsilon &\approx \left(\frac{\lambda^2-1}{\lambda}\right) \frac{1}{\lambda^{2(N+1)} + \lambda^2 + 1 - 2(\lambda^2-1)(N+1)}
\end{aligned} \tag{B.87}$$

Here higher order ($\propto \epsilon^2$) were neglected.
In the case of

$$\begin{aligned}
(\lambda)^{2(N+1)} &>> \lambda^2 + 1 - 2(\lambda^2-1)(N+1) \\
&\rightarrow \epsilon \approx \frac{\lambda^2-1}{\lambda}(\frac{1}{\lambda^2})^{N+1}
\end{aligned} \tag{B.88}$$

This is true in the regime of $\lambda > 1$, where the localized state exists (for $\lambda < 1$ no imaginary solution in the condition for the k-values exists). Thus

$$\begin{aligned}
&\rightarrow \left(\frac{E}{2t}\right)^2 = 1 + \lambda^2 - \lambda(\frac{1}{\lambda} + \epsilon + \frac{1}{1/\lambda + \epsilon}) \\
&\approx 1 + \lambda^2 - \lambda(\frac{1}{\lambda} + \epsilon + \lambda - \lambda^2\epsilon) \\
&= \epsilon\lambda(\lambda^2 - 1)
\end{aligned} \tag{B.89}$$

B.10 Wave function of the localized state

$$\phi_n \propto \sinh(qn) \tag{B.90}$$

$$\psi_n \propto \sinh(q(N+1-n)) \tag{B.91}$$

The normalization constant can be calculated by

$$\begin{aligned}
\sum_n (|v_n|^2 + |u_n|^2) &= \sum_n \frac{1}{4}\left(\phi_n^2 + \psi_n^2 - 2\psi_n\phi_n + \psi_n^2 + \phi_n^2 + 2\phi_n\psi_n\right) \\
&= \sum_n \frac{1}{2}\left(\phi_n^2 + \psi_n^2\right) = \sum_n \phi_n^2 \,,
\end{aligned} \tag{B.92}$$

since $\sum_n \phi_n^2 = \sum_n \psi_n^2$.

$$\sum_n \sinh^2(nq) = \sum_{n=0}^{N} \frac{1}{4}\left(e^{2nq} + e^{-2nq} - 2\right) = \frac{1}{4}\left(\frac{e^{2q(N+1)}-1}{e^{2q}-1} + \frac{1-e^{-2q(N+1)}}{1-e^{-2q}} - 2(N+1)\right)$$

$$\rightarrow \frac{1}{\sum_n \sinh^2(nq)} = 4\frac{1}{\frac{e^{2q(N+1)}-1}{e^{2q}-1} + \frac{1-e^{-2q(N+1)}}{1-e^{-2q}} - 2(N+1)}$$

$$\approx \frac{1}{\frac{e^{2q(N+1)}-1}{e^{2q}-1} - \frac{1}{e^{2q}-1} + \frac{1}{1-e^{-2q}} - 2(N+1)} \approx 4\frac{e^{2q}-1}{e^{2q(N+1)}}$$

$$\approx 4\frac{\lambda^2-1}{(\lambda^2)^{N+1}}$$

$$\rightarrow \psi_n = 2\frac{\sqrt{\lambda^2-1}}{\lambda^{N+1}}\sinh(q(N+1-n)) \approx \sqrt{\lambda^2-1}e^{-qn} \tag{B.93}$$

$$\rightarrow \phi_n = 2\frac{\sqrt{\lambda^2-1}}{\lambda^{N+1}}\sinh(qn) \approx \sqrt{\lambda^2-1}e^{-q(N+1-n)} \tag{B.94}$$

B.11 Normalization for the transformation of the open chain

With

$$\phi_{kn} = u_{kn} - v_{kn} \propto s_k \sin(kn)$$

$$\psi_{kn} = u_{kn} + v_{kn} \propto \sin(k(N+1-n))$$

$$\rightarrow v_{kn} = \frac{1}{2}\left(c_1 \sin(k(N+1-n)) - c_2 s_k \sin(kn)\right) \tag{B.95}$$

$$\rightarrow u_{kn} = \frac{1}{2}\left(c_1 \sin(k(N+1-n)) + c_2 s_k \sin(kn)\right) \tag{B.96}$$

From the normalization condition we have

$$\sum_n |\phi_n|^2 = 1 = \sum_n |\psi_n|^2$$

$$\sum_n |\phi_n|^2 = \sum_n |c_1 \sin(kn)|^2 = c_1^2 \sum_n sin^2(kn) = c_1^2 \frac{1}{2}\left(N - \frac{\sin(kN)\cos(k(N+1))}{\sin(k)}\right)$$

$$\sum_n |\psi_n|^2 = c_2^2 \sum_{n=1}^{N} sin^2(k(N+1-n)) = c_2^2 \sum_{n=N}^{1} sin^2(k(N+1-n)) = c_2^2 \sum_{n=1}^{N} sin^2(kn)$$

$$\rightarrow c_1^2 = c_2^2 = \frac{2}{N - \frac{\sin(kN)\cos(k(N+1))}{\sin(k)}}\,. \tag{B.97}$$

Assuming that k is real (for imaginary k see B.10).

B.12 Majorana representation

To derive the zero energy mode in the thermodynamic limit one can introduce the Majorana modes:

$$\hat{a}_n = \hat{c}_n + \hat{c}_n^\dagger \tag{B.98}$$

$$\hat{b}_n = \frac{\hat{c}_n - \hat{c}_n^\dagger}{i} \tag{B.99}$$

With $\{\hat{a}_n, \hat{b}_j\} = 2\delta_{nj}$ and $\hat{a}^2 = \hat{b}^2 = 1$.
And the reverse transformation:

$$\hat{c}_n = \frac{\hat{a}_n + i\hat{b}_n}{2} \tag{B.100}$$

$$\hat{c}_n^\dagger = \frac{\hat{a}_n - i\hat{b}_n}{2} \tag{B.101}$$

Thus one can transform the hopping as

$$\hat{c}_{n+1}^\dagger \hat{c}_n = \frac{1}{4}\left(\hat{a}_{n+1}\hat{a}_n + \hat{b}_{n+1}\hat{b}_n + i\hat{a}_{n+1}\hat{b}_n - i\hat{b}_{n+1}\hat{a}_n\right) \tag{B.102}$$

$$\rightarrow \hat{c}_{n+1}^\dagger \hat{c}_n + \hat{c}_n^\dagger \hat{c}_{n+1} = \frac{i}{2}\left(\hat{a}_n\hat{b}_{n+1} - \hat{b}_n\hat{a}_{n+1}\right) , \tag{B.103}$$

And the pairing term to

$$\hat{c}_{n+1}\hat{c}_n = \frac{1}{4}\left(\hat{a}_{n+1}\hat{a}_n - \hat{b}_{n+1}\hat{b}_n + i\hat{a}_{n+1}\hat{b}_n + i\hat{b}_{n+1}\hat{a}_n\right) \tag{B.104}$$

$$\rightarrow \hat{c}_{n+1}\hat{c}_n + \hat{c}_n^\dagger \hat{c}_{n+1}^\dagger = \frac{i}{2}\left(\hat{a}_{n+1}\hat{b}_n + \hat{b}_{n+1}\hat{a}_n\right) . \tag{B.105}$$

The kinetic term transforms to

$$2\hat{n}_n = 1 + i\hat{a}_n\hat{b}_n . \tag{B.106}$$

Hence the total Hamiltonian reads with the Majorana operators

$$\begin{aligned} H &= -J\sum_{n=1}^{N-1}\left(\hat{c}_n^\dagger\hat{c}_{n+1} + \hat{c}_{n+1}\hat{c}_n + h.c.\right) - t\left(\sum_{n=1}^{N} 1 - 2\hat{n}_n\right) \\ &= -iJ\sum_{n=1}^{N-1}\hat{a}_{n+1}\hat{b}_n + it\sum_{n}^{N}\hat{a}_n\hat{b}_n \end{aligned} \tag{B.107}$$

To diagonalize define the following transformation:

$$\hat{a}_n = \sum_m f_{nm}\alpha_m \tag{B.108}$$

$$\hat{b}_n = \sum_m g_{nm}\beta_m . \tag{B.109}$$

Here α and β are also Majorana operators. Due to the properties of $\hat{a}_n$ and $\hat{b}_n$ the transformation matrix f_{nm} and g_{nm} has to be real and normalized to

$$1 = \sum_m f_{nm}^2 = \sum_m g_{nm}^2 . \tag{B.110}$$

The diagonalized Hamiltonian reads

$$\begin{aligned} H &= \frac{i}{2}\sum_m E_m\alpha_m\beta_m \\ &= -iJ\sum_{n=1}^{N-1}\sum_{m,l} f_{n+1,m}\alpha_m g_{n,l}\beta_l + it\sum_{n=1}^{N}\sum_{m,l} f_{n,m}g_{n,l}\alpha_m\beta_l . \end{aligned} \tag{B.111}$$

As the transformation has to diagonalize the Hamiltonian, all the terms with $m \neq l$ have to be zero such that:

$$\frac{1}{2}\sum_m E_m \alpha_m \beta_m = t\sum_{n=1}^{N}\sum_m f_{n,m} g_{n,m} \alpha_m \beta_m - J\sum_{n=1}^{N-1} f_{n+1,m} g_{n,m} \alpha_m \beta_m$$
$$\rightarrow E_m = 2t\sum_{n=1}^{N} f_{n,m} g_{n,m} \alpha_m \beta_m - 2J\sum_{n=1}^{N-1} f_{n+1,m} g_{n,m} \alpha_m \beta_m \,. \tag{B.112}$$

Since we want to focus here on the zero mode (Majorana mode) with zero energy, one can set $E_m = 0$ for this mode as an Ansatz. Hence one arrives at the condition

$$2t\sum_{n=1}^{N} f_{n,m} g_{n,m} = 2J\sum_{n=1}^{N-1} f_{n+1,m} g_{n,m} \,. \tag{B.113}$$

If one assumes $f_{n,m} = f_{1,m}^n$ and $g_{n,m} = g_{1,m}^n$:

$$t\sum_{n=1}^{N}(f_1 g_1)^n = J f_1 \sum_{n=1}^{N-1}(f_1 g_1)^n \tag{B.114}$$
$$\tag{B.115}$$

If one further assumes that the prefactors have the form $f_1 = 1/g_1$ we have

$$Nt = (N-1)J f_1$$
$$\rightarrow f_1 = \frac{N}{N-1}\frac{t}{J} \tag{B.116}$$
$$f_n = e^{n \ln \frac{Nt}{(N-1)J}} \tag{B.117}$$

Since one has also a normalizing condition:

$$1 = \sum_m f_{n,m}^2 \tag{B.118}$$
$$1 = f_{n,m_0}^2 + \underbrace{\sum_{m\neq m_0} f_{n,m}^2}_{\geq 0}$$
$$1 = e^{n \ln \frac{Nt}{(N-1)J}} + \underbrace{\sum_{m\neq m_0} f_{n,m}^2}_{\geq 0}$$
$$= \left(\frac{Nt}{(N-1)J}\right)^n + \underbrace{\sum_{m\neq m_0} f_{n,m}^2}_{\geq 0} \tag{B.119}$$

Here the zero mode has the notation m_0.
One can see from the last condition the zero mode can only exists if

$$\left(\frac{Nt}{(N-1)J}\right)^n \leq 1$$
$$\rightarrow \left(\frac{Nt}{(N-1)J}\right)^N \leq 1 \tag{B.120}$$

Thus for $N \to \infty$ we have

$$\frac{t}{J} \leq 1\, y \tag{B.121}$$

which is the condition for the existence of the zero mode (for $N \to \infty$).

C Lindblad for the closed chain

C.1 Delta functions

We have

$$\frac{1}{N}\sum_n e^{i\pi/N(k_1-k_2)n} = \begin{cases} 1 & k_1 = k_2 \\ e^{i\pi/N(k_1-k_2)}\frac{1-e^{i\pi(k_1-k_2)}}{1-e^{i\pi/N(k_1-k_2)}} = 0 & k_1 - k_2 = even \\ e^{i\pi/N(k_1-k_2)}\frac{1-e^{i\pi(k_1-k_2)}}{1-e^{i\pi/N(k_1-k_2)}} = e^{i\pi/N(k_1-k_2)}\frac{2}{1-e^{i\pi/N(k_1-k_2)}} & k_1 - k_2 = \text{odd} \end{cases} \tag{C.1}$$

If k_1 and k_2 are both even or both odd the difference or sum has always to be even, hence the third case for $k_1 - k_2 = \text{odd}$ drops out.

C.2 Global coupling

One can define the Fourier transform of the bath correlator

$$\Gamma(\omega) = \int_{t_0}^{t} dt^{'} e^{i\omega(t-t^{'})} F(t-t^{'}) \tag{C.2}$$

$$\Gamma^{*}(\omega) = \int_{t_0}^{t} dt^{'} e^{-i\omega(t-t^{'})} F(t^{'}-t) \tag{C.3}$$

Using the Rotating Wave Approximation will lead for the first two parts of the master equation (where only one subspace is involved):

$$\begin{aligned}
\frac{d\rho_s}{dt} &= -\Gamma(0)\left(N-2\sum_{k_1}\left(u_{k1}^2-v_{k1}^2\right)\gamma_{k1}^\dagger\gamma_{k1}\right)\left(N-2\sum_{k_2}\left(u_{k2}^2-v_{k2}^2\right)\gamma_{k2}^\dagger\gamma_{k2}\right)\rho_s \\
&+\Gamma(0)\left(N-2\sum_{k_1}\left(u_{k1}^2-v_{k1}^2\right)\gamma_{k1}^\dagger\gamma_{k1}\right)\rho_s\left(N-2\sum_{k_2}\left(u_{k2}^2-v_{k2}^2\right)\gamma_{k2}^\dagger\gamma_{k2}\right) \\
&+\Gamma^*(0)\left(N-2\sum_{k_1}\left(u_{k1}^2-v_{k1}^2\right)\gamma_{k1}^\dagger\gamma_{k1}\right)\rho_s\left(N-2\sum_{k_2}\left(u_{k2}^2-v_{k2}^2\right)\gamma_{k2}^\dagger\gamma_{k2}\right) \\
&-\Gamma^*(0)\left(N-2\sum_{k_1}\left(u_{k1}^2-v_{k1}^2\right)\gamma_{k1}^\dagger\gamma_{k1}\right)\left(N-2\sum_{k_2}\left(u_{k2}^2-v_{k2}^2\right)\gamma_{k2}^\dagger\gamma_{k2}\right)\rho_s \\
&-\sum_{k1,k2}\Gamma(2E_{k1})\delta_{E_{k1},E_{k2}}4u_{k1}v_{-k_1}u_{k2}v_{-k2}\left(\gamma_{k1}^\dagger\gamma_{-k1}^\dagger\right)\left(\gamma_{-k2}\gamma_{k2}\right)\rho_s \\
&+\sum_{k1,k2}\Gamma(2E_{k1})\delta_{E_{k1},E_{k2}}4u_{k1}v_{-k_1}u_{k2}v_{-k2}\left(\gamma_{-k2}\gamma_{k2}\right)\rho_s\left(\gamma_{k1}^\dagger\gamma_{-k1}^\dagger\right) \\
&+\sum_{k1,k2}\Gamma^*(2E_{k1})\delta_{E_{k1},E_{k2}}4u_{k1}v_{-k_1}u_{k2}v_{-k2}\left(\gamma_{-k2}\gamma_{k2}\right)\rho_s\left(\gamma_{k1}^\dagger\gamma_{-k1}^\dagger\right) \\
&-\sum_{k1,k2}\Gamma^*(2E_{k1})\delta_{E_{k1},E_{k2}}4u_{k1}v_{-k_1}u_{k2}v_{-k2}\rho_s\left(\gamma_{k1}^\dagger\gamma_{-k1}^\dagger\right)\left(\gamma_{-k2}\gamma_{k2}\right) \\
&-\sum_{k1,k2}\Gamma(-2E_{k1})\delta_{E_{k1},E_{k2}}4u_{k1}v_{-k_1}u_{k2}v_{-k2}\left(\gamma_{-k2}\gamma_{k2}\right)\left(\gamma_{k1}^\dagger\gamma_{-k1}^\dagger\right)\rho_s \\
&+\sum_{k1,k2}\Gamma(-2E_{k1})\delta_{E_{k1},E_{k2}}4u_{k1}v_{-k_1}u_{k2}v_{-k2}\left(\gamma_{k1}^\dagger\gamma_{-k1}^\dagger\right)\rho_s\left(\gamma_{-k2}\gamma_{k2}\right) \\
&+\sum_{k1,k2}\Gamma^*(-2E_{k1})\delta_{E_{k1},E_{k2}}4u_{k1}v_{-k_1}u_{k2}v_{-k2}\left(\gamma_{k1}^\dagger\gamma_{-k1}^\dagger\right)\rho_s\left(\gamma_{-k2}\gamma_{k2}\right) \\
&-\sum_{k1,k2}\Gamma^*(-2E_{k1})\delta_{E_{k1},E_{k2}}4u_{k1}v_{-k_1}u_{k2}v_{-k2}\rho_s\left(\gamma_{-k2}\gamma_{k2}\right)\left(\gamma_{k1}^\dagger\gamma_{-k1}^\dagger\right)
\end{aligned} \tag{C.4}$$

Note that the projection operators on the two parity subspaces were omitted for simplification (e.g. $\gamma_{k1}\gamma_{k2} \sim \hat{P}^{\pm}\gamma_{k1}\gamma_{k2}\hat{P}^{\pm}$).
One can divide these equation into the real part with $\kappa(\omega) = \Gamma(\omega) + \Gamma^*(\omega)$ and all Lamb-shift terms with $2iS(\omega) = \Gamma(\omega) - \Gamma^*(\omega)$. Such that:

$$\Gamma(\omega)[A, B\rho_s] + \Gamma^*(\omega)[\rho_s A, B] = -\kappa(\omega)\left(B\rho_s A - \frac{1}{2}\{AB, \rho_s\}\right) + iS[AB, \rho_s] \tag{C.5}$$

Neglecting the Lamb shift terms, to obtain only the dissipative part, leads to:

$$\begin{aligned}
\frac{d\rho_s}{dt} &= 4\kappa(0)\sum_{k1,k2}(u_{k1}^2-v_{k1}^2)(u_{k2}^2-v_{k2}^2)\left(\gamma_{k1}^\dagger\gamma_{k1}\rho_s\gamma_{k2}^\dagger\gamma_{k2} - \frac{1}{2}\left\{\gamma_{k1}^\dagger\gamma_{k1}\gamma_{k2}^\dagger\gamma_{k2}, \rho_s\right\}\right) \\
&+4\sum_{k1,k2}\delta_{E_{k1},E_{k2}}\kappa(2E_{k1})4u_{k1}v_{-k_1}u_{k2}v_{-k2}\left(\gamma_{-k1}\gamma_{k1}\rho_s\gamma_{k2}^\dagger\gamma_{-k2}^\dagger - \frac{1}{2}\left\{\gamma_{k2}^\dagger\gamma_{k2}^\dagger\gamma_{-k1}\gamma_{k1}, \rho_s\right\}\right) \\
&+4\sum_{k1,k2}\delta_{E_{k1},E_{k2}}\kappa(-2E_{k1})4u_{k1}v_{-k_1}u_{k2}v_{-k2}\left(\gamma_{k1}^\dagger\gamma_{-k1}\rho_s\gamma_{-k2}\gamma_{k2} - \frac{1}{2}\left\{\gamma_{-k2}\gamma_{k2}\gamma_{k1}^\dagger\gamma_{-k1}^\dagger, \rho_s\right\}\right)
\end{aligned} \tag{C.6}$$

With $u_k^2 - v_k^2 = \xi_k/E_k$ and $u_k v_k = \Delta_k/2E_k$.
The last part from the master equation can be transformed in the same way as before, but due to the rotating wave approximation and the fact that the even and odd parity subspace have different single particle spectrum, the only term left, is the one with $\omega = 0$:

$$\begin{aligned}
\frac{d\rho_s}{dt} &= \Gamma(0)\left(2\sum_{k_1^+}\left(u_{k1}^2 - v_{k1}^2\right)P^+\gamma_{k1}^\dagger\gamma_{k1}P^+\right)\rho_s\left(2\sum_{k_2^-}\left(u_{k2}^2 - v_{k2}^2\right)P^-\gamma_{k2}^\dagger\gamma_{k2}P^-\right) \\
&+ \Gamma^*(0)\left(2\sum_{k_1^+}\left(u_{k1}^2 - v_{k1}^2\right)P^+\gamma_{k1}^\dagger\gamma_{k1}P^+\right)\rho_s\left(2\sum_{k_2^-}\left(u_{k2}^2 - v_{k2}^2\right)P^-\gamma_{k2}^\dagger\gamma_{k2}P^-\right) \\
&+ \Gamma(0)\left(2\sum_{k_1^-}\left(u_{k1}^2 - v_{k1}^2\right)P^-\gamma_{k1}^\dagger\gamma_{k1}P^-\right)\rho_s\left(2\sum_{k_2^-}\left(u_{k2}^2 - v_{k2}^2\right)P^+\gamma_{k2}^\dagger\gamma_{k2}P^+\right) \\
&+ \Gamma^*(0)\left(2\sum_{k_1^+}\left(u_{k1}^2 - v_{k1}^2\right)P^-\gamma_{k1}^\dagger\gamma_{k1}P^-\right)\rho_s\left(2\sum_{k_2^-}\left(u_{k2}^2 - v_{k2}^2\right)P^+\gamma_{k2}^\dagger\gamma_{k2}P^+\right)) \\
&= \kappa_0\sum_{k1^+,k_2^-}\frac{\xi_{k1}\xi_{k2}}{E_{k1}E_{k2}}P^+\gamma_{k1}^\dagger\gamma_{k1}P^+\rho_s P^-\gamma_{k2}^\dagger\gamma_{k2}P^- \\
&+ \kappa_0\sum_{k1^-,k_2^+}\frac{\xi_{k1}\xi_{k2}}{E_{k1}E_{k2}}P^-\gamma_{k1}^\dagger\gamma_{k1}P^-\rho_s P^+\gamma_{k2}^\dagger\gamma_{k2}P^+
\end{aligned} \tag{C.7}$$

C.3 Diagonalization of the first excited subspace

To find the solution of this set of equation

$$t\left[f_{(n+1,m)} + f_{(n-1,m)} + f_{(n,m+1)} + f_{(n,m-1)}\right] = \varepsilon f_{(n,m)}\,, \tag{C.8}$$

for $|n-m| > 1$ and $|N+n-m| < 1$ whereas for $n = m+1$ we have

$$t\left[f_{(n+1,m)} + f_{(n,m-1)}\right] = \varepsilon f_{(n,m)}\,, \tag{C.9}$$

or for $n = m-1$ we have

$$t\left[f_{(n-1,m)} + f_{(n,m+1)}\right] = \varepsilon f_{(n,m)}\,, \tag{C.10}$$

one can solve the problem connected to the tight binding model in the effective lattice shown in Fig.3.8. Define the vertical direction of this effective lattice as x-direction and the horizontal direction of the effective lattice as y-direction. As there are periodic boundary conditions along x, we have $\Psi(x) = \Psi(x+2N)$ and open boundary condition (due to the loose ends) along y with $\Psi(0) = \Psi(N) = 0$. Hence with $\Psi = f_{x,y}\,|x,y\rangle$ (x,y define the position in the effective lattice) we have

$$f_{x,y} = \frac{\sqrt{2}}{N}\sin\left(\frac{pi}{N}ky\right)e^{i\frac{pi}{N}qx} \tag{C.11}$$

$$\varepsilon(k,q) = 2t\left(\cos(\pi(k-q)/N) + \cos(\pi(k+q)/N)\right) \tag{C.12}$$

using the usual Ansatz for the tight binding model.
To express the solution in the basis of the two domain walls has to project the position $|x, y\rangle$ back to $|n, m\rangle$ with:

$$x = \begin{cases} n+m & \text{for } n < m \\ n+m \pm N & \text{for } n > m \end{cases} \tag{C.13}$$

$$y = \begin{cases} m-n & \text{for } n < m \\ m-n+N & \text{for } n > m \end{cases} \tag{C.14}$$

Hence the result in the basis of $|n, m\rangle$ is

$$\begin{aligned} f_{n,m} &= \begin{cases} \frac{\sqrt{2}}{N} \sin(\frac{\pi}{N} k(m-n)) e^{i\frac{\pi}{N} q(m+n)} & n < m \\ e^{i\pi(k+q)} \frac{\sqrt{2}}{N} \sin(\frac{\pi}{N} k(m-n)) e^{i\frac{\pi}{N} q(m+n)} & n > m \end{cases} \\ \varepsilon(k,q) &= 2t \left[\cos\left(\pi(k-q)/N\right) + \cos\left(\pi(k+q)/N\right)\right] \end{aligned} \tag{C.15}$$

C.4 Lindblad operator by Projection onto the eigenstates

For the Lindblad operator connecting the ground states with the excited subspace we have

$$\begin{aligned} \hat{A}(4J + \varepsilon(k,q)) &= (|u\rangle\langle u| + |d\rangle\langle u|) \sum_i \sigma_i^z |k,q\rangle\langle k,q| \\ &= (|u\rangle\langle u| + |d\rangle\langle u|) \sum_i \sigma_i^z \sum_{n,m} f_{n,m} |n,m\rangle\langle k,q| \\ &= (|u\rangle\langle u| + |d\rangle\langle u|) \sum_n \left(f_{n,n+1} |u\rangle + f_{n+1,n} |d\rangle\right)\langle k,q| \ , \end{aligned} \tag{C.16}$$

and with

$$\begin{aligned} \sum_n f_{n,n+1} &= \frac{\sqrt{2}}{N} \sin\left(\frac{\pi}{N}k\right) \sum_n \left(e^{\frac{i\pi}{N} q(2n+1)}\right) \\ &= \sqrt{2} \sin\left(\frac{\pi}{N}k\right) \delta_{q,N} \\ \sum_n f_{n+1,n} &= -e^{i\pi(k+N)} \sqrt{2} \sin\left(\frac{\pi}{N}k\right) \delta_{q,N} \end{aligned} \tag{C.17}$$

we have

$$\hat{A}(4J + \varepsilon(k,q)) = 2 \sin\left(\frac{\pi k}{N}\right) |g_s\rangle\langle k, N| \ . \tag{C.18}$$

C.5 Local coupling

The Redfield equation for one subspace reads as (note that the projector operators are neglected):

$$\begin{aligned}\frac{d\rho_s}{dt} = -\int_{t_0}^{t} dt' \sum_{n_1,n_2} \Big(& F_{n_1,n_2}(t-t')\sigma^z_{n_1}(t)\sigma^z_{n_2}(t')\rho_s(t) \\ & - F_{n_1,n_2}(t-t')\sigma^z_{n_2}(t')\rho_s(t)\sigma^z_{n_1}(t) \\ & - F_{n_2,n_1}(t'-t)\sigma^z_{n_1}(t)\rho_s(t)\sigma^z_{n_2}(t') \\ & + F_{n_2,n_1}(t'-t)\rho_s(t)\sigma^z_{n_2}(t')\sigma^z_{n_1}(t)\Big)\end{aligned} \tag{C.19}$$

Under the Rotating Wave Approximation (or secular approximation) only the terms, which rotate with the same frequency are taken into account (every other term refers to fast oscillating terms and can be neglected). Thus one can define the Fourier transformation of the correlation function of the bath to

$$\Gamma_{n_1,n_2}(\omega) = \int_{t_0}^{t} dt' e^{i\omega(t-t')} F_{n_1,n_2}(t-t') \tag{C.20}$$

$$\Gamma^*_{n_2,n_1}(\omega) = \int_{t_0}^{t} dt' e^{-i\omega(t-t')} F_{n_2,n_1}(t'-t) \tag{C.21}$$

To have the whole dependence of the spin sites in one term one can define

$$\Gamma_\omega(k_1-k_2,k_3-k_4) = \frac{1}{N^2}\sum_{n_1,n_2}\Gamma_{n_1,n_2}(\omega)e^{-i\frac{\pi}{N}(k_1-k_2)n_1}e^{-i\frac{\pi}{N}(k_3-k_4)n_2} \tag{C.22}$$

adding the n-dependent terms of $\sigma^z_n(t)$.
For local coupling one can assume that $F_{n_1,n_2} = c(t-t')\delta_{n_1,n_2}$, such that the bath correlator is only nonzero at the same spin site (the bathes of different spin sites are uncorrelated)

$$\begin{aligned}\Gamma_\omega(k_1-k_2,k_3-k_4) &= \frac{1}{N^2}\sum_{n_1,n_2}\Gamma_{n_1,n_2}(\omega)e^{-i\frac{\pi}{N}(k_1-k_2)n_1}e^{-i\frac{\pi}{N}(k_3-k_4)n_2} \\ &= \frac{1}{N^2}\sum_{n_1,n_2} c(\omega)\cdot\delta_{n1,n2}e^{-i\frac{\pi}{N}(k_1-k_2)n_1}e^{-i\frac{\pi}{N}(k_3-k_4)n_2} \\ &= \frac{1}{N^2}\sum_{n_1} c(\omega)\cdot e^{-i\frac{\pi}{N}(k_1-k_2+k_3-k_4)n_1} \\ &= \frac{1}{N}c(\omega)\cdot\delta_{k_1-k_2,k_4-k_3}\end{aligned} \tag{C.23}$$

Such that the master equation can be expressed as (omitting the projection operators for simplification e.g. $\gamma_{k1}\gamma_{k2} \sim \hat{P}^{\pm}\gamma_{k1}\gamma_{k2}\hat{P}^{\pm}$))

$$
\begin{aligned}
\hat{L}^{\pm}(\rho_s) = \Bigg(& \frac{2}{N}\sum_{k_1,k_2} A_{k_1,k_2} c(0)\delta_{k_1-k_2,0}\delta_{E_{k1}-E_{k2},0}[\gamma_{k1}^{\dagger}\gamma_{k2},\rho_s] \\
& + \frac{2}{N}\sum_{k_1,k_2} u_{k1}v_{k2}c(0)\delta_{k_1+k_2,0}\delta_{E_{k1}+E_{k2},0}[\gamma_{k1}^{\dagger}\gamma_{k2}^{\dagger}+\gamma_{k2}\gamma_{k1},\rho_s] \\
& + \frac{4}{N}\sum_{k_1,k_2k_3,k_4} A_{k_1,k_2}A_{k_3,k_4}c((E_{k1}-E_{k2}))\delta_{k_1-k_2,k_4-k_3}\delta_{E_{k1}-E_{k2},E_{k4}-E_{k3}}[\gamma_{k1}^{\dagger}\gamma_{k2},\gamma_{k3}^{\dagger}\gamma_{k4}\rho_s] \\
& + 4\sum_{k_1,k_2k_3,k_4} A_{k_1,k_2}u_{k_3}v_{k_4}c(E_{k1}-E_{k2})\delta_{k_1-k_2,-k_3-k_4}\delta_{E_{k1}-E_{k2},-E_{k3}-E_{k4}}[\gamma_{k1}^{\dagger}\gamma_{k2},\gamma_{k3}^{\dagger}\gamma_{k4}^{\dagger}\rho_s] \\
& + 4\sum_{k_1,k_2k_3,k_4} A_{k_1,k_2}u_{k_3}v_{k_4}c(E_{k1}-E_{k2})\delta_{k_1-k_2,k_3+k_4}\delta_{E_{k1}-E_{k2},E_{k3}E_{k4}}[\gamma_{k1}^{\dagger}\gamma_{k2},\gamma_{k4}\gamma_{k3}\rho_s] \\
& + \frac{4}{N}\sum_{k_1,k_2k_3,k_4} u_{k1}v_{k2}A_{k_3,k_4}c(E_{k1}+E_{k2})\delta_{k_1+k_2,k_4-k_3}\delta_{E_{k1}+E_{k2},-E_{k3}+E_{k4}}[\gamma_{k1}^{\dagger}\gamma_{k2}^{\dagger},\gamma_{k3}^{\dagger}\gamma_{k4}\rho_s] \\
& + \frac{4}{N}\sum_{k_1,k_2k_3,k_4} u_{k1}v_{k2}u_{k3}v_{k4}c(E_{k1}+E_{k2})\delta_{k_1+k_2,-k_3-k_4}\delta_{E_{k1}+E_{k2},-E_{k3}-E_{k4}}[\gamma_{k1}^{\dagger}\gamma_{k2}^{\dagger},\gamma_{k3}^{\dagger}\gamma_{k4}^{\dagger}\rho_s] \\
& + \frac{4}{N}\sum_{k_1,k_2k_3,k_4} u_{k1}v_{k2}u_{k3}v_{k4}c(E_{k1}+E_{k2})\delta_{k_1+k_2,k_3+k_4}\delta_{E_{k1}+E_{k2},E_{k3}+E_{k4}}[\gamma_{k1}^{\dagger}\gamma_{k2}^{\dagger},\gamma_{k4}\gamma_{k3}\rho_s] \\
& + \frac{4}{N}\sum_{k_1,k_2k_3,k_4} u_{k1}v_{k2}u_{k3}v_{k4}c(-E_{k1}-E_{k2})\delta_{-k_1-k_2,k_3+k_4}\delta_{-E_{k1}-E_{k2},E_{k3}+E_{k4}}[\gamma_{k2}\gamma_{k1},\gamma_{k4}\gamma_{k3}\rho_s] \\
& + \frac{4}{N}\sum_{k_1,k_2k_3,k_4} u_{k1}v_{k2}u_{k3}v_{k4}c(-E_{k1}-E_{k2})\delta_{-k_1-k_2,-k_3-k_4}\delta_{-E_{k1}-E_{k2},-E_{k3}-E_{k4}}[\gamma_{k2}\gamma_{k1},\gamma_{k3}^{\dagger}\gamma_{k4}^{\dagger}\rho_s] \\
& + \frac{4}{N}\sum_{k_1,k_2k_3,k_4} u_{k1}v_{k2}A_{k1,k2}c(-E_{k1}-E_{k2})\delta_{-k_1-k_2,k_4-k_3}\delta_{-E_{k1}-E_{k2},-E_{k3}+E_{k4}}[\gamma_{k2}\gamma_{k1},\gamma_{k3}^{\dagger}\gamma_{k4}\rho_s]
\end{aligned}
$$

$$
\begin{aligned}
&+\frac{2}{N}\sum_{k_1,k_2} A_{k_1,k_2}c^*(0)\delta_{k_1-k_2,0}\delta_{E_{k1}-E_{k2},0}[\rho_s,\gamma^\dagger_{k1}\gamma_{k2}]\\
&+\frac{2}{N}\sum_{k_1,k_2} u_{k1}v_{k2}c^*(0)\delta_{k_1+k_2,0}\delta_{E_{k1}+E_{k2},0}[\rho_s,\gamma^\dagger_{k1}\gamma^\dagger_{k2}+\gamma_{k2}\gamma_{k1}]\\
&+\frac{4}{N}\sum_{k_1,k_2k_3,k_4} A_{k_1,k_2}A_{k_3,k_4}c^*(E_{k1}-E_{k2})\delta_{k_1-k_2,k_4-k_3}\delta_{E_{k1}-E_{k2},E_{k4}-E_{k3}}[\rho_s\gamma^\dagger_{k1}\gamma_{k2},\gamma^\dagger_{k3}\gamma_{k4}]\\
&+\frac{4}{N}\sum_{k_1,k_2k_3,k_4} A_{k_1,k_2}u_{k_3}v_{k_4}c^*(E_{k1}-E_{k2})\delta_{k_1-k_2,-k_3-k_4}\delta_{E_{k1}-E_{k2},-E_{k3}-E_{k4}}[\rho_s\gamma^\dagger_{k1}\gamma_{k2},\gamma^\dagger_{k3}\gamma^\dagger_{k4}]\\
&+\frac{4}{N}\sum_{k_1,k_2k_3,k_4} A_{k_1,k_2}u_{k_3}v_{k_4}c^*(E_{k1}-E_{k2})\delta_{k_1-k_2,k_3+k_4}\delta_{E_{k1}-E_{k2},E_{k3}E_{k4}}[\rho_s\gamma^\dagger_{k1}\gamma_{k2},\gamma_{k4}\gamma_{k3}]\\
&+\frac{4}{N}\sum_{k_1,k_2k_3,k_4} u_{k1}v_{k2}A_{k_3,k_4}c^*(E_{k1}+E_{k2})\delta_{k_1+k_2,k_4-k_3}\delta_{E_{k1}+E_{k2},-E_{k3}+E_{k4}}[\rho_s\gamma^\dagger_{k1}\gamma^\dagger_{k2},\gamma^\dagger_{k3}\gamma_{k4}]\\
&+\frac{4}{N}\sum_{k_1,k_2k_3,k_4} u_{k1}v_{k2}u_{k3}v_{k4}c^*(E_{k1}+E_{k2})\delta_{k_1+k_2,-k_3-k_4}\delta_{E_{k1}+E_{k2},-E_{k3}-E_{k4}}[\rho_s\gamma^\dagger_{k1}\gamma^\dagger_{k2},\gamma^\dagger_{k3}\gamma^\dagger_{k4}]\\
&+\frac{4}{N}\sum_{k_1,k_2k_3,k_4} u_{k1}v_{k2}u_{k3}v_{k4}c^*(E_{k1}+E_{k2})\delta_{k_1+k_2,k_3+k_4}\delta_{E_{k1}+E_{k2},E_{k3}+E_{k4}}[\rho_s\gamma^\dagger_{k1}\gamma^\dagger_{k2},\gamma_{k4}\gamma_{k3}]\\
&+\frac{4}{N}\sum_{k_1,k_2k_3,k_4} u_{k1}v_{k2}u_{k3}v_{k4}c^*_{-k_1-k_2}(-2(E_{k1}+E_{k2}))\delta_{-k_1-k_2,k_3+k_4}\delta_{-E_{k1}-E_{k2},E_{k3}+E_{k4}}[\rho_s\gamma_{k2}\gamma_{k1},\gamma_{k4}\gamma_{k3}]\\
&+\frac{4}{N}\sum_{k_1,k_2k_3,k_4} u_{k1}v_{k2}u_{k3}v_{k4}c^*(-E_{k1}-E_{k2})\delta_{-k_1-k_2,-k_3-k_4}\delta_{-E_{k1}-E_{k2},-E_{k3}-E_{k4}}[\rho_s\gamma_{k2}\gamma_{k1},\gamma^\dagger_{k3}\gamma^\dagger_{k4}]\\
&+\frac{4}{N}\sum_{k_1,k_2k_3,k_4} u_{k1}v_{k2}A_{k1,k2}c^*(-E_{k1}-E_{k2})\delta_{-k_1-k_2,k_4-k_3}\delta_{-E_{k1}-E_{k2},-E_{k3}+E_{k4}}[\rho_s\gamma_{k2}\gamma_{k1},\gamma^\dagger_{k3}\gamma_{k4}]\Big)
\end{aligned}
\tag{C.24}
$$

With $A_{k_1,k_2}=(v_{k1}v_{k2}-u_{k1}u_{k2})$.
Some terms contains delta-functions, which cannot be fulfilled e.g. $\delta_{k_1+k_2,0}\delta_{E_{k1}+E_{k2},0}$:

$$k_1=-k_2 \tag{C.25}$$
$$E_{k1}=-E_{k2} \tag{C.26}$$

One can see that this cannot be fulfilled with the given energy relation for $t>J$ and $t<J$ (only at $t=J$ with $E_0=0$).
Besides the cases $\delta_{k_1+k_2,-k_3-k_4}\delta_{E_{k1}+E_{k2},-E_{k3}-E_{k4}}$ and $\delta_{-k_1-k_2,k_3+k_4}\delta_{-E_{k1}-E_{k2},E_{k3}+E_{k4}}$ can also be never fulfilled as $E_k>0$ for all k. Besides there is also a non-trivial case that drops out

$$k_1-k_2=k_3+k_4 \tag{C.27}$$
$$E_{k1}-E_{k2}=E_{k3}+E_{k4}\,, \tag{C.28}$$

which is also impossible to fulfill as it can be seen in Fig.17.
All the rest can be fulfilled (depending on t, J, N). Dropping out these terms simplify

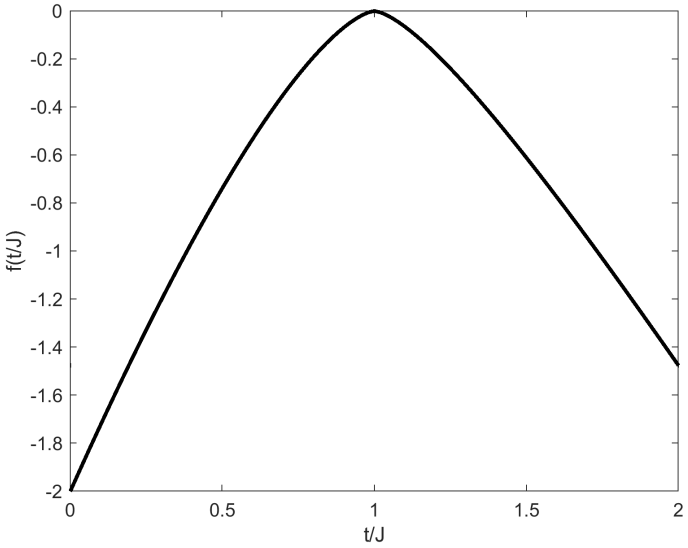

Figure 17: The function $f(t/J) = max_{\Delta_k}(max_{k1}(E_{k1} - E_{k1-\Delta_k}) - min_{k3}(E_{k3} + E_{\Delta_k - k3}))$ with $\Delta_k = k_1 - k_2$ plotted over t/J. The function f is always smaller than zero for $t > J$ and $t < J$, meaning there cannot be a solution for $\delta_{k1-k2,k3+k4}\delta_{E_{k1}-E_{k2},E_{k3}+E_{k4}}$ as $E_{k1} - E_{k2} < E_{k3} + E_{k4}$ under the condition that $k_1 - k_2 = k_3 + k_4$. Only at the critical point $t = J$ there can be a solution with $E_k - E_0 = E_k + E_0$ ($E_0 = 0$ at the critical point), but for $t < J$ and $t > J$ all terms containing these delta-functions can be dropped.

the master equation to:

$$
\begin{aligned}
\hat{L}(\rho_s) = -\Bigg(& \frac{2}{N} \sum_{k_1} A_{k_1,k_2} c(0) [\gamma_{k1}^\dagger \gamma_{k1}, \rho_s] \\
& + \frac{4}{N} \sum_{k_1,k_2 k_3,k_4} A_{k_1,k_2} A_{k_3,k_4} c(E_{k1} - E_{k2}) \delta_{k_1-k_2,k_4-k_3} \delta_{E_{k1}-E_{k2},E_{k4}-E_{k3}} [\gamma_{k1}^\dagger \gamma_{k2}, \gamma_{k3}^\dagger \gamma_{k4} \rho_s] \\
& + \frac{4}{N} \sum_{k_1,k_2 k_3,k_4} u_{k1} v_{k2} u_{k3} v_{k4} c(E_{k1} + E_{k2}) \delta_{k_1+k_2,k_3+k_4} \delta_{E_{k1}+E_{k2},E_{k3}+E_{k4}} [\gamma_{k1}^\dagger \gamma_{k2}^\dagger, \gamma_{k4} \gamma_{k3} \rho_s] \\
& + \frac{4}{N} \sum_{k_1,k_2 k_3,k_4} u_{k1} v_{k2} u_{k3} v_{k4} c(-E_{k1} - E_{k2}) \delta_{-k_1-k_2,-k_3-k_4} \delta_{-E_{k1}-E_{k2},-E_{k3}-E_{k4}} [\gamma_{k2} \gamma_{k1}, \gamma_{k3}^\dagger \gamma_{k4}^\dagger \rho_s] \\
& + \frac{4}{N} \sum_{k_1} A_{k_1,k_1} c^*(0) [\rho_s, \gamma_{k1}^\dagger \gamma_{k1}] \\
& + \frac{4}{N} \sum_{k_1,k_2 k_3,k_4} A_{k_1,k_2} A_{k_3,k_4} c^*(E_{k1} - E_{k2}) \delta_{k_1-k_2,k_4-k_3} \delta_{E_{k1}-E_{k2},E_{k4}-E_{k3}} [\rho_s \gamma_{k1}^\dagger \gamma_{k2}, \gamma_{k3}^\dagger \gamma_{k4}] \\
& + \frac{4}{N} \sum_{k_1,k_2 k_3,k_4} u_{k1} v_{k2} u_{k3} v_{k4} c^*(E_{k1} + E_{k2}) \delta_{k_1+k_2,k_3+k_4} \delta_{E_{k1}+E_{k2},E_{k3}+E_{k4}} [\rho_s \gamma_{k1}^\dagger \gamma_{k2}^\dagger, \gamma_{k4} \gamma_{k3}] \\
& + \frac{4}{N} \sum_{k_1,k_2 k_3,k_4} u_{k1} v_{k2} u_{k3} v_{k4} c^*(-E_{k1} - E_{k2})) \delta_{-k_1-k_2,-k_3-k_4} \delta_{-E_{k1}-E_{k2},-E_{k3}-E_{k4}} [\rho_s \gamma_{k2} \gamma_{k1}, \gamma_{k3}^\dagger \gamma_{k4}^\dagger]
\end{aligned}
\tag{C.29}
$$

One can see that there are several terms which have the following structure:

$$\begin{aligned} c[A, B\rho_s] + c^*[\rho_s A, B] &= c(AB\rho_s - B\rho_s A) + c^*(\rho_s AB - B\rho_s A) \\ &= -(c + c^*)B\rho_s A + cAB\rho_s + c^*\rho_s AB \\ &= -\underbrace{(c + c^*)}_{\kappa}\left(B\rho_s A - \frac{1}{2}(AB\rho_s + \rho_s AB)\right) + \underbrace{\frac{1}{2}(c - c^*)}_{iS}(AB\rho_s - \rho_s AB) \\ &= -\kappa\left(B\rho_s A - \frac{1}{2}\{AB, \rho_s\}\right) + iS[AB, \rho_s] \end{aligned} \tag{C.30}$$

Where κ is the real part of c and S the imaginary part of c.
Thus the total equation can be expressed in Lindblad form as (neglecting the Lamb shift from the imaginary part):

$$\begin{aligned} \hat{L}(\rho_s) = \frac{4}{N} &\sum_{k1,k2,k3,k4} A_{k1,k2}A_{k3,k4}\delta_{k_1-k_2,k_4-k_3}\delta_{E_{k1}-E_{k2},E_{k4}-E_{k3}} \\ &\left(\kappa(E_{k1} - E_{k2})\left(\gamma^\dagger_{k3}\gamma_{k4}\rho_s\gamma^\dagger_{k1}\gamma_{k2} - \frac{1}{2}\{\gamma^\dagger_{k1}\gamma_{k2}\gamma^\dagger_{k3}\gamma_{k4}, \rho_s\}\right)\right) \\ &+ \frac{4}{N}\sum_{k1,k2,k3,k4} u_{k1}v_{k2}u_{k3}v_{k4}\delta_{k_1+k_2,k_4+k_3}\delta_{E_{k1}+E_{k2},E_{k4}+E_{k3}} \\ &\left(\kappa(E_{k1} + E_{k2})\left(\gamma_{k4}\gamma_{k3}\rho_s\gamma^\dagger_{k1}\gamma^\dagger_{k2} - \frac{1}{2}\{\gamma^\dagger_{k1}\gamma^\dagger_{k2}\gamma_{k4}\gamma_{k3}, \rho_s\}\right)\right) \\ &+ \frac{4}{N}\sum_{k1,k2,k3,k4} u_{k1}v_{k2}u_{k3}v_{k4}\delta_{-k_1-k_2,-k_4-k_3}\delta_{-E_{k1}-E_{k2},-E_{k4}-E_{k3}} \\ &\left(\kappa(-E_{k1} - E_{k2})\left(\gamma^\dagger_{k3}\gamma^\dagger_{k4}\rho_s\gamma_{k2}\gamma_{k1} - \frac{1}{2}\{\gamma_{k2}\gamma_{k1}\gamma^\dagger_{k3}\gamma^\dagger_{k4}, \rho_s\}\right)\right) \end{aligned} \tag{C.31}$$

The expression above will be defined as the Lindblad master operator $L^{\pm}$ for the respective subspace (only the sum over the possible k-values are different for the two subspaces).
The same can be done for the master equation part with mixing parity, leading to

$$\begin{aligned} \hat{L}^{\pm\mp}(\rho_s) = \frac{4}{N} &\sum_{k1^-,k2^-,k3^+,k4^+} A_{k1,k2}A_{k3,k4}\delta_{k_1-k_2,k_4-k_3}\delta_{E_{k1}-E_{k2},E_{k4}-E_{k3}}\kappa(E_{k1} - E_{k2}) \\ &\left(\hat{P}^+\gamma^\dagger_{k3}\gamma_{k4}\hat{P}^+\rho_s\hat{P}^-\gamma^\dagger_{k1}\gamma_{k2}\hat{P}^-\right) \\ &+ \frac{4}{N}\sum_{k1^-,k2^-,k3^+,k4^+} u_{k1}v_{k2}u_{k3}v_{k4}\delta_{k_1+k_2,k_4+k_3}\delta_{E_{k1}+E_{k2},E_{k4}+E_{k3}}\kappa(E_{k1} + E_{k2}) \\ &\left(\hat{P}^+\gamma_{k4}\gamma_{k3}\hat{P}^+\rho_s\hat{P}^-\gamma^\dagger_{k1}\gamma^\dagger_{k2}\hat{P}^-\right) \\ &+ \frac{4}{N}\sum_{k1^-,k2^-,k3^+,k4^+} u_{k1}v_{k2}u_{k3}v_{k4}\delta_{-k_1-k_2,-k_4-k_3}\delta_{-E_{k1}-E_{k2},-E_{k4}-E_{k3}}\kappa(-E_{k1} - E_{k2}) \\ &\left(\hat{P}^+\gamma^\dagger_{k3}\gamma^\dagger_{k4}\hat{P}^+\rho_s\hat{P}^-\gamma_{k2}\gamma_{k1}\hat{P}^-\right) \end{aligned} \tag{C.32}$$

C.6 Additional solutions for the delta functions for 10 spins

Every time there is a crossing in Fig.18 or Fig.19 there is a additional solution in the Lindblad equation, e.g. at the point $t/J = 1.5$ (for $N = 10$), $\delta_{k1-k2,k4-k3}\delta_{E_{k1}-E_{k2},E_{k3}-E_{k4}}$ has additionally the solution $k_1 = 5$, $k_2 = 3$, $k_3 = 3$ and $k_4 = 1$, which leads to the extra term in the Lindblad:

$$\frac{2}{N}(u_5u_3 - v_5v_3)(u_3u_1 - v_3v_1)\gamma_3^\dagger\gamma_1\rho_s\gamma_5^\dagger\gamma_3 - \frac{1}{2}\{\gamma_5^\dagger\gamma_3\gamma_3^\dagger\gamma_1, \rho_s\} \tag{C.33}$$

As one can see this term only leads to an additional coupling and decay of matrix elements with excitation with the k-values of the additional solution and thus do not influence e.g. the decoherence of the ground states. Besides the influence of this single term at the point $t/J = 1.5$ should be small due to the large number of other terms in the Lindblad ($\sim N^2$). All the other additional solution (at different t/J ratios) have similar behavior and thus can be neglected for deriving a general solution for arbitrary t/J and N.

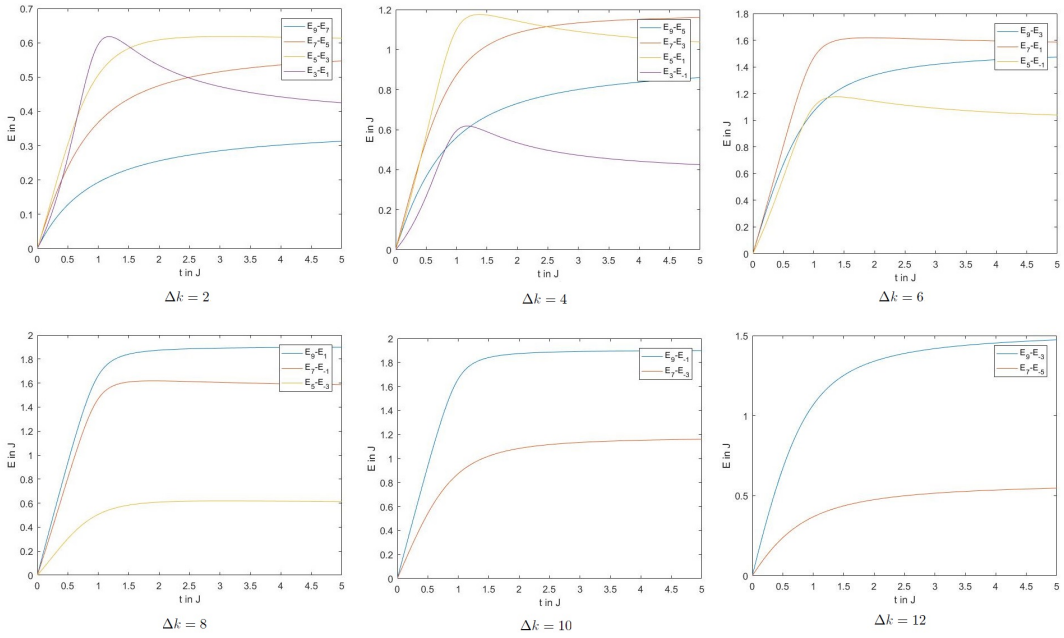

Figure 18: Energy differences with the same difference $\Delta k = k_1 - k_2$ for the even parity subspace. Note that the possibilities with negative k lead to the same figure with negative energy since $E_k = E_{-k}$.

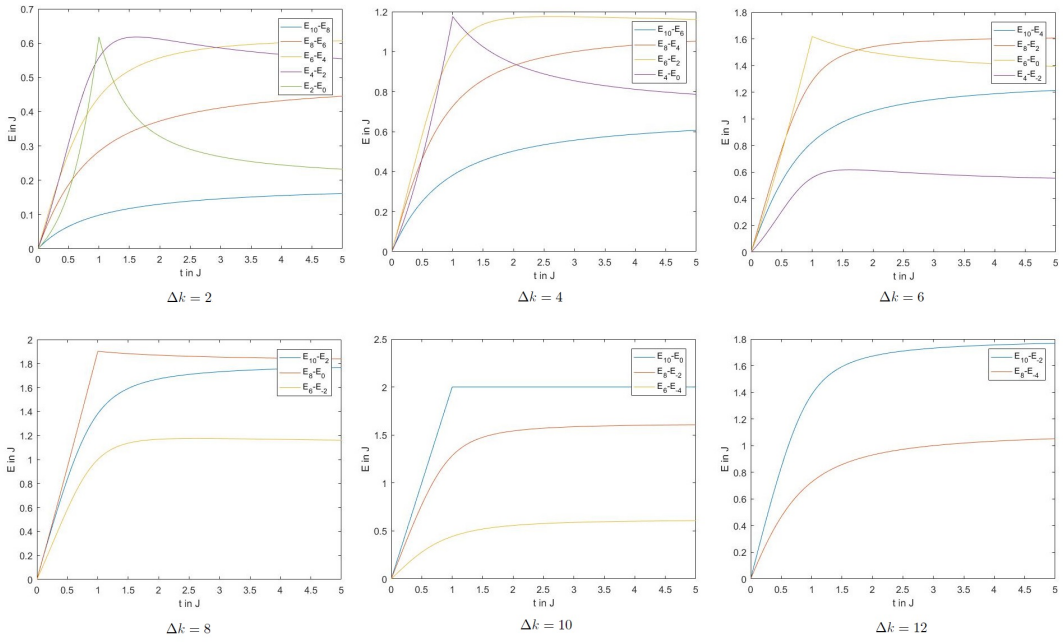

Figure 19: Energy differences with the same difference $\Delta k = k_1 - k_2$ for the odd parity subspace. Note that the possibilities with negative k lead to the same figure with negative energy since $E_k = E_{-k}$.

D Lindblad for the closed chain

Inserting the time dependent interaction into the Redfield equation and using the Rotating Wave Approximation leads to:

$$
\begin{aligned}
\frac{d\rho_s}{dt} = -\sum_{n1,n2}\Bigg(
&2\sum_{i,j}\Gamma_{n1,n2}(0)A_{i,j,n_1}\delta_{E_i,E_j}[\gamma_i^\dagger\gamma_j,\rho_s] \\
&+2\sum_{i,j}\Gamma_{n1,n2}(0)v_{i,n1}u_{j,n1}\delta_{E_i,-E_j}[\gamma_i\gamma_j,\rho_s] \\
&+2\sum_{i,j}\Gamma_{n1,n2}(0)v^*_{i,n1}u^*_{j,n1}\delta_{E_i,-E_j}[\gamma_j^\dagger\gamma_i^\dagger,\rho_s] \\
&+4\sum_{i1,i2,j1,j2}\Gamma_{n1,n2}(E_{i1}-E_{j1})A_{i1,j1,n1}A_{i2,j2,n2}\delta_{E_{i1}-E_{j1},E_{j2}-E_{i2}}[\gamma_{i1}^\dagger\gamma_{j1},\gamma_{i2}^\dagger\gamma_{j2}\rho_s] \\
&+4\sum_{i1,i2,j1,j2}\Gamma_{n1,n2}(E_{i1}-E_{j1})A_{i1,j1,n1}v_{i2,n2}u_{j2,n2}\delta_{E_{i1}-E_{j1},E_{i2}+E_{j2}}[\gamma_{i1}^\dagger\gamma_{j1},\gamma_{i2}\gamma_{j2}\rho_s] \\
&+4\sum_{i1,i2,j1,j2}\Gamma_{n1,n2}(E_{i1}-E_{j1})A_{i1,j1,n1}v^*_{i2,n2}u^*_{j2,n2}\delta_{E_{i1}-E_{j1},-E_{i2}-E_{j2}}[\gamma_{i1}^\dagger\gamma_{j1},\gamma_{j2}^\dagger\gamma_{i2}^\dagger\rho_s] \\
&+4\sum_{i1,i2,j1,j2}\Gamma_{n1,n2}(-E_{i1}-E_{j1})v_{i1,n1}u_{j1,n1}A_{i2,j2,n2}\delta_{-E_{i1}-E_{j1},E_{j2}-E_{i2}}[\gamma_{i1}\gamma_{j1},\gamma_{i2}^\dagger\gamma_{j2}\rho_s] \\
&+4\sum_{i1,i2,j1,j2}\Gamma_{n1,n2}(-E_{i1}-E_{j1})v_{i1,n1}u_{j1,n1}v_{i2,n2}u_{j2,n2}\delta_{-E_{i1}-E_{j1},E_{j2}+E_{i2}}[\gamma_{i1}\gamma_{j1},\gamma_{i2}\gamma_{j2}\rho_s] \\
&+4\sum_{i1,i2,j1,j2}\Gamma_{n1,n2}(-E_{i1}-E_{j1})v_{i1,n1}u_{j1,n1}v^*_{i2,n2}u^*_{j2,n2}\delta_{E_{i1}+E_{j1},E_{j2}+E_{i2}}[\gamma_{i1}\gamma_{j1},\gamma_{j2}^\dagger\gamma_{i2}^\dagger\rho_s] \\
&+4\sum_{i1,i2,j1,j2}\Gamma_{n1,n2}(E_{i1}+E_{j1})v^*_{i1,n1}u^*_{j1,n1}A_{i2,j2,n2}\delta_{E_{i1}+E_{j1},E_{j2}-E_{i2}}[\gamma_{j1}^\dagger\gamma_{i1}^\dagger,\gamma_{i2}^\dagger\gamma_{j2}\rho_s] \\
&+4\sum_{i1,i2,j1,j2}\Gamma_{n1,n2}(E_{i1}+E_{j1})v^*_{i1,n1}u^*_{j1,n1}v_{i2,n2}u_{j2,n2}\delta_{E_{i1}+E_{j1},E_{j2}+E_{i2}}[\gamma_{j1}^\dagger\gamma_{i1}^\dagger,\gamma_{i2}\gamma_{j2}\rho_s] \\
&+4\sum_{i1,i2,j1,j2}\Gamma_{n1,n2}(E_{i1}+E_{j1})v^*_{i1,n1}u^*_{j1,n1}v^*_{i2,n2}u^*_{j2,n2}\delta_{E_{i1}+E_{j1},-E_{j2}-E_{i2}}[\gamma_{j1}^\dagger\gamma_{i1}^\dagger,\gamma_{j2}^\dagger\gamma_{i2}^\dagger\rho_s]
\end{aligned}
$$

$$
\begin{aligned}
&+2\sum_{k,j}\Gamma^{*}_{n1,n2}(0)A_{i,j,n_1}\delta_{E_i,E_j}[\rho_s,\gamma_i^{\dagger}\gamma_j]\\
&+2\sum_{i,j}\Gamma_{n1,n2}(0)v_{i,n1}u_{j,n1}\delta_{E_i,-E_j}[\rho_s,\gamma_i\gamma_j]\\
&+2\sum_{i,j}\Gamma_{n1,n2}(0)v^{*}_{i,n1}u^{*}_{j,n1}\delta_{E_i,-E_j}[\rho_s,\gamma_j^{\dagger}\gamma_i^{\dagger}]\\
&+4\sum_{i1,i2,j1,j2}\Gamma_{n1,n2}(E_{i1}-E_{j1})A_{i1,j1,n1}A_{i2,j2,n2}\delta_{E_{i1}-E_{j1},E_{j2}-E_{i2}}[\rho_s\gamma_{i1}^{\dagger}\gamma_{j1},\gamma_{i2}^{\dagger}\gamma_{j2}]\\
&+4\sum_{i1,i2,j1,j2}\Gamma^{*}_{n1,n2}(E_{i1}-E_{j1})A_{i1,j1,n1}v_{i2,n2}u_{j2,n2}\delta_{E_{i1}-E_{j1},E_{i2}+E_{j2}}[\rho_s\gamma_{i1}^{\dagger}\gamma_{j1},\gamma_{i2}\gamma_{j2}]\\
&+4\sum_{i1,i2,j1,j2}\Gamma^{*}_{n1,n2}(E_{i1}-E_{j1})A_{i1,j1,n1}v^{*}_{i2,n2}u^{*}_{j2,n2}\delta_{E_{i1}-E_{j1},-E_{i2}-E_{j2}}[\rho_s\gamma_{i1}^{\dagger}\gamma_{j1},\gamma_{j2}^{\dagger}\gamma_{i2}^{\dagger}]\\
&+4\sum_{i1,i2,j1,j2}\Gamma^{*}_{n1,n2}(-E_{i1}-E_{j1})v_{i1,n1}u_{j1,n1}A_{i2,j2,n2}\delta_{-E_{i1}-E_{j1},E_{j2}-E_{i2}}[\rho_s\gamma_{i1}\gamma_{j1},\gamma_{i2}^{\dagger}\gamma_{j2}]\\
&+4\sum_{i1,i2,j1,j2}\Gamma^{*}_{n1,n2}(-E_{i1}-E_{j1})v_{i1,n1}u_{j1,n1}v_{i2,n2}u_{j2,n2}\delta_{-E_{i1}-E_{j1},E_{j2}+E_{i2}}[\rho_s\gamma_{i1}\gamma_{j1},\gamma_{i2}\gamma_{j2}]\\
&+4\sum_{i1,i2,j1,j2}\Gamma^{*}_{n1,n2}(-E_{i1}-E_{j1})v_{i1,n1}u_{j1,n1}v^{*}_{i2,n2}u^{*}_{j2,n2}\delta_{E_{i1}+E_{j1},E_{j2}+E_{i2}}[\rho_s\gamma_{i1}\gamma_{j1},\gamma_{j2}^{\dagger}\gamma_{i2}^{\dagger}]\\
&+4\sum_{i1,i2,j1,j2}\Gamma^{*}_{n1,n2}(E_{k1}+E_{j1})v^{*}_{i1,n1}u^{*}_{j1,n1}A_{i2,j2,n2}\delta_{E_{i1}+E_{j1},E_{j2}-E_{i2}}[\rho_s\gamma_{j1}^{\dagger}\gamma_{i1}^{\dagger},\gamma_{i2}^{\dagger}\gamma_{j2}]\\
&+4\sum_{i1,i2,j1,j2}\Gamma^{*}_{n1,n2}(E_{i1}+E_{j1})v^{*}_{i1,n1}u^{*}_{j1,n1}v_{i2,n2}u_{j2,n2}\delta_{E_{i1}+E_{j1},E_{j2}+E_{i2}}[\rho_s\gamma_{j1}^{\dagger}\gamma_{i1}^{\dagger},\gamma_{i2}\gamma_{j2}]\\
&+4\sum_{i1,i2,j1,j2}\Gamma^{*}_{n1,n2}(E_{i1}+E_{j1})v^{*}_{i1,n1}u^{*}_{j1,n1}v^{*}_{i2,n2}u^{*}_{j2,n2}\delta_{E_{i1}+E_{j1},-E_{j2}-E_{i2}}[\rho_s\gamma_{j1}^{\dagger}\gamma_{i1}^{\dagger},\gamma_{j2}^{\dagger}\gamma_{i2}^{\dagger}]\Bigg)
\end{aligned}
\tag{D.1}
$$

with

$$
A_{i,j,n}=v_{k_jn}v^{*}_{k_in}-u^{*}_{k_in}u_{k_jn}\,. \tag{D.2}
$$

As one can see some terms drop out due to the delta functions. Thus several terms like the following can be dropped out:

$$
\delta_{E_{i1}+E_{j1},-E_{j2}-E_{i2}}[\gamma_{j1}^{\dagger}\gamma_{i1}^{\dagger},\gamma_{j2}^{\dagger}\gamma_{i2}^{\dagger}\rho_s]=[\underbrace{\gamma_0^{\dagger}\gamma_0^{\dagger}}_{0},\gamma_0^{\dagger}\gamma_0^{\dagger}\rho_s] \tag{D.3}
$$

as the $|0\rangle$ state is the only excitation with zero energy (for $t < J$).
Thus the total equation simplifies to:

$$\begin{aligned}
\frac{d\rho_s}{dt} = -\sum_{n1,n2} \Bigg(& 2\sum_{i,j} \Gamma_{n1,n2}(0) A_{i,j,n_1} \delta_{E_i,E_j} [\gamma_i^\dagger \gamma_j, \rho_s] \\
& + 4 \sum_{i1,i2,j1,j2} \Gamma_{n1,n2}(E_{i1} - E_{j1}) A_{i1,j1,n1} A_{i2,j2,n2} \delta_{E_{i1}-E_{j1},E_{j2}-E_{i2}} [\gamma_{i1}^\dagger \gamma_{j1}, \gamma_{i2}^\dagger \gamma_{j2} \rho_s] \\
& + 4 \sum_{i1,i2,j1,j2} \Gamma_{n1,n2}(E_{i1} - E_{j1}) A_{i1,j1,n1} v_{i2,n2} u_{j2,n2} \delta_{E_{i1}-E_{j1},E_{i2}+E_{j2}} [\gamma_{i1}^\dagger \gamma_{j1}, \gamma_{i2} \gamma_{j2} \rho_s] \\
& + 4 \sum_{i1,i2,j1,j2} \Gamma_{n1,n2}(E_{i1} - E_{j1}) A_{i1,j1,n1} v_{i2,n2}^* u_{j2,n2}^* \delta_{E_{i1}-E_{j1},-E_{i2}-E_{j2}} [\gamma_{i1}^\dagger \gamma_{j1}, \gamma_{j2}^\dagger \gamma_{i2}^\dagger \rho_s] \\
& + 4 \sum_{i1,i2,j1,j2} \Gamma_{n1,n2}(-E_{i1} - E_{j1}) v_{i1,n1} u_{j1,n1} A_{i2,j2,n2} \delta_{-E_{i1}-E_{j1},E_{j2}-E_{i2}} [\gamma_{i1} \gamma_{j1}, \gamma_{i2}^\dagger \gamma_{j2} \rho_s] \\
& + 4 \sum_{i1,i2,j1,j2} \Gamma_{n1,n2}(-E_{i1} - E_{j1}) v_{i1,n1} u_{j1,n1} v_{i2,n2}^* u_{j2,n2}^* \delta_{E_{i1}+E_{j1},E_{j2}+E_{i2}} [\gamma_{i1} \gamma_{j1}, \gamma_{j2}^\dagger \gamma_{i2}^\dagger \rho_s] \\
& + 4 \sum_{i1,i2,j1,j2} \Gamma_{n1,n2}(E_{i1} + E_{j1}) v_{i1,n1}^* u_{j1,n1}^* A_{i2,j2,n2} \delta_{E_{i1}+E_{j1},E_{j2}-E_{i2}} [\gamma_{j1}^\dagger \gamma_{i1}^\dagger, \gamma_{i2}^\dagger \gamma_{j2} \rho_s] \\
& + 4 \sum_{i1,i2,j1,j2} \Gamma_{n1,n2}(E_{i1} + E_{j1}) v_{i1,n1}^* u_{j1,n1}^* v_{i2,n2} u_{j2,n2} \delta_{E_{i1}+E_{j1},E_{j2}+E_{i2}} [\gamma_{j1}^\dagger \gamma_{i1}^\dagger, \gamma_{i2} \gamma_{j2} \rho_s] \\
& + 2\sum_{i,j} \Gamma_{n1,n2}^*(0) A_{i,j,n_1} \delta_{E_i,E_j} [\rho_s, \gamma_i^\dagger \gamma_j] \\
& + 4 \sum_{i1,i2,j1,j2} \Gamma_{n1,n2}(E_{i1} - E_{j1}) A_{i1,j1,n1} A_{i2,j2,n2} \delta_{E_{i1}-E_{j1},E_{j2}-E_{i2}} [\rho_s \gamma_{i1}^\dagger \gamma_{j1}, \gamma_{i2}^\dagger \gamma_{j2}] \\
& + 4 \sum_{i1,i2,j1,j2} \Gamma_{n1,n2}^*(E_{i1} - E_{j1}) A_{i1,j1,n1} v_{i2,n2} u_{j2,n2} \delta_{E_{i1}-E_{j1},E_{i2}+E_{j2}} [\rho_s \gamma_{i1}^\dagger \gamma_{j1}, \gamma_{i2} \gamma_{j2}] \\
& + 4 \sum_{i1,i2,j1,j2} \Gamma_{n1,n2}^*(E_{i1} - E_{j1}) A_{i1,j1,n1} v_{i2,n2}^* u_{j2,n2}^* \delta_{E_{i1}-E_{j1},-E_{i2}-E_{j2}} [\rho_s \gamma_{i1}^\dagger \gamma_{j1}, \gamma_{j2}^\dagger \gamma_{i2}^\dagger] \\
& + 4 \sum_{i1,i2,j1,j2} \Gamma_{n1,n2}^*(-E_{i1} - E_{j1}) v_{i1,n1} u_{j1,n1} A_{i2,j2,n2} \delta_{-E_{i1}-E_{j1},E_{j2}-E_{i2}} [\rho_s \gamma_{i1} \gamma_{j1}, \gamma_{i2}^\dagger \gamma_{j2}] \\
& + 4 \sum_{i1,i2,j1,j2} \Gamma_{n1,n2}^*(-E_{i1} - E_{j1}) v_{i1,n1} u_{j1,n1} v_{i2,n2}^* u_{j2,n2}^* \delta_{E_{i1}+E_{j1},E_{j2}+E_{i2}} [\rho_s \gamma_{i1} \gamma_{j1}, \gamma_{j2}^\dagger \gamma_{i2}^\dagger] \\
& + 4 \sum_{i1,i2,j1,j2} \Gamma_{n1,n2}^*(E_{i1} + E_{j1}) v_{i1,n1}^* u_{j1,n1}^* A_{i2,j2,n2} \delta_{E_{i1}+E_{j1},E_{j2}-E_{i2}} [\rho_s \gamma_{j1}^\dagger \gamma_{i1}^\dagger, \gamma_{i2}^\dagger \gamma_{j2}] \\
& + 4 \sum_{i1,i2,j1,j2} \Gamma_{n1,n2}^*(E_{i1} + E_{j1}) v_{i1,n1}^* u_{j1,n1}^* v_{i2,n2} u_{j2,n2} \delta_{E_{i1}+E_{j1},E_{j2}+E_{i2}} [\rho_s \gamma_{j1}^\dagger \gamma_{i1}^\dagger, \gamma_{i2} \gamma_{j2}] \Bigg)
\end{aligned} \tag{D.4}$$

One can see that there are several terms, which have the following structure:

$$\begin{aligned}
\Gamma[A, B\rho_s] + \Gamma^*[\rho_s A, B] &= \Gamma(AB\rho_s - B\rho_s A) + \Gamma^*(\rho_s AB - B\rho_s A) \\
&= -(\Gamma + \Gamma^*) B\rho_s A + \Gamma AB\rho_s + \Gamma^* \rho_s AB \\
&= -\underbrace{(\Gamma + \Gamma^*)}_{\gamma} \left(B\rho_s A - \frac{1}{2}(AB\rho_s + \rho_s AB) \right) + \underbrace{\frac{1}{2}(\Gamma - \Gamma^*)}_{iS} (AB\rho_s - \rho_s AB) \\
&= -\gamma \left(B\rho_s A - \frac{1}{2}\{AB, \rho_s\} \right) + iS[AB, \rho_s]
\end{aligned} \tag{D.5}$$

Where γ is the real part of Γ and S the imaginary part of Γ.
Thus the total equation can be expressed in a Lindblad like form

$$
\begin{aligned}
\frac{d\rho_s}{dt} = \sum_{n1,n2} \Bigg(& -4i \sum_{i,j} S_{n1,n2}(0) A_{i,j,n1} \delta_{E_i,E_j} [\gamma_i^\dagger \gamma_j, \rho_s] \\
& + 4 \sum_{i1,i2,j1,j2} A_{i1,j1,n1} A_{i2,j2,n2} \delta_{E_{i1}-E_{j1},E_{j2}-E_{i2}} \Bigg(-iS_{n1,n2}(E_{i1}-E_{j1}) [\gamma_{i1}^\dagger \gamma_{j1} \gamma_{i2}^\dagger \gamma_{j2}, \rho_s] \\
& + \gamma_{n1,n2}(E_{i1}-E_{j1}) \left(\gamma_{i2}^\dagger \gamma_{j2} \rho_s \gamma_{i1}^\dagger \gamma_{j1} - \frac{1}{2} \{ \gamma_{i1}^\dagger \gamma_{j1} \gamma_{i2}^\dagger \gamma_{j2}, \rho_s \} \right) \Bigg) \\
& + 4 \sum_{i1,i2,j1,j2} A_{i1,j1,n1} u_{j2,n2} v_{i2,n2} \delta_{E_{i1}-E_{j1},E_{i2}+E_{j2}} \Bigg(-iS_{n1,n2}(E_{i1}-E_{i2}) [\gamma_{i1}^\dagger \gamma_{j1} \gamma_{i2} \gamma_{j2}, \rho_s] \\
& + \gamma_{n1,n2}(E_{i1}-E_{j1}) \left(\gamma_{i2} \gamma_{j2} \rho_s \gamma_{i1}^\dagger \gamma_{j1} - \frac{1}{2} \{ \gamma_{i1}^\dagger \gamma_{j1} \gamma_{i2} \gamma_{j2}, \rho_s \} \right) \Bigg) \\
& + 4 \sum_{i1,i2,j1,j2} A_{i1,j1,n1} u_{j2,n2}^* v_{i2,n2}^* \delta_{E_{i1}-E_{j1},-E_{i2}-E_{j2}} \Bigg(-iS_{n1,n2}(E_{i1}-E_{j1}) [\gamma_{i1}^\dagger \gamma_{j1} \gamma_{i2}^\dagger \gamma_{j2}^\dagger, \rho_s] \\
& + \gamma_{n1,n2}(E_{i1}-E_{j1}) \left(\gamma_{j2}^\dagger \gamma_{i2}^\dagger \rho_s \gamma_{i1}^\dagger \gamma_{j1} - \frac{1}{2} \{ \gamma_{i1}^\dagger \gamma_{j1} \gamma_{j2}^\dagger \gamma_{i2}^\dagger, \rho_s \} \right) \Bigg) \\
& + 4 \sum_{i1,i2,j1,j2} u_{j1,n1} v_{i1,n2} A_{i2,j2,n2} \delta_{E_{i1}+E_{j1},E_{i2}-E_{j2}} \Bigg(-iS_{n1,n2}(-E_{i1}-E_{j1}) [\gamma_{i1} \gamma_{j1} \gamma_{i2}^\dagger \gamma_{j2}, \rho_s] \\
& + \gamma_{n1,n2}(-E_{i1}-E_{j1}) \left(\gamma_{i2}^\dagger \gamma_{j2} \rho_s \gamma_{i1} \gamma_{j1} - \frac{1}{2} \{ \gamma_{i1} \gamma_{j1} \gamma_{i2}^\dagger \gamma_{j2}, \rho_s \} \right) \Bigg) \\
& + 4 \sum_{i1,i2,j1,j2} u_{j1} v_{i1} u_{j2}^* v_{i2}^* \delta_{E_{i1}+E_{j1},E_{i2}+E_{j2}} \Bigg(-iS_{n1,n2}(-E_{i1}-E_{j1}) [\gamma_{i1} \gamma_{j1} \gamma_{j2}^\dagger \gamma_{i2}, \rho_s] \\
& + \gamma_{n1,n2}(-E_{i1}-E_{j1}) \left(\gamma_{j2}^\dagger \gamma_{k2}^\dagger \rho_s \gamma_{i1} \gamma_{j1} - \frac{1}{2} \{ \gamma_{i1} \gamma_{j1} \gamma_{j2}^\dagger \gamma_{i2}^\dagger, \rho_s \} \right) \Bigg) \\
& + 4 \sum_{i1,i2,j1,j2} u_{j1,n1}^* v_{i1,n1}^* u_{j2,n2} v_{i2,n2} \delta_{E_{i1}+E_{j1},E_{i2}+E_{j2}} \Bigg(-iS_{n1,n2}(E_{i1}+E_{j1}) [\gamma_{j1}^\dagger \gamma_{i1}^\dagger \gamma_{i2} \gamma_{j2}, \rho_s] \\
& + \gamma_{n1,n2}(E_{i1}+E_{j1}) \left(\gamma_{i2} \gamma_{j2} \rho_s \gamma_{j1}^\dagger \gamma_{i1}^\dagger - \frac{1}{2} \{ \gamma_{j1}^\dagger \gamma_{i1}^\dagger \gamma_{i2} \gamma_{j2}, \rho_s \} \right) \Bigg) \\
& + 4 \sum_{i1,i2,j1,j2} u_{j1,n1}^* v_{i1,n1}^* A_{i2,j2,n2} \delta_{E_{i1}+E_{j1},E_{j2}-E_{i2}} \Bigg(-iS_{n1,n2}(E_{i1}+E_{j1}) [\gamma_{j1}^\dagger \gamma_{i1}^\dagger \gamma_{i2}^\dagger \gamma_{j2}, \rho_s] \\
& + \gamma_{n1,n2}(E_{i1}+E_{j1}) \left(\gamma_{i2}^\dagger \gamma_{j2} \rho_s \gamma_{j1}^\dagger \gamma_{i1}^\dagger - \frac{1}{2} \{ \gamma_{j1}^\dagger \gamma_{i1}^\dagger \gamma_{i2}^\dagger \gamma_{j2}, \rho_s \} \right) \Bigg) \Bigg) \, , . \qquad \text{(D.6)}
\end{aligned}
$$

And by neglecting the Lamb shift terms the total Lindblad equation reads

$$
\begin{aligned}
\frac{d\rho_s}{dt} = \sum_{n1,n2} \Bigg(& 4 \sum_{i1,i2,j1,j2} A_{i1,j1,n1} A_{i2,j2,n2} \delta_{E_{i1}-E_{j1},E_{j2}-E_{i2}} \\
& \left(\kappa_{n1,n2}(E_{i1}-E_{j1}) \left(\gamma_{i2}^\dagger \gamma_{j2} \rho_s \gamma_{i1}^\dagger \gamma_{j1} - \frac{1}{2} \{ \gamma_{i1}^\dagger \gamma_{j1} \gamma_{i2}^\dagger \gamma_{j2}, \rho_s \} \right) \right) \\
& + 4 \sum_{i1,i2,j1,j2} A_{i1,j1,n1} u_{j2,n2} v_{i2,n2} \delta_{E_{i1}-E_{j1},E_{i2}+E_{j2}} \\
& \left(\kappa_{n1,n2}(E_{i1}-E_{j1}) \left(\gamma_{i2} \gamma_{j2} \rho_s \gamma_{i1}^\dagger \gamma_{j1} - \frac{1}{2} \{ \gamma_{i1}^\dagger \gamma_{j1} \gamma_{i2} \gamma_{j2}, \rho_s \} \right) \right) \\
& + 4 \sum_{i1,i2,j1,j2} A_{i1,j1,n1} u_{j2,n2}^* v_{i2,n2}^* \delta_{E_{i1}-E_{j1},-E_{i2}-E_{j2}} \\
& \left(\kappa_{n1,n2}(E_{i1}-E_{j1}) \left(\gamma_{j2}^\dagger \gamma_{i2}^\dagger \rho_s \gamma_{i1}^\dagger \gamma_{j1} - \frac{1}{2} \{ \gamma_{i1}^\dagger \gamma_{j1} \gamma_{j2}^\dagger \gamma_{i2}^\dagger, \rho_s \} \right) \right) \\
& + 4 \sum_{i1,i2,j1,j2} u_{j1,n1} v_{i1,n2} A_{i2,j2,n2} \delta_{E_{i1}+E_{j1},E_{i2}-E_{j2}} \\
& \left(\kappa_{n1,n2}(-E_{i1}-E_{j1}) \left(\gamma_{i2}^\dagger \gamma_{j2} \rho_s \gamma_{i1} \gamma_{j1} - \frac{1}{2} \{ \gamma_{i1} \gamma_{j1} \gamma_{i2}^\dagger \gamma_{j2}, \rho_s \} \right) \right) \\
& + 4 \sum_{i1,i2,j1,j2} u_{j1,n1} v_{i1,n1} u_{j2,n2}^* v_{i2,n2}^* \delta_{E_{i1}+E_{j1},E_{i2}+E_{j2}} \\
& \left(\kappa_{n1,n2}(-E_{i1}-E_{j1}) \left(\gamma_{j2}^\dagger \gamma_{i2}^\dagger \rho_s \gamma_{i1} \gamma_{j1} - \frac{1}{2} \{ \gamma_{i1} \gamma_{j1} \gamma_{j2}^\dagger \gamma_{i2}^\dagger, \rho_s \} \right) \right) \\
& + 4 \sum_{i1,i2,j1,j2} u_{j1,n1}^* v_{i1,n1}^* u_{j2} v_{i2} \delta_{E_{i1}+E_{j1},E_{i2}+E_{j2}} \\
& \left(\kappa_{n1,n2}(E_{i1}+E_{j1}) \left(\gamma_{i2} \gamma_{j2} \rho_s \gamma_{j1}^\dagger \gamma_{k1}^\dagger - \frac{1}{2} \{ \gamma_{j1}^\dagger \gamma_{i1}^\dagger \gamma_{i2} \gamma_{j2}, \rho_s \} \right) \right) \\
& + 4 \sum_{i1,i2,j1,j2} u_{j1,n1}^* v_{i1,n1}^* A_{i2,j2,n2} \delta_{E_{i1}+E_{j1},E_{j2}-E_{i2}} \\
& \left(\kappa_{n1,n2}(E_{i1}+E_{j1}) \left(\gamma_{i2}^\dagger \gamma_{j2} \rho_s \gamma_{j1}^\dagger \gamma_{i1}^\dagger - \frac{1}{2} \{ \gamma_{j1}^\dagger \gamma_{i1}^\dagger \gamma_{i2}^\dagger \gamma_{j2}, \rho_s \} \right) \right) . \qquad \text{(D.7)}
\end{aligned}
$$